

**Mapping and Monitoring of Croplands in a  
Complex Urban/ Peri-urban Landscape Using  
Multi-sensor Satellite Imagery: A Case Study of  
Japan**

February 2018



**CHIBA  
UNIVERSITY**

Graduate School of Science  
Division of Geosystem and Biological Science  
Department of Earth Science  
Eunice Nduati

## **Declaration**

This thesis is an account of research undertaken at The Department of Earth Science, Faculty of Science, Chiba University. Except where acknowledged in the customary manner, the material presented in this thesis is, to the best of my knowledge, original and has not been submitted in whole or part for a degree in any other university.

---

Eunice Nduati

February, 2019

## Abstract

Rapid increase in the world's population, urbanization and allocation of agricultural products towards non-food use has propelled pressure on arable land and poses a threat to food and nutrition security. In the coming years, it is expected that there will be additional encumbrances on existing agricultural production due to the need to intensify and enhance production and efficiency, while maintaining environmentally friendly and sustainable practices. There is thus an urgent need for up-to-date spatial information on agricultural production enterprises and continuous monitoring in order to support key decision and policy making activities at various administrative levels. This is particularly imperative for urban populations since more than half the world's population currently reside in urban areas and this figure is set to rise.

While food production in urban and peri-urban areas is fast becoming entrenched and integrated into the fabric of urban life, it is market demand driven and caters to provision of the most perishable food products. It is therefore highly dynamic in terms of spatial location, due to conversion of valuable agricultural land to urban land-use, and what is produced, as land owners seek to maximize returns on the land. As such, methods used to acquire information on cropland location and what is produced in urban and peri-urban areas need to be spatially and temporally flexible. Remote Sensing allows for repetitive acquisition of information pertaining to land cover use and type and can be easily operationalized compared to classical methods such as field surveys. However, limitations imposed by spatial-temporal resolution trade-offs of imaging systems and atmospheric artefacts inhibit the acquisition of spatially and temporally conterminous data that is necessary for agricultural mapping and monitoring applications.

Towards meeting the need for consistent and timely information on urban and peri-urban agricultural production, this study seeks to evaluate the application

of intra-annual optical earth observation data with exploitation of the simple phenological metric, the Normalized Difference Vegetation Index (NDVI). A high density NDVI time series data set is generated via fusion of daily MODIS NDVI and intermittent Landsat NDVI images within one year for seven municipalities in Chiba Prefecture, which is adjacent to the Tokyo metropolis. Pixel-based classification using the ensemble-learning Random Forest classifier is then applied to the time series stack with training data derived from the maximum value composite NDVI stack of the available Landsat imagery and corroborated by Google earth and Google Maps. The methodology presented serves as an analytical framework for operational annual mapping and estimation of cropland extent and cropping regimes, using a creative means of acquiring reference data thus eliminating the need for time and cost intensive field surveys.

## Acknowledgements

I would like to extend my utmost gratitude to the Japan International Cooperation Agency (JICA) and members of its affiliate project in Kenya, the Japan Africa-Innovation Project (Japan-ai-Project), whose financial, logistical and moral support made this research possible. In particular, I would like to thank Prof. Manabu Tsunoda, Ms. Kato Megumi, Ms. Oda Sachiko and last but not least, Ms. Toda Mai.

I would also like to sincerely thank Prof. Jong Geol Park of Tokyo University of Information Science for his unwavering patience, kindness and guidance in the course of my studies. I remain indebted to my supervisors, Prof. Akihiko Kondoh and Dr. Yang Wei for their guidance throughout my research.

To my family, my parents Gidraph J. Nduati and Ruth W. Nduati, my sisters Loise, Faith and Serah and my niece and nephew, Audrey and Tyler, your love, support and encouragement can never be overstated.

*Your reason and your passion are the rudder and The sails of your seafaring soul.*

*If either your sails or your rudder be broken, you can but toss and drift, or else be held at a standstill in mid-seas.*

*For reason, ruling alone, is a force confining; and passion, unattended, is a flame that burns to its own destruction.*

*Therefore, let your soul exalt your reason to the height of passion, that it may sing;*

*And let it direct your passion with reason, that your passion may live through its own daily resurrection, and like the phoenix rise above its own ashes.*

— Khalil Gibran, *The Prophet*

# Contents

<b>Declaration</b>	<b>i</b>
<b>Abstract</b>	<b>ii</b>
<b>Acknowledgements</b>	<b>iv</b>
<b>1 Introduction</b>	<b>1</b>
1.1 Background . . . . .	1
1.2 Motivations and Problem statement . . . . .	3
1.3 Objectives . . . . .	9
1.3.1 General Objective . . . . .	9
1.3.2 Specific objectives . . . . .	9
1.4 Outline . . . . .	10
<b>2 Literature Review</b>	<b>11</b>
2.1 Land-use and Land Cover Mapping . . . . .	11

---

2.2	Cropland Mapping . . . . .	23
2.3	Urban and Peri-urban Agriculture (UPA) . . . . .	26
2.4	Spatio-temporal Image Fusion . . . . .	29
<b>3</b>	<b>Methodology</b>	<b>40</b>
3.1	Study area . . . . .	40
3.2	Data and Methods . . . . .	43
3.2.1	Application requirements evaluation . . . . .	43
3.2.2	Data acquisition and processing . . . . .	48
3.3	Classification . . . . .	54
3.3.1	Training and Validation Samples . . . . .	54
3.3.2	Crop-type Mapping Experiment . . . . .	58
<b>4</b>	<b>Results and Discussion</b>	<b>61</b>
4.1	MODIS-Landsat Fusion . . . . .	61
4.2	Cropland identification and discrimination . . . . .	68
4.2.1	JAXA HRLULC map comparison . . . . .	71
4.2.2	GFSAD30m map comparison . . . . .	72
4.3	Estimation of cropping regimes . . . . .	77
4.4	Peanuts Mapping . . . . .	82



<b>5</b>	<b>Conclusions and Future Work</b>	<b>90</b>
5.1	Conclusions . . . . .	90
5.2	Contributions . . . . .	93
5.3	Future Work . . . . .	93
	<b>Bibliography</b>	<b>94</b>
	Appendix	
A.1	Methodology Test Case: Kenya . . . . .	121
A.1.1	Introduction . . . . .	121
A.1.2	Results of preliminary processing and analysis . . . . .	129
A.2	Peer Reviewed Journal Paper . . . . .	134

# List of Tables

2.1	Summary of studies on cropland mapping and monitoring methods by application . . . . .	25
2.2	Categorization of fusion methods based on type of data sets fused and dimension enhanced by fusion. ( <i>Adapted from Pohl and Van Genderen, 1998</i> ) . . . . .	37
2.3	Proposed categorization of pixel-based image fusion algorithms. ( <i>Adapted from Pohl and Van Genderen, 2015</i> ) . . . . .	39
4.1	Confusion matrix of cropland extent classification . . . . .	70
4.2	Best periods for some of Chiba prefecture's representative crops	78
4.3	Confusion matrix of peanuts classification . . . . .	89

# List of Figures

2.1	Preview of ESA CCI-LC Map v2.0.7 for year 2015 . . . . .	19
2.2	Legend of the global CCI-LC Maps . . . . .	20
2.3	Count of Regional LC maps by location. <i>Source: Grekousis, Mountrakis and Kavouras (2015)</i> . . . . .	21
2.4	LULC categories in JAXA HRLULC maps . . . . .	22
2.5	Fusion methods categorized by representational elements fused from multi-source data. ( <i>Adapted from Ghassemian, 2016</i> ) . . .	36
2.6	Pixel-level fusion. ( <i>After Pohl and Van Genderen, 1998</i> ) . . . .	38
3.1	The seven municipalities constituting the study area in this research. . . . .	42
3.2	Proportional distribution of cultivated area size per farmer . . .	46
3.3	Sentinel 2A coverage (T54SVE) of the study area on various dates	47
3.4	MOD09GA and MOD09GQ pre-processing workflow . . . . .	49
3.5	Relative temporal distribution of Landsat-8 OLI and MODIS NDVI images for the study epoch . . . . .	51

---

3.6	Anomalous NDVI time-series profiles for various land use/cover types after fusion using fully reconstructed MODIS images . . . . .	53
3.7	RGB composites of the seasonal Maximum Value Composite NDVI (MVC-NDVI) for a subset of the study area. . . . .	56
3.8	Google Earth image on 9 <sup>th</sup> October 2015 for the same area subset shown in Figure 3.7 . . . . .	57
3.9	Google Maps Street View and Google Earth views of peanuts post-harvest practice on (9 <sup>th</sup> October, 2015) used for identification of location cultivation (N35°37', E140°14) . . . . .	60
4.2	Scatterplots showing results of comparison of synthetic fusion NDVI images with original Landsat images . . . . .	64
4.3	Comparison of synthetic and original Landsat NDVI time series profiles of major land cover types . . . . .	67
4.4	Land use/cover map of 2015 as mapped in this study . . . . .	69
4.5	Comparison of cropland extent of this study's result with JAXA HRLULC map . . . . .	74
4.6	GFSAD30 cropland extent . . . . .	75
4.7	Comparison of this study's paddy and cropland extent with GF-SAD30 cropland extent . . . . .	76
4.8	Cropping regimes estimated in this study for the year 2015 . . . . .	80

4.9	Locations where land cover change was detected in the Land Use/Cover Map and Cropping Regimes Estimation maps respectively . . . . .	84
4.10	Detailed view of locations 1 and 2 where rapid conversion of land cover from 'Grassland' to 'Urban' was detected . . . . .	85
4.11	2014 Google Earth image of locations 1 and 2 where rapid conversion of land cover from 'Grassland' to 'Urban' was detected .	86
4.12	2015 Google Earth image of locations 1 and 2 where rapid conversion of land cover from 'Grassland' to 'Urban' was detected .	87
4.13	Distinction of peanuts cultivation from other crops within the study area for the year 2015 . . . . .	88
A.1.1	The European Space Agency Climate Change Initiative (ESA CCI) Land use/ cover map of Kenya for 2016 . . . . .	124
A.1.2	Percentage monthly total cloud cover in the west, east and southern Africa regions . . . . .	125
A.1.3	MODIS Terra daily corrected surface reflectance data for January 2019 . . . . .	126
A.1.4	The test study area in Kenya located in the central highlands .	127
A.1.5	Relative temporal distribution of Landsat and MODIS surface reflectance images acquired for the year 2016 for the Kenyan test study area . . . . .	128
A.1.6	Scatterplots showing results of comparison of synthetic NDVI images with original Landsat NDVI images . . . . .	132

A.1.7 Land Use/ Cover map of 2016 for the test study area in Kenya . 133

# Chapter 1

## Introduction

### 1.1 Background

Regional food security is threatened by uncertain global climatic conditions and global commodity price fluctuations which have resulted in decreased yields and dependence on local food production respectively (Brown and Funk, 2008). In addition, due to urbanization and an increase in demand for settlement land, production of food crops in urban areas and the regions neighbouring them is increasingly becoming necessary. This is especially the case for the highly perishable but nutritious food crops which are progressively becoming harder to access in urban areas (Opitz *et al.*, 2016). However, urban and peri-urban food production units are limited in size due to competing land use demands and the high value attached to land in urban and peri-urban areas (Eigenbrod and Gruda, 2015). To counter these challenges, adaptation strategies are imperative and are aimed towards achieving food security as defined by the Food and Agriculture Organization (FAO, 2004). Adaptation and mitigation strategies include but are not limited to, formulation of short

---

and long-term policies for improvement, sustenance, and protection of natural resources, modification of farming practices via technological uptake and adaptation of new crops and cropping systems (Jat *et al.*, 2016; Waldner and Defourny, 2015). There is therefore exigency for timely and dependable information on agricultural production for capacity building, forecasting and constitution of contingency plans for vulnerable areas (Jat *et al.*, 2016; Waldner and Defourny, 2015 ; Toma *et al.*, 2016).

As a precursor to the aforementioned activities relating to monitoring of agricultural production and formulation of policies towards improvement of agricultural practices, it is necessary to know where crop production is taking place, what crops are being produced and when they are produced, that is, cropland and crop-type mapping and inventorying. Currently, there is an opportunity to develop a cohesive analytical framework suitable for assessing spatial and temporal trends in land cover and land use at local scales in agricultural landscapes. Such a framework involves collection and analysis of information that will enable integration with other information databases necessary for agricultural development such as soil and weather information databases (Teluguntla *et al.*, 2015). The time sensitive nature of data related to the environment and agriculture, demands that such a framework be capable of acquiring consistent and timely information to enhance integration with other regional environmental reporting frameworks. Towards this goal, this thesis presents a method that allows for processing of earth observation imagery and agricultural land use information in a cohesive manner suitable for annual regional agricultural land-use/cover mapping and monitoring.



## 1.2 Motivations and Problem statement

Cropland and crop-type mapping and assessment activities using remote sensing have been around for a long time but have recently gained momentum due to advancements in data collection and ingestion technologies that have resulted in 'big data' (Bronson and Knezevic, 2016). Formerly restricted by spatial resolution of imaging systems, higher spatial resolutions are now possible with higher revisit frequency and therefore better temporal resolution, thus providing more information on the agricultural landscape. While there have been major advancements in optical imaging systems, agricultural land use mapping, monitoring and assessment activities require temporally continuous data. A major limitation to acquisition of continuous optical remote sensing data is the presence of atmospheric artefacts such as haze or cloud cover. Sensor failures and atmospheric artefacts result in acquisition of images where information about the ground surface cannot be directly retrieved and hence missing data and irregular sampling of the phenomena under investigation (Petitjean, Inglada and Gançarski, 2012).

Various techniques have been developed to deal with missing data in remote sensing imagery (Julien and Sobrino, 2010; Shukla *et al.*, 2011; Cheng *et al.*, 2017; Ramoino *et al.*, 2017). According to Shen *et al.* (2015), these techniques can be broadly classified into four main categories, on the basis of the source of ancillary information for filling in the missing data:

1. Spatial-based methods: The most basic category of methods in which the supplemental information comes from the remaining parts of the data. They are based on the assumption that the missing data and the remaining parts have a statistical or geometrical relationship.

2. Spectral-based methods: Methods that utilize redundant information in the spectral dimension of multispectral and hyperspectral data, on the basis that for a given dataset, there are both complete and incomplete spectral bands, and that the incomplete bands have some residual information that can be used to model their relationship.
3. Temporal-based methods: They include the temporal replacement, temporal filter and temporal learning methods which use the information about a spatial location acquired at different periods in time.
4. Hybrid methods: These methods take advantage of the correlations in the spatial, spectral and temporal domains and include the spatio-temporal, and spatio-spectral methods.

Spatial methods are relatively simple and efficient to implement since they require no complementary information from another data source or domain. However, they are not well suited for large regions or areas with complex ground features (Shen *et al.*, 2015; Cheng *et al.*, 2017). Spectral methods on the one hand, reconstruct a singular image based on all the spectral information available in it in order to differentiate cloud cover from other features (Julien and Sobrino, 2010). Although spectral reconstruction methods are suitable for detection of cloud cover, they do not provide a means for estimation of the missing data, resulting in non-continuous imagery and hence loss of information, (Julien and Sobrino, 2010). On the other hand, temporal interpolation methods do not depend on detection of atmospheric contaminants, instead estimating missing information by modelling the continuous temporal behaviour of biophysical phenomena. However, in order to accurately fit the model, high regular temporal frequency imaging of the phenomena is required. The high temporal resolution necessary for temporal interpolation methods

restricts their application to low resolution imagery such as NOAA's AVHRR (National Oceanic and Atmospheric Administration Advanced Very High Resolution Radiometer) and MODIS (Moderate Resolution Imaging Spectroradiometer) data. As such, spatially and temporally heterogeneous agricultural landscapes, such as those prevalent in urban and peri-urban areas, requiring high spatial and temporal resolution data, cannot be adequately mapped and monitored using data reconstructed using either of the two broad satellite data reconstruction methods on their own (Hazaymeh and Hassan, 2015; Shen *et al.*, 2015).

Techniques for generation of synthetic high spatial and temporal resolution images via spatio-temporal data fusion have emerged as an important area of remote sensing (Hazaymeh and Hassan, 2015). This is due to the fact that, even as imaging systems' technology advances, satellite payload limitations impose a spatial-temporal resolution trade-off where high spatial resolution imaging systems tend to have low temporal resolution and contrariwise (Zhu *et al.*, 2016; Liao *et al.*, 2017). The overarching objective of spatio-temporal image fusion is to estimate missing high spatial resolution data that may be as a result of imaging systems' trade-offs, sensor failures or noise and atmospheric artefacts such as cloud cover by using a combination of high spatial - low temporal resolution data (e.g., Landsat 8 Operational Land Imager (OLI)) with high temporal - low spatial resolution data (e.g., MODIS) ( Zhao, Huang, and Song, 2018). Spatio-temporal fusion methods may be broadly categorized into four groups including; weighted function based, unmixing based, data-assimilation based and dictionary-pair learning based algorithms (Zhu *et al.*, 2016; Liao *et al.*, 2017). These methods all require as inputs, one or more pairs of observed low and high spatial resolution images, and a low spatial resolution image for the desired high spatial resolution prediction time or date.

The choice of fusion method is highly dependent on the application (e.g., agricultural or disaster monitoring and assessment), the nature of the landscape under observation, that is, homogeneous or heterogeneous landscapes, quality and availability of the data, and complexity of the method *vis-a-vis* available computational resources and technical skills (Alparone *et al.*, 2015; Pohl and van Genderen, 2015; Schmitt and Zhu, 2016; Pohl and van Genderen, 2016; Zhu *et al.*, 2018). Despite the growth of interest in spatio-temporal fusion, the diversity inherent in the large number of algorithms proposed, lack of standardized approaches to implementation and accuracy assessment of fusion results, and computational complexity and inefficiency have limited widespread operational application (Pohl and van Genderen, 2016; Zhu *et al.*, 2018).

In addition to quality continuous data acquisition constraints, further challenges in mapping and monitoring of croplands and crop-type in urban areas arise from the unavailability of, or lack of access to timely ground-truth data necessary for classification and validation. Generally, satellite images are, for most applications, processed and analysed retrospectively unless the data acquisition and processing are real-time or near real-time, as is the case for meteorological prediction applications. For agricultural applications, inter-annual cropland and crop-type mapping has been successfully implemented in the case of field crops such as wheat, paddy rice and maize using a variety of sensors at global, regional and national scales (Jakubauskas, Legates and Kastens, 2002; Mingwei *et al.*, 2008; McNairn *et al.*, 2009; Siachalou, Mallinis and Tsakiri-Strati, 2015; Inglada *et al.*, 2015). This has been made possible by, among other factors, the fact that field crops are cultivated over larger areas than most of the horticultural food crops typically cultivated in urban and peri-urban croplands and that they tend to be national staple foods, hence they are of great social, economical and political importance (Eigenbrod and

Gruda, 2015). As such, detection and extraction of their phenological properties has been the focus of most research works since they are more extensively and intensively cultivated and have for a long-time been deemed to be the key to building food security (Eigenbrod and Gruda, 2015; Hisano, 2015). In contrast, studies on production of horticultural food crops in the geospatial context have been far fewer, in part due to the focus on global and regional food production systems especially in developing countries and regions and under appreciation of the importance of urban horticulture in advancing food and nutritional security (Eigenbrod and Gruda, 2015; Hisano, 2015).

Further, the intra- and inter-annual variability of horticultural food crop types produced in urban and peri-urban holdings, presents a challenge in terms of continuous monitoring even at local scales. In order to counter the challenges of acquiring up-to-date ground-truth data, various country's mapping and research agencies have adopted ground-truth information acquisition modalities that involve inter-governmental agency cooperation with farmers and regular surveys by officials affiliated with agricultural agencies and private agribusiness enterprises. However, these approaches can be time, cost and resource intensive. The Agricultural Land Information System (ALIS) used in Japan and Phillipines estimates agricultural land and crop area using the most recent detailed satellite map derived from Google Earth imagery but requires ground surveys in order to verify the results, albeit on a subsample of observations (<https://www.adb.org/publications/crop-monitoring-improved-food-security>). Similarly, the Agriculture and Agri-Food Canada agency (AAFC) geospatial science, which has been in operation for over 20 years and is currently in the operational application mode, utilizes satellite earth observation data for among other applications, monitoring of land cover, annual national crop inventorying, estimation of agricultural land use

change indicators and near real-time weekly crop condition assessment ([https://ec.europa.eu/jrc/sites/jrcsh/files/09\\_champagne.pdf](https://ec.europa.eu/jrc/sites/jrcsh/files/09_champagne.pdf)). The AAFC's success in acquisition, processing and dissemination of information relevant to agricultural monitoring and forecasting can be attributed to a tenacious accumulation of data and expertise over time. Accordingly collection and accumulation of ground-truth information remains a daunting task, especially for spatially and temporally complex croplands, that requires investigation of application of novel approaches. Innovative approaches include but are not limited to, using the freely accessible high resolution satellite imagery with near ubiquitous repetitive coverage such as Google Earth and Bing, and crowdsourcing initiatives such as the Geo-Wiki platform (Xiao *et al.*, 2011; Fritz *et al.*, 2012).

This research focuses on mapping cropland area and crop types intra-annually in Chiba Prefecture which is a hinterland of the Japan Capital Region (JCR) as defined in Porter *et al.* (2014). While Japan is a developed country and is widely considered to be food secure, decreasing food self-sufficiency ratio and nutritional insufficiency are major issues which are highlighted in the Annual Report on Food, Agriculture and Rural Areas in Japan (MAFF, 1999). Hisano (2015) elaborates on these issues by pointing out that more than 60% of Japanese caloric intake is imported and the domestic agricultural sector relies on small-scale producers whose aging and declining population is facing production challenges further exacerbated by external and internal trade pressures. In Porter *et al.* (2014), the JCR is presented as a model example of how huge cities may feed themselves by relying on overseas land areas with production surplus to meet their own deficit via economic power. Notably, Porter *et al.* (2014) focussed on food availability and accessibility, in other words, volume aspect of food security, thus demonstrating the importance of urban

and peri-urban horticultural production in the JCR, from a nutritional security perspective. This study seeks to characterize these food production units using satellite earth observation data acquired in one year, by identifying horticultural croplands and distinguishing them from other land cover types and uses, including paddy fields. Using the Normalized Difference Vegetation Index (NDVI) as a phenological indicator, the parcel level intra- and inter-seasonal characteristics of various crop production units are investigated at pixel level in order to estimate croplands using reference data corroborated by Google Earth imagery for the same time as the study's period and expert knowledge on post-harvest practices for some crops. The methodology presented herein, provides an operational application framework for cropland mapping at local scales in spatially and temporally heterogeneous and dynamic landscapes.

## 1.3 Objectives

### 1.3.1 General Objective

The primary objective of this research is mapping and monitoring of urban and peri-urban agriculture in a complex landscape by exploiting multi-resolution spatio-temporal information.

### 1.3.2 Specific objectives

Towards achievement of the overall aim of this study, the following are the specific objectives:

1. To evaluate the application of fusion of multi-source satellite imagery to

generation of synthetic high spatio-temporal resolution time series

2. To distinguish cropland from non-cropland and make a distinction between upland cropland and paddy rice fields with limited reference data
3. To extract temporal phenological metrics to enable cropping pattern or cropping intensity estimation in a limited reference data scenario
4. To test the applicability of empirical data, specifically post-harvest practices information, in distinguishing peanuts from other crops in the study area

## 1.4 Outline

This thesis is organized into five chapters. Chapter 2 presents a review of research on land-use/cover mapping, spatio-temporal image fusion, cropland mapping and urban and peri-urban agriculture (UPA). Chapter 3 outlines the methodology used in this research including the rationale behind the data and methods as presented in the application requirements evaluation. The results and discussion of the outcomes of the processes implemented including image fusion and classification are described in Chapter 4. Conclusions and future prospects of the study are presented in chapter 5.



# Chapter 2

## Literature Review

### 2.1 Land-use and Land Cover Mapping

Information pertaining to land use activities and land cover has long been recognized as pertinent to the core business of many governments and non-governmental agencies and institutions (Anderson *et al.*, 1976; Kerr and Ostrovsky, 2003; Hermosilla *et al.*, 2014). Anderson *et al.* (1976) noted the importance of land-use and land cover information for a better understanding of living conditions towards maintaining or improving them by addressing problems such as haphazard and uncontrolled urban development, loss of biodiversity and agricultural land and assessment of environmental processes. Beyond the terrestrial biosphere, it is widely known and understood that both natural and anthropogenic-induced land cover changes have an effect on atmospheric and hydrological phenomena such as carbon concentrations, hydrological cycles and the surface-atmosphere interface energy balance, all of which influence local, regional and global climates (Ramankutty and Foley, 1999; Lepers *et al.*, 2005; Monteith and Unsworth, 2007; Houghton *et al.*, 2012; Gomez *et al.*,

2016).

Land cover has been variously defined as the observed biophysical cover on the earth's surface or the terrestrial biosphere cover, upon which humans depend in order to derive resources such as food, water and energy (Ramankutty and Foley, 1999; Bartholome and Belward, 2005; Di Gregario, 2005; Grekousis, Mountrakis and Kavouras, 2015; Gomez *et al.*, 2016). Numerous studies have been carried out to document and predict the nature and extent of changes in land cover as a result of human activities (Findell, Shevliakova and Stouffer, 2007; Kaplan *et al.*, 2011; Ellis *et al.*, 2013). In Lepers *et al.* (2005), an analysis via synthesis of information on land cover changes based on previous studies in the last twenty years of the twentieth century and the data generated thereof found that at regional scales, deforestation was the most significantly measured process but found gaps in spatially definitive data. Further, the study found that cropland increase was pervasive and associated with large-scale deforestation, most notably in Southeast Asia. In addition, most of the tropical studies used in the information synthesis were derived from remotely-sensed data due to unavailability of reliable statistical data. Therefore, at the close of the twentieth century, land-use and land cover change characterization and monitoring was largely based on remote sensing data and geographical information analysis techniques, with increased frequency of dissemination of datasets, made accessible to a wide range of users for diverse applications.

However, as noted by Anderson *et al.* (1976) and later by Comber, Fisher and Wadsworth (2005), the collection and dissemination of geographical information on land-use and land cover is carried out against a backdrop of the conceptualized representations of the real world with respect to the intended application and end-user needs, which are diverse and dynamic. Various re-

searchers and institutions have developed definitions of land cover and carried out associated classifications at varied spatial scales using multifarious methods (Anderson et al. 1976; Bartholome and Belward, 2005; Bontemps et al., 2011; Takahashi et al., 2013). The increasing ease of access to these datasets and eventual use by non-specialist users is having a negative effect due to a failure, on the part of the users, to understand or interact with information specifications and the contextual background of its generation (Comber, Fisher and Wadsworth, 2005). This section presents an overview of some of the various remote sensing-based classifications adopted for global, regional and national scale land-use/ land cover mapping, the classification methods used in their implementation and accuracy assessment of the subsequent products. The review is carried out in order to illuminate the various ways in which the real world is represented, and the relationship and underlying logic or motivation to the categories or classes in various products, thus laying a basis for the importance of the classification work carried out in this study.

The first global land cover mapping products exploiting remote sensing arose out of the need for datasets to support international efforts towards understanding and monitoring of environmental changes and the coordination of adaptation and mitigation strategies (Mora *et al.*, 2014). These datasets had low spatial resolution (e.g. 1°NDVI-derived land cover classification by DeFries and Townshend (1994)), but have since been improved to yield higher spatial resolution products (e.g. 300m ESA CCI global LC maps) through incorporation of the temporal dimension (Bontemps *et al.*, 2013; Mora *et al.*, 2014; Gomez *et al.*, 2016). In response to the Essential Climate Variables (ECV's) list established by the Global Climate Observing System (GCOS), the European Space Agency (ESA) initiated the Climate Change Initiative Land Cover project (CCI-LC) with a primary focus on land cover character-

ization (Bontemps *et al.*, 2013). Through a system needs assessment carried out in consultation with climate modelling users, CCL-LC found that the need for stable and dynamic information about land cover far outstripped all other user requirements for this particular user group. This necessitated a revision of the land cover concept (LC concept) which was dichotomized into 'LC *state*' and 'LC *condition*', the former of which was found to be adequately described within the United Nations Land Cover Classification System (UN-LCCS) (Bontemps *et al.*, 2013). LC *state* refers to the set of land cover features that do not change over time as a result of non-permanent or natural variability, while LC *condition* is related to the biogeophysical processes that drive temporary changes in land cover features, such as phenology, that do not alter its integral characteristics. In other words, any changes in the LC state, result in a permanent change in the definition of land cover by its observable and measurable attributes, while changes in the LC condition are temporary and do not alter the essential definition of the land cover.

The UN-LCCS is predicated on some assumptions as outlined by Di Gregorio *et al.* (2016) including:

1. Mapping is a local activity therefore there may be need to establish unique classification systems to fit local conditions;
2. At a certain scale, any feature can be heterogeneous and the variety of standards for representation and generalization of land characteristics can be as diverse as the heterogeneity of the land itself;
3. In geographic information, truth as a distinct, incontrovertible and correct fact, cannot exist since a classification of geographic phenomena is inherently subject to indeterminacy and relativism mostly reflected in

its ontology;

4. No classification system can fully capture or reflect the social and/or natural world accurately;
5. Classification or categorization is a highly dynamic process related to geographical areas, time and culture;
6. The process of classification is a “balancing act” that must strike a balance between the huge complexity of the “continuum” nature of the real world and the necessity to represent or utilize it in a database with a finite boundary;
7. There are and there will always be multiple ways to categorize (segment) real world phenomena, and all are equally legitimate;
8. In the process of classifying or categorizing the real world, both standardization and harmonization efforts are needed. The effectiveness of a classification process depends on the levels at which standardization and harmonization are used.

The LCCS was formalized as an international standard for LC classification systems in 2012 by the International Standards Organization (ISO) and is referred to as the Land Cover Meta Language (LCML) (Di Gregorio *et al.*, 2016). In the LCML ontology, land cover classes are linked to clearly defined diagnostic attributes rather than text descriptions, thus allowing for specification of land cover features anywhere in the world using a set of independent diagnostic criteria that allow for linkage with other existing classifications at global, regional and national scales (Di Gregorio *et al.*, 2016). There are two main LC hierarchies within the LCML framework; Biotic and Abiotic, from which

sub-classes can be derived but are still related to a measurable, observable attribute of the LC feature. The assumptions inherent in the UN-LCCS and the robust LCML ontology inform the land cover classification methodology employed by CCI-LC for the generation of 300m global LC state and condition maps centered to the years 2000, 2005, 2010 and 2015, and derived from MERIS and SPOT-VGT datasets (Bontemps *et al.*, 2013; Lamarche *et al.*, 2013). Figure 2.1 shows the ESA CCI-LC map v2.0.7 which has twenty two macro-classes excluding 'No data' as shown in Figure 2.2. Of the twenty two macro-classes, eighteen belong to the biotic macro-class as per the UN-LCCS and are sub-categorized on the basis of growth forms, leaf type and phenology, while four belong to the abiotic macro-class, with sub-categories derived on the basis of artificial or natural surface elements and water bodies. The use of multi-year Earth Observation (EO) datasets makes the classification less sensitive to the period of observation assuming that no LC state changes have occurred in the multi-year period, thus satisfying the climate modelling user group's requirement of stability and dynamicity in land cover information. Moreover, categorization based on the UN-LCCS ensures compatibility with plant functional types which are used in many models. The ESA CCI-LC maps are generated via machine learning and unsupervised classification processes whose input is the 7-day time series of MERIS FR and RR L1 and SPOT-VGT global composites. Prior to classification, a reference LC dataset from existing global, regional and local land cover maps is generated. The reference LC dataset acts as an *a-priori* stratification of the world into equal-reasoning areas upon which the classification algorithms are run and also enables change detection. Validation of this dataset is underway (Grekousis, Mountrakis and Kavouras, 2015).

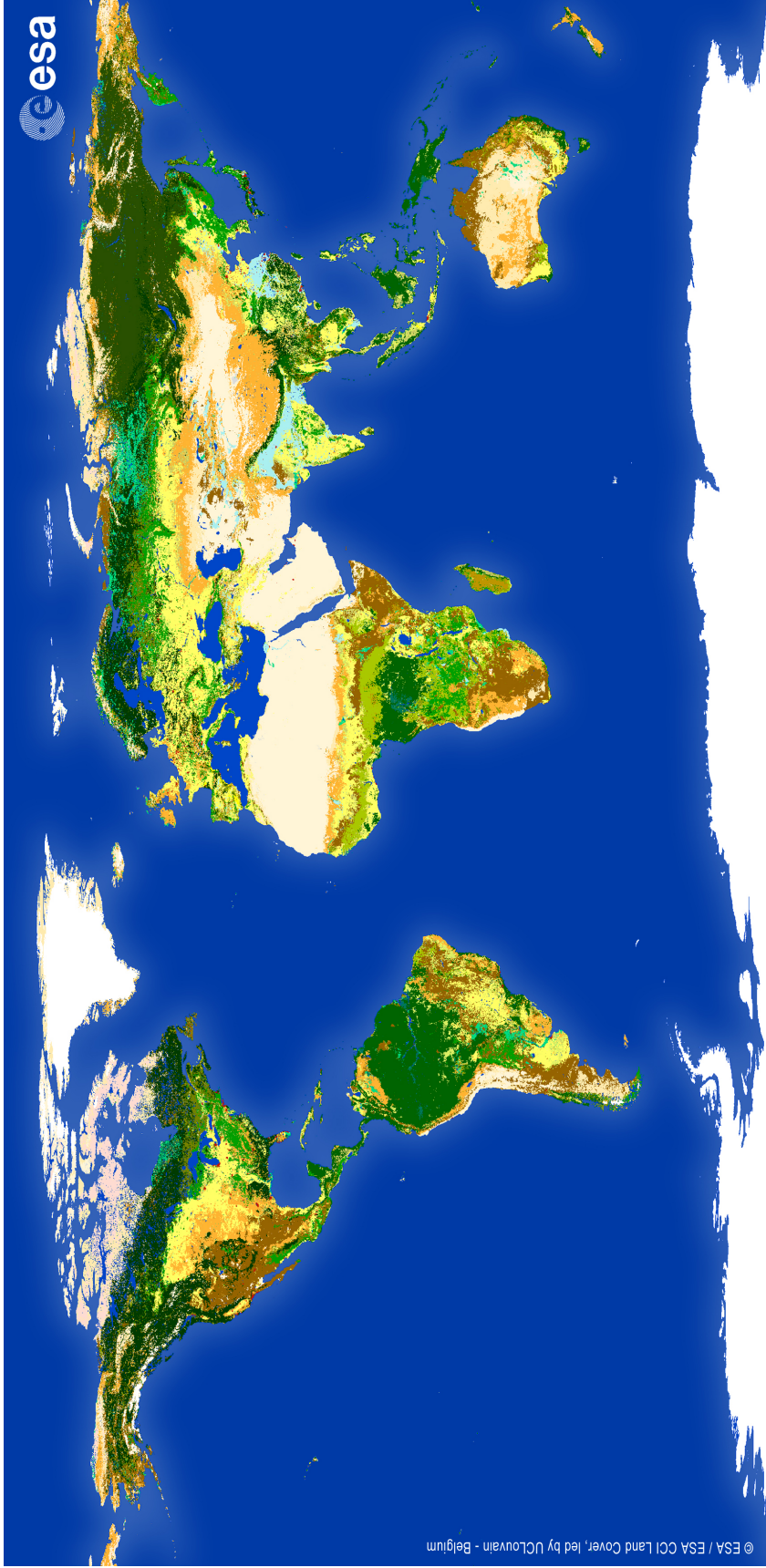
According to Lepers *et al.* (2005), the greatest concentration of rapid land-

cover changes observed in that study were in Asia and the study recommended that "operational monitoring of land cover should be extended to regions that are not known as hotspots but where rapid changes may still take place and catch the scientific community by surprise". Figure 2.3 shows the locational distribution of Regional LC maps according to Grekousis, Mountrakis and Kavouras (2015), which highlights the fact that Asia and Africa are not fully covered by regional maps solely developed for those regions but are covered by maps generated by national agencies such as the Japan Aerospace Exploration Agency (JAXA) which produces high resolution land cover maps for Japan and Vietnam (Takahashi *et al.*, 2013; JAXA, 2018).

Takahashi *et al.* (2013) describes the production process of the JAXA High Resolution LULC Map of Japan (JHR LULC Map) version 13.02 which was released in March 2013. The latest JAXA High Resolution LULC map is the HRLULC map version 18.03 which in addition to providing continuity for the earlier versions has been time-pegged as a LC map of Japan for 2015 with data inputs ranging from 2014 to 2016. The reported overall accuracy for version 16.09 was 78% while that for version 18.03 is 81.6%. Improvements made include the use of Landsat 8 (OLI) imagery, application of cloud masks, introduction of terrain correction and visual collection of training and validation data. The JAXA HRLULC map has ten classes excluding the 'Unclassified' or 'unknown' and 'No data' or 'nodata' as shown in Figure 2.4. An integration of bayesian estimation, likelihood estimation by kernel density (Hashimoto *et al.* 2014) and post-classification editing were used for version 18.03 (JAXA, 2018). The class definitions within the JAXA HRLULC mapping framework are consistent with the UN-LCCS. However, in the course of this review, no comparison of the consistency of these products with any global LC products was found. The research community would benefit from a qualitative and/or

quantitative comparison of the JAXA products to other global LC mapping products since they contribute to regional LC coverage of the southeast Asia region.





**Climate Change Initiative | Land Cover 2015 | 300 m**

© ESA / ESA CCI Land Cover, led by UCLouvain - Belgium

**Figure 2.1:** Preview of ESA CCI-LC Map v2.0.7 for year 2015

Value	Label	Color
0	No Data	
10	Cropland, rainfed	
11	Herbaceous cover	
12	Tree or shrub cover	
20	Cropland, irrigated or post-flooding	
30	Mosaic cropland (>50%) / natural vegetation (tree, shrub, herbaceous cover) (<50%)	
40	Mosaic natural vegetation (tree, shrub, herbaceous cover) (>50%) / cropland (<50%)	
50	Tree cover, broadleaved, evergreen, closed to open (>15%)	
60	Tree cover, broadleaved, deciduous, closed to open (>15%)	
61	Tree cover, broadleaved, deciduous, closed (>40%)	
62	Tree cover, broadleaved, deciduous, open (15-40%)	
70	Tree cover, needleleaved, evergreen, closed to open (>15%)	
71	Tree cover, needleleaved, evergreen, closed (>40%)	
72	Tree cover, needleleaved, evergreen, open (15-40%)	
80	Tree cover, needleleaved, deciduous, closed to open (>15%)	
81	Tree cover, needleleaved, deciduous, closed (>40%)	
82	Tree cover, needleleaved, deciduous, open (15-40%)	
90	Tree cover, mixed leaf type (broadleaved and needleleaved)	
100	Mosaic tree and shrub (>50%) / herbaceous cover (<50%)	
110	Mosaic herbaceous cover (>50%) / tree and shrub (<50%)	
120	Shrubland	
121	Evergreen shrubland	
122	Deciduous shrubland	
130	Grassland	
140	Lichens and mosses	
150	Sparse vegetation (tree, shrub, herbaceous cover) (<15%)	
151	Sparse tree (<15%)	
152	Sparse shrub (<15%)	
153	Sparse herbaceous cover (<15%)	
160	Tree cover, flooded, fresh or brakish water	
170	Tree cover, flooded, saline water	
180	Shrub or herbaceous cover, flooded, fresh/saline/brakish water	
190	Urban areas	
200	Bare areas	
201	Consolidated bare areas	
202	Unconsolidated bare areas	
210	Water bodies	
220	Permanent snow and ice	

Figure 2.2: Legend of the global CCI-LC Maps

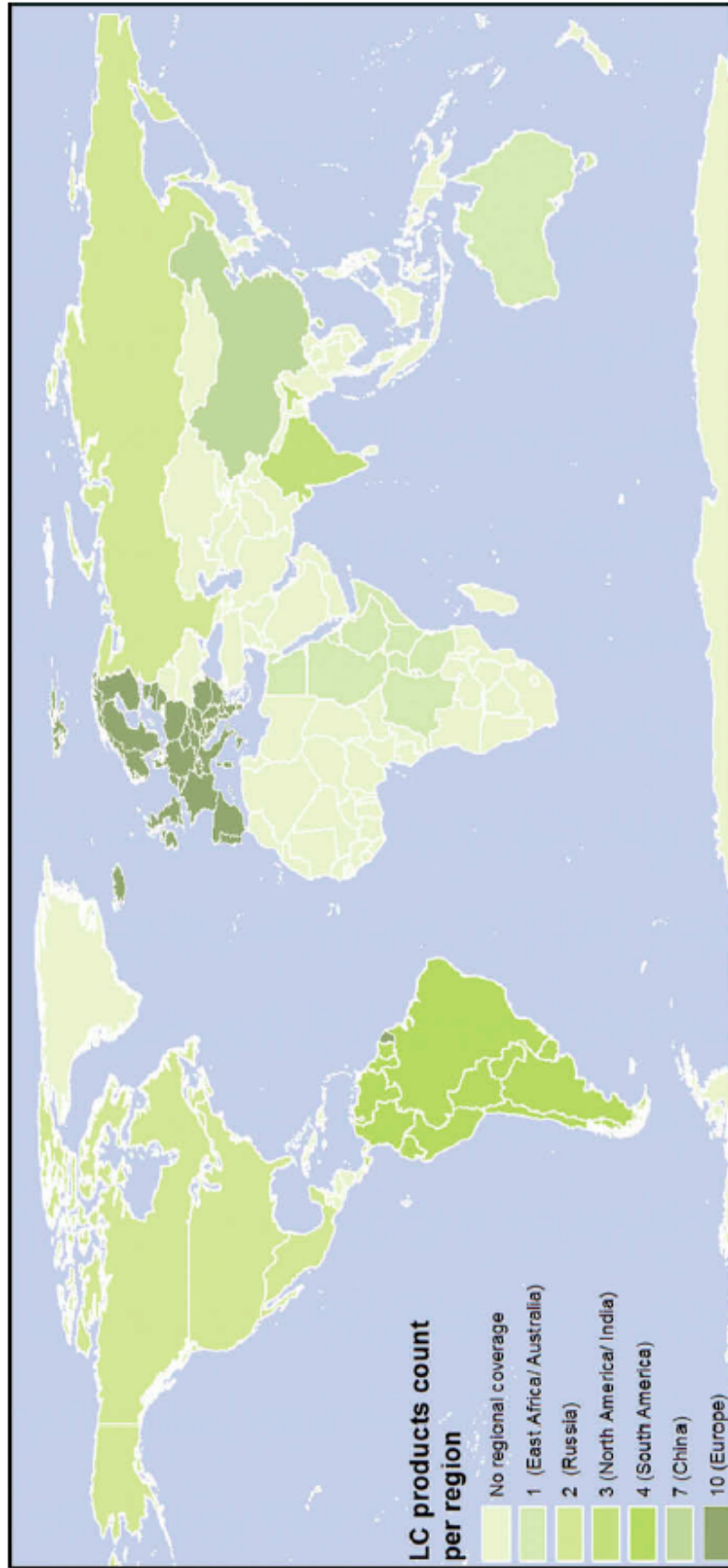


**Figure 2.3:** Count of Regional LC maps by location. *Source: Grekousis, Mountrakis and Kavouras (2015)*



色	コード	カテゴリ
	1	水域 (water)
	2	都市 (urban)
	3	水田 (rice paddy)
	4	畑地 (crop)
	5	草地 (grass)
	6	落葉広葉樹 (DBF)
	7	落葉針葉樹 (DNF)
	8	常緑広葉樹 (EBF)
	9	常緑針葉樹 (ENF)
	10	裸地 (bareland)

Figure 2.4: LULC categories in JAXA HRLULC maps

## 2.2 Cropland Mapping

Population growth leading to an increase in labour and land productivity led to the advent of the agricultural revolution and with it the modification of vast amounts of the natural landscape for the growth of food crops and animal husbandry. The need to manage land resources in order to enhance efficiency of production and a greater awareness of the impacts of anthropogenic land use has led to ever increasing efforts to not only know where production is taking place via mapping, but to quantify, monitor and predict production efforts (Pongratz *et al.*, 2008). In addition, food security challenges at global, regional and spatial scales, necessitate the generation of information relating to agricultural production at varying spatial and temporal scales. In See *et al.*, (2015), approaches to cropland information generation are broadly classified on the basis of spatial scale and the type of data used in terms of its acquisition, processing, temporal and spatial consistency and relative cost of acquisition and maintenance.

Climate variability and its associated impacts on food production has created an urgent need for timely and cost effective agricultural production information especially for croplands due to the fact that croplands are space intensive and have been found to have a direct impact on climate. As such, cropland mapping approaches that are scalable and hence easily generated operationally are of great importance (Inglada *et al.*, 2015; Torbick *et al.*, 2018). In the application of remote sensing to cropland mapping and monitoring, the underlying principles of image classification and the data needs or final application dictate the methods used to generate the maps. Table 2.1 summarizes by application, various studies as presented in Atzberger (2013) that have been employed

in remote sensing for cropland mapping and monitoring and their drawbacks or limitations.

Pixel-based and object-based image analysis approaches have been implemented in various studies for classifying broad land cover classes over agricultural landscapes using a variety of classification algorithms including decision tree (DT), random forest (RF), and the support vector machine (SVM) algorithms and machine learning classifiers. While pixel-based analysis have long been the mainstay for classifying remotely sensed imagery due to their relative ease of implementation, object-based image analysis have become increasingly popular (Blaschke, 2010). Whether pixels or objects are used as underlying units for the purposes of classifying remotely derived imagery, the information contained within and among these units can be subjected to a variety of classification algorithms. Previous comparative studies have been conducted that examine the relative performance of different classification algorithms using pixel-based, and/or object-based image analysis, and conclude that the choice of classification methods for cropland mapping is contingent on availability of data and the intended application (Teluguntla *et al.*, 2015; Matton *et al.*, 2015; Waldner *et al.*, 2016).

**Table 2.1:** Summary of studies on cropland mapping and monitoring methods by application

Application	Method	Drawback	Study
Biomass and yield estimation	Regression; Yield correlation masking; Crop growth models	Cropland Mask is necessary	Rembold, F., Atzberger, C., Savin, I., & Rojas, O. (2013)
Vegetation vigor and drought stress monitoring	Drought indices e.g. PDI, TDI & VDI	Reliance on one parameter; Need for near-real-time data	Balint, Z., Mutua, F., Mudiiri, P., & Onuto, C. T. (2013)
Crop phenology assessment	Time series modelling e.g. curve fitting using pre-defined functions	Need for a priori information to inform the model	Beck, P. S., Atzberger, C., Høgda, K. A., Johansen, B., & Skidmore, A. K. (2006)
Crop acreage estimation and Cropland Mapping	Time series analysis (graphical and statistical)	Evaluation only for regional scale	Wardlow, B. D., Egbert, S. L., & Kastens, J. H. (2007)
Mapping of Disturbances and LUCC	Pre- and Post-classification change detection		Singh, A. (1989)

## 2.3 Urban and Peri-urban Agriculture (UPA)

Over half of the world's population (55 per cent) reside in urban areas with a projected increase to 68 percent by 2050 (UN, 2018). As the population increases, demand for food and settlement areas is set to rise in tandem. The fringe areas or zones abounding, rapidly growing urban areas have long been recognized to have a transformational influence on the societies and economies of rural areas they abut and in turn respond to changes in the urban areas (Zasada, 2012). Traditionally, peri-urban areas are considered to be zones of spatial transition from 'urban' to 'rural', while simultaneously in temporal transition to 'urban' land use (Iaqinta and Drescher, 2000; Castles, 2014). The dynamic nature of peri-urban areas necessitates proper definition of fundamental terminology associated with these regions in order to understand the social, environmental and economic changes they drive and respond to (Iaqinta and Drescher, 2003).

The term 'peri' is a prefix meaning 'about' or 'around' and therefore has geographical implications (Castles, 2014). While there is no universally agreed upon definition of the compound term peri-urban, these areas are commonly understood to be the transitional zones between distinctly urban and unambiguously rural areas (Simon, 2008). The role and importance of these areas with respect to planning and policy development in both rural and urban areas has been brought into sharp relief through various studies (Iaqinta and Drescher, 2000; Allen, 2003; Thornton, 2008; Zasada, 2011; McGregor and Simon, 2012; Schneider, 2012). Iaqinta and Drescher (2003) highlight the difficulty in distilling a singular definition concluding that existing definitions are based on operational variables that are subject to the research discipline. In



this section, multi-disciplinary definitions are presented with a view of particularizing the selection of regions considered in this study. Further, the definition and characterization of peri-urban agriculture is presented in the context of various studies.

There exist various modalities for definition of the term peri-urban as identified by Iaquina and Drescher (2003) including but not limited to: implicit definition where an area is defined as peri-urban if it is neither rural nor urban and is located in the fringes of an urban area; conceptual theoretical definition where a peri-urban area is defined based on its demographic and geographical characteristics with respect to an urban area; land-use definition where an area is deemed to be peri-urban based on the factors that influence it derived from land-use relations, and definition via characterization of the physical configuration, economic activities and social relationships. The aforementioned methods of definition are surmised primarily from sociology studies and draw on three components used to define 'urban', that is, the demographic (high population density), economic (primarily non-agricultural economic activities) and social-psychological (urban consciousness) components. The study concludes that a peri-urban area is a variation of these components. In the realm of Remote Sensing and Geospatial Information Science, the definitions of peri-urban largely focus on institutional physical definition (zoning) or lack thereof, demographic, land-use and economic characteristics of a region (Mbiba and Huchzermeyer, 2002; Thapa and Murayama, 2008; Thornton, 2008).

Variations in global, regional and local socio-cultural-economic characteristics, flows and interactions, and their relationship with urban and rural development rend the task of eliciting a universal definition of peri-urban arduous. In developing countries, particularly in Africa, distinction between peri-urban

and rural areas on the basis of demographics and land-use is exacerbated by a rapidly increasing rural population density, growing infrastructure and cultural and colonial influences on land-use and land tenure systems (Smith and Memon, 1994; Atukunda and Maxwell, 1996; Foeken and Mboganie-Mwangi, 2000, Thapa and Murayama, 2008). The complexities associated with characterization of peri-urban areas extend to the distinction between urban and peri-urban agriculture (Mougeot, 2000; Thornton, 2008; Schneider, 2012). However, the importance of urban and peri-urban agriculture and their role in food security and sustainable livelihoods is widely recognized and has been the subject of numerous studies in the last three decades (Appeaning Addo, 2010; Lwasa *et al.*, 2014; Thebo, Drechsel and Lambin, 2014; Opitz *et al.*, 2016). Key to distinguishing urban agriculture from peri-urban agriculture are the dimensions of urban agriculture outlined by Mougeot (2000) as: types of economic activities, types of products, characteristics of production locations, destination of products and production scale. Preeminently contentious among these facets is location since it broaches the issue of the dichotomous typification of rural and urban areas in which it is assumed that agriculture is the primary economic activity of rural populations and thus fails to acknowledge urban agriculture (Tacoli, 1998; Mougeot, 2000). However, the locational aspect is critical to defining peri-urban agriculture since the benefits and challenges accrued from proximity to urban areas while maintaining non-urban characteristics provide a means of spatial delineation. Farming in peri-urban areas is carried out on small non-contiguous units which result in a heterogeneous landscape as land-use competes with non-agricultural uses as a result of urban pressures (Zasada, 2011; Schneider, 2012).

## 2.4 Spatio-temporal Image Fusion

Image fusion refers to the combination of two or more images from different sensors or sources using an appropriate algorithm, in order to obtain a new image from which, more precise information regarding the scene, than that available from a singular image source independently, can be derived (Pohl and Van Genderen, 1998; Solberg, 2006; Hazaymeh and Hassan, 2015; Schmitt and Zhu, 2016). Earth observation using satellite-based sensors has been around since the 1970s and has evolved over time to include multiple sensors capturing data about the earth's surface at ever increasing spatial detail, acquired for the same location at a higher temporal frequency, over an increasingly discretized electromagnetic spectrum, that is, high spatial, temporal and spectral resolution. The increasing coverage of the earth in space, time and spectrum has enabled expansion of earth observation data analysis techniques, formerly confined to single source or sensor images, to allow for multi-source, multi-scale, multi-polarization, multi-frequency and multi-temporal image analysis (Solberg, 2006).

In addition to technological advancements, limitations in currently available data *vis-a-vis* application requirements have spurred the growth in image fusion techniques for application specific exploitation of the most advantageous attributes of this data. Applications like cropland mapping, drought monitoring and irrigation and grassland management, which involve monitoring of dynamics require high temporal resolution data (Hazaymeh and Hassan, 2015; Liao *et al.*, 2017). From national to global scales, low spatial-high temporal resolution data sets such as NOAA-AVHRR, SPOT-VGT and MODIS have been used to map and monitor vegetation cover and changes through programmes

such as the International Geosphere-Biosphere Program’s Global Land Cover Characterization (IGBP-GLCC), which used 1-km AVHRR 10-day NDVI composites for 1992 to 1993 (<https://lta.cr.usgs.gov/GLCC>; Xie, Sha and Yu, 2008). An example of large scale vegetation monitoring with regional coverage is Copernicus’s pan-European High Resolution Layers data set which provides information on specific land cover characteristics such as forests, grassland and imperviousness for 39 countries and is complementary to the CORINE land use/ cover datasets which are produced using medium resolution and high resolution images including Landsat, SPOT-5, IRS and RapidEye (<https://land.copernicus.eu/pan-european>). However, some land use/cover features cannot be adequately captured using the datasets and methods heretofore mentioned. For instance, Lefebvre (2014) underscores the importance of Green Linear Features (GLF) including:

1. Soil and water conservation through filtration of pesticides and other pollutants from water by grass filter strips before it reaches surface water features
2. Aiding climate protection through carbon storage and sequestration and promoting climate adaptation through mitigation of landslides and floods
3. Promoting biodiversity by facilitating movement of some species between disparate habitat patches
4. Preservation of cultural identity since they compose and structure rural landscapes

The accurate mapping and monitoring of GLFs such as those found along the banks of many hydrological features and roads, as well as hedges that aid in demarcation of land is therefore relevant and the report concludes that

satellite images or aerial images with high or very high spatial resolution and manual delineation methods provide the best results, (Lefebvre, 2014). However, typically, sensors with very high or high spatial resolution have a small spatial footprint thus limiting their application for non-local scale monitoring purposes due to prohibitive acquisition costs and limited coverage. Manual delineation is also time consuming and the inevitable recourse tends towards automatic methods that are pixel or object-based, (Lefebvre, 2014).

Prior to any vegetation extraction processes, image preprocessing is imperative in order to remove the effects of noise and enhance interpretability of image data, especially so for time series and mosaicked imagery, since it is essential that the images are spatially and spectrally consistent and compatible (McCoy, 2005; Solberg, 2006; Xie, Sha and Yu, 2008; Han, Pei and Kamber, 2011; Young *et al.*, 2017). Preprocessing is comprised of a series of tasks, the extent of which is influenced by among other factors, type of data (i.e. optical or non-optical), the preprocessing level of data at the point of acquisition which is contingent on the disseminating agency, spatial extent of the area of interest and the intended application. For optical data, one of the main sources of noise and a major drawback to its application in fields requiring regular data is atmospheric artefacts such as cloud cover. For vegetation mapping and monitoring, a pertinent preprocessing step for optical datasets is handling of cloud inundated images through removal or reconstruction (Xie, Sha and Yu, 2008; Julien and Sobrino, 2010; Ramoino *et al.*, 2017 ).

Microwave remote sensing, also referred to as Long-wave, such as Synthetic Aperture Radar (SAR), are relatively insusceptible to atmospheric noise due to their penetrative capabilities, are available day and night as well as under any meteorological event and have high resolution capabilities (Lillesand, Keifer

and Chipman, 2014; Alparone *et al.*, 2015; Du *et al.*, 2015). For these and other reasons including, direct relation of recorded data to the physical properties of natural features such as surface roughness and dielectric properties, subsurface penetration, sensitivity to man-made objects and high temporal resolution, microwave remote sensing has been used in a wide range of remote sensing applications including environmental disaster detection and management, deformation monitoring, crop-type mapping and preeminently in urban mapping with capabilities of extension from two-dimensional analysis to three dimensions using LiDAR and interferometric SAR (Donnay, Barnsley and Longley, 2014; Du *et al.*, 2015; Kenduiywo, Bargie and Soergel, 2015; Notti *et al.*, 2015; Abdikan, *et al.*, 2016).

Nevertheless, there are some impediments to the widespread operational application of active remote sensing data. Due to the significant differences in imaging geometry between optical and microwave systems, optical data is richer in detail at similar resolutions and is more amenable to human interpretation in comparison to SAR data (Zhu *et al.*, 2012; Schmitt, Tupin and Zhu, 2017; Haack and Mahabir, 2018). While microwave systems have been around for a long time and the theoretical principles related to their utilization in urban and natural environments are fairly well established, there has been a dearth of agency in comparison to optical data, attributed to an overall lack of understanding of the data structures and feasible exploitation of the same, insufficient or convoluted methods of processing and analysis, and differential performance in characterizing certain land cover types especially in heterogeneous landscapes (Kerr and Ostrovsky, 2003; Rogan and Chen, 2004; (Zhu *et al.*, 2012; Van Tricht *et al.*, 2018). In a comparative assessment of the relative importance of the spectral, polarimetric, temporal and spatial dimensions of remote sensing data for urban and peri-urban land cover classification, Zhu

*et al.* (2012) observed that when using PALSAR data by itself, the classification accuracy was outmatched by the use of a single Landsat image, even with the addition of the spatial dimension of PALSAR data. In another study evaluating synergistic application of radar Sentinel-1 and Optical Sentinel-2 imagery for crop mapping within a season, Van Tricht *et al.* (2018) found that overall classification accuracy of optical-only data performed better than SAR- only data but was improved by increasing the number of images made available to the classifier. In both studies, combined use of SAR and optical data significantly improved classification results (Zhu *et al.*, 2012; Van Tricht *et al.*, 2018).

Both optical and microwave imaging and non-imaging systems have demonstrable value in acquisition of data and information on the earth's surface and even to some extent, sub-surface features, in order to address various problems. However, limitations inherent in the nature of available data and the common processing and analysis mechanisms, versus specific application demands and non-uniform distribution of land use/cover features (i.e. landscape heterogeneity), have led to the need for image fusion and development of fusion methods amid a deluge of optical and microwave remote sensing data that is held in archives and is currently being acquired (Schmitt and Zhu, 2016; Schmitt, Tupin and Zhu, 2017). An initial categorization of multi-sensor data fusion is on the basis of the representational elements fused. Fusion can be implemented at the signal level where signals from different sensors are blended in order to obtain a signal with improved signal-to-noise ratio compared to the original independent signals (Solberg, 2006). From a remote sensing perspective, the lowest element refinement level is at the pixel level, which requires multi-source data that are aligned (co-registered) and involves attribute estimation by combining information on a pixel-by-pixel basis and resulting in a new enhanced

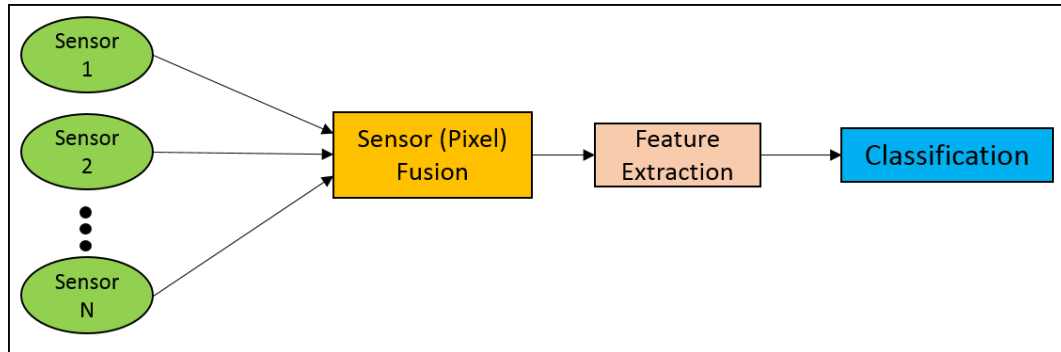
image (Pohl and Van Genderen, 1998; Solberg, 2006; Schmitt and Zhu, 2016). The other level is the feature-based fusion methods which operate at a higher level of processing compared to the pixel-based fusion methods and require extraction of features via segmentation from the multi-source data prior to fusion (Pohl and Van Genderen, 1998; Solberg, 2006; Ghassemian, 2016). Decision level fusion methods, also referred to as interpretation level or symbol-level, are the highest level of fusion and involve merging information from various sources, post preliminary classification (Pohl and Van Genderen, 1998; Solberg, 2006; Ghassemian, 2016). In all levels of fusion, matching and coregistration of data is essential and while it has been investigated rigorously, it remains a significant challenge especially for heterogeneous sensor data fusion (Schmitt and Zhu, 2016). Moreover, among the three levels of fusion, the best fusion level and methodology depends on the application and is influenced by among other factors, availability of data, complexity of the classification problem and the primary objective of the analysis (Solberg, 2006). Figure 2.5 depicts the three fusion levels as categorized by representation features fused. The remainder of this review will focus on pixel-level fusion methods.

Pixel-based fusion methods may be categorized on the basis of the type of data fused and the dimension enhanced by the fusion process, that is, spatial or temporal, as shown in Table 2.2 as proposed in Pohl and Van Genderen (1998). An alternative approach to grouping of pixel-level fusion based on the techniques exploited towards achieving either spatial or temporal enhancement was detailed in Pohl and Van Genderen (1998), dividing them into colour-related and statistical/numerical methods, with further subgroupings as shown in 2.6, (Pohl and Van Genderen, 1998; Pohl and Van Genderen, 2015). The colour-based techniques include RGB, which is a simple overlay of multi-source data in the *Red-Green-Blue* colour space and colour transformations including

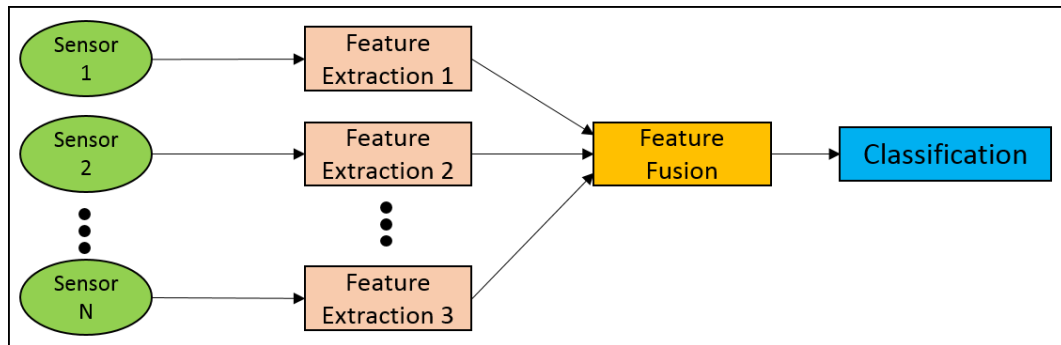


*Intensity-Hue-Saturation* (IHS) in which, spatial ( $I$ ) and spectral ( $H, S$ ) information from a standard RGB image is separated and YIQ, which is a colour encoding system that combines RGB signals in proportion to the sensitivity of the human eye thus enhancing visual interpretation (Pohl and Van Genderen, 1998; Pohl and Van Genderen, 2015; Ghassemian, 2016). The arithmetic methods within the approach shown in Figure 2.6 include Brovey Transform (BT), high-pass filtering (HPF), Component Substitution (CS), Principal Component Analysis (PCA), Regression Variable Substitution (RVS) and Wavelet Transform (WT). Following an earlier taxonomy proposed by Schowengerdt (2006), in which fusion methods were divided into spectral, spatial and space scale techniques, and its subsequent adoption by various other scientists, Pohl and Van Genderen (2015) proposed a general categorization, summarised in Table 2.3, with five groups including:

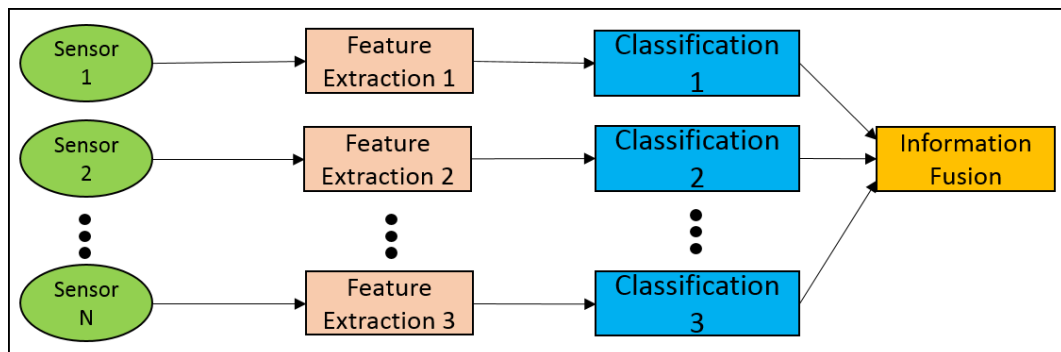
1. Component Substitution
2. Numerical and statistical image fusion
3. Modulation-based techniques
4. Multi-resolution approaches (MRA)
5. Hybrid techniques



(a) Pixel-level fusion



(b) Feature-level fusion



(c) Decision-level fusion

**Figure 2.5:** Fusion methods categorized by representational elements fused from multi-source data. (Adapted from Ghassemian, 2016)

**Table 2.2:** Categorization of fusion methods based on type of data sets fused and dimension enhanced by fusion. (*Adapted from Pohl and Van Genderen, 1998*)

<b>Data Set Type</b>	<b>Dimension</b>	<b>Sample Application Reference</b>
Single sensor	Temporal	Kussul <i>et al.</i> (2017)
Multi sensor	Temporal	Shimoni <i>et al.</i> (2015)
Single sensor	Spatial	Vivone <i>et al.</i> (2017)
Multi sensor	Spatial	Yokoya (2017)
Multi sensor	Spatio-temporal	Zhao <i>et al.</i> (2017)

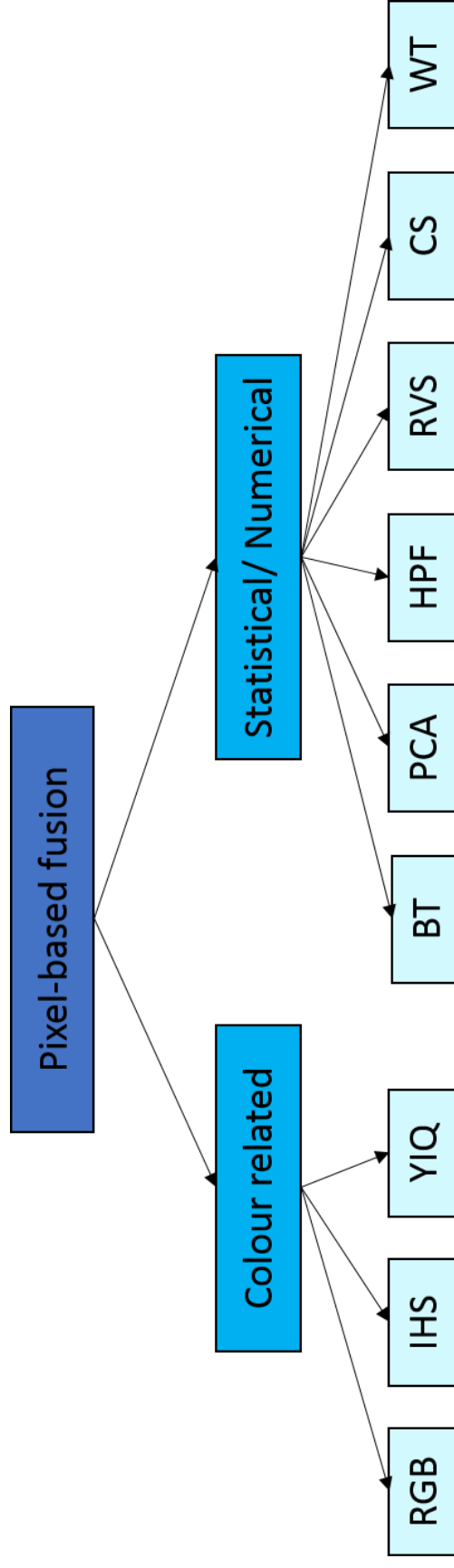


Figure 2.6: Pixel-level fusion. (After Pohl and Van Genderen, 1998)

**Table 2.3:** Proposed categorization of pixel-based image fusion algorithms.  
(Adapted from Pohl and Van Genderen, 2015)

	CS	Num/Stat	Modulation	MRA	Hybrid
BT		x			
IHS	x				
YIQ	x				
PCA		x			
WT				x	
LP				x	
IHS/BT					x
Modulation/SFIM			x		

# Chapter 3

## Methodology

### 3.1 Study area

The study area is made up of seven municipalities within Chiba prefecture which is located in the Southeastern part of Japan and is adjacent to the Tokyo Metropolis to the east. The seven municipalities are Yotsukaido-shi, Inzai-shi, Yachimata-shi, Narita-shi, Sakura-shi, Tomisato-shi and Shisui-machi, with a total area and population of 623.15 km<sup>2</sup> and 668,603 respectively as shown in Figure 3.1. Chiba prefecture has an annual average temperature of 16.3°C, with annual monthly average maximum and minimum temperatures of 30.8°C and 2°C respectively. The annual average precipitation is 1496mm and approximately 2113 hours of sunlight are received yearly, making it highly favorable for agricultural production. Chiba prefecture is a valuable source of agricultural food crops and was ranked sixth in vegetable production in Japan with vegetable production worth more than half a billion yen in 2015 according to the Ministry of Agriculture, Forestry and Fisheries 2016 report on food, agriculture and rural areas in Japan. The main crops in the regions selected are

---

rice, which is cultivated on irrigated paddy fields and vegetables including but not limited to carrots, daikon radish, taro, cabbages and spinach. It has a highly heterogeneous landscape comprised of urban or built-up areas, Forests (Evergreen and Deciduous), grasslands (land covered with grass or shrubs), paddy fields, croplands (also described as upland cropland) and water bodies. There are two types of grasslands, natural as in the case of land covered by grass and shrubs not managed by man, as well as abandoned cropland or paddy fields and artificial or man-made grasslands such as golf courses.

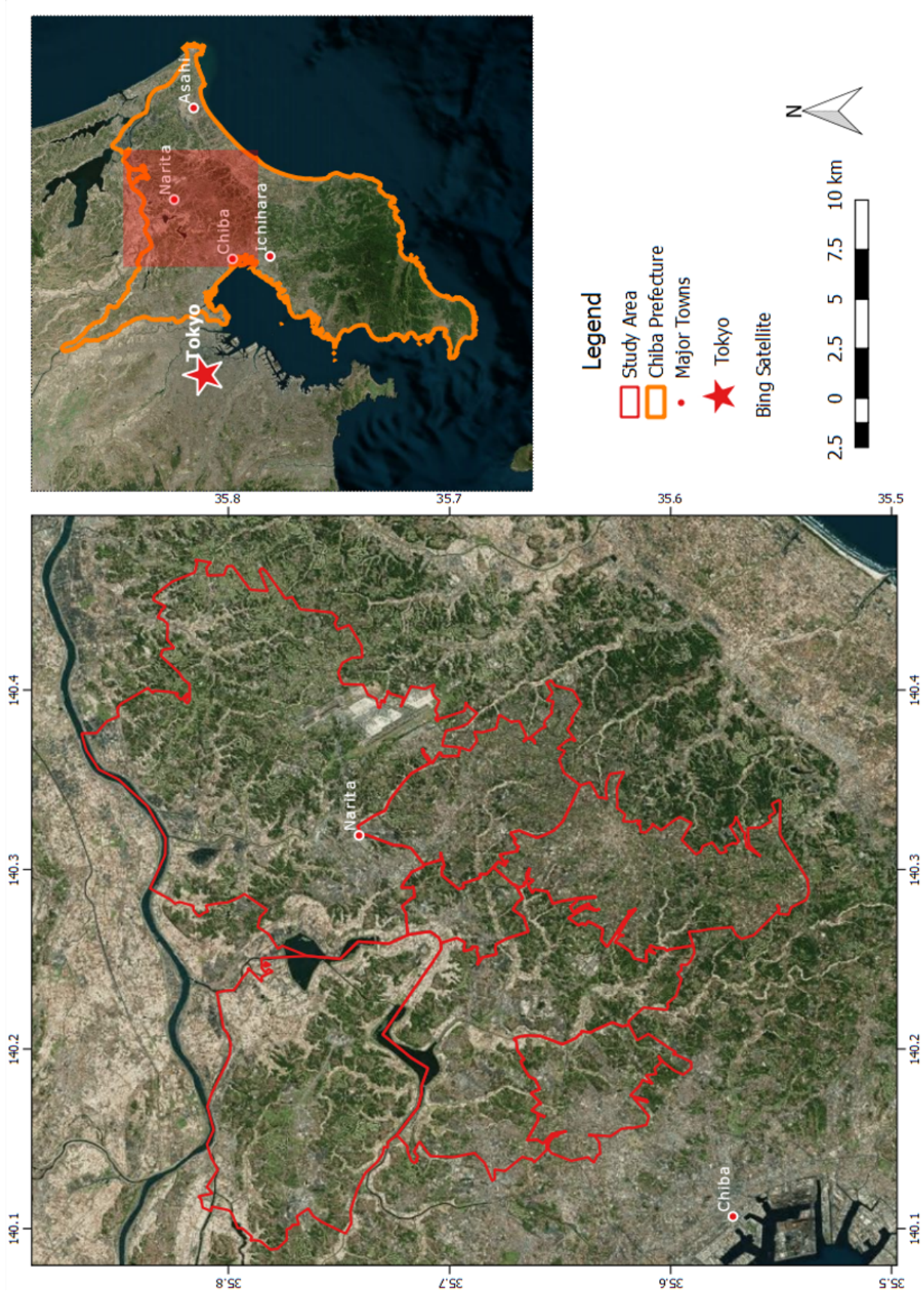


**Figure 3.1:** The seven municipalities constituting the study area in this research.



## 3.2 Data and Methods

### 3.2.1 Application requirements evaluation

In this section, the data and technological factors considered in designing and settling on the final research design are discussed with respect to this study's objectives. The overarching goal of this study was to describe the distinctive nature of upland croplands used for cultivation of horticultural food crops at pixel-level, by identifying and distinguishing them from other land use/ land cover, within a complex urban/peri-urban landscape and with data acquired within one year. In Oliphant *et al.* (2017), the Global Food Security-Support Analysis Data at 30m (GFSAD30) project identifies some limitations of current cropland extent map products as:

1. Absence of precise spatial location of cultivated areas
2. Coarse resolution nature of map products with significant uncertainties in areas, locations and detail
3. Absence of crop types and cropping intensities
4. Absence of a dedicated dissemination portal for cropland information products

Key to addressing the aforementioned limitations is the development of techniques for mapping croplands routinely, rapidly, consistently and with sufficient accuracy (Teluguntla *et al.*, 2015). Croplands are spatio-temporally dynamic in nature and their changes are subject to inter-related factors including climatic factors (e.g. precipitation and temperature), bio-geophysical factors (e.g.

soil type and topography) and human factors (e.g. management practices and choice of crop type to cultivate). As such, the data requirements for mapping of croplands demand spatio-temporal continuity and detail in order to estimate distinguishing characteristics such as biophysical changes, thus necessitating high spatial and temporal resolution data. For all imaging systems, there exists a primary trade-off between spatial and temporal resolution, with systems having one of each at a time but not both at the same time. The Sentinel 2 constellation of satellites aims to bridge this gap by acquiring images at a high spatial resolution (10 — 20m) and high temporal frequency (5 — 10 days). However, presence of cloud cover and other atmospheric artefacts imposes the trade-off by having spatial discontinuity where they occur despite regular imaging frequency. In order to address the issue of discontinuity, spatio-temporal image fusion methods have been developed.

An assessment of agricultural statistical survey data for the year 2015 for the seven municipalities under consideration and Chiba prefecture as a whole, laid out some initial criteria for our data needs. Figure 3.2 shows the proportions of area according to size of cultivated area managed by farmers surveyed during the Agriculture and Forestry census of 2015. Majority of the farmers surveyed (23 %) had parcels of land ranging from 2 to 3 ha, while 22 % had parcels of between 3 to 5 ha. Bearing in mind the need for continuous data, MODIS daily surface reflectance data at 250m spatial resolution provide continuity at a high frequency. However, the area of one pixel (62,500 m<sup>2</sup>) is much larger than the area of the highest proportion of parcels of land under cultivation (20000 m<sup>2</sup> — 50000 m<sup>2</sup>). On the other hand, Landsat moderate resolution images at 30m spatial resolution, provide adequate spatial detail for characterization of croplands at parcel level (approx. 20 — 30 Landsat pixels) but are spatially and temporally intermittent due to cloud cover. Similarly, Sentinel 2 images

---

provide much greater detail but are limited by cloud cover and the fact that for the study area, the tile coverage is not always the same as seen in Figure 3.3. Further, the latest agricultural statistical data available was released in 2015 and it was desired in this study, to see how remote sensing based estimation of cropland extents compares to statistical data. As such, Sentinel 2 data was inadequate for a time series in that year since the earliest available image for the study area is in August (7<sup>th</sup> August, 2015) and only two images meet the cloud cover threshold of less than 10%. It was therefore decided that the fusion of MODIS and Landsat products was the best approach.

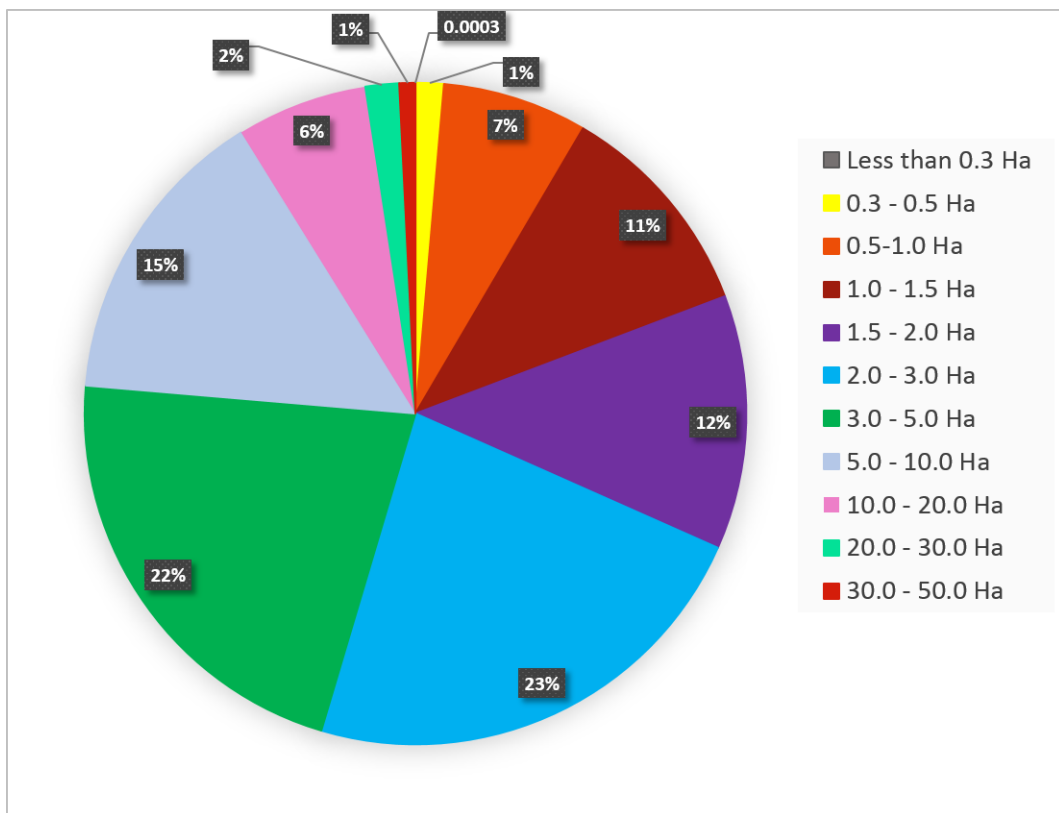
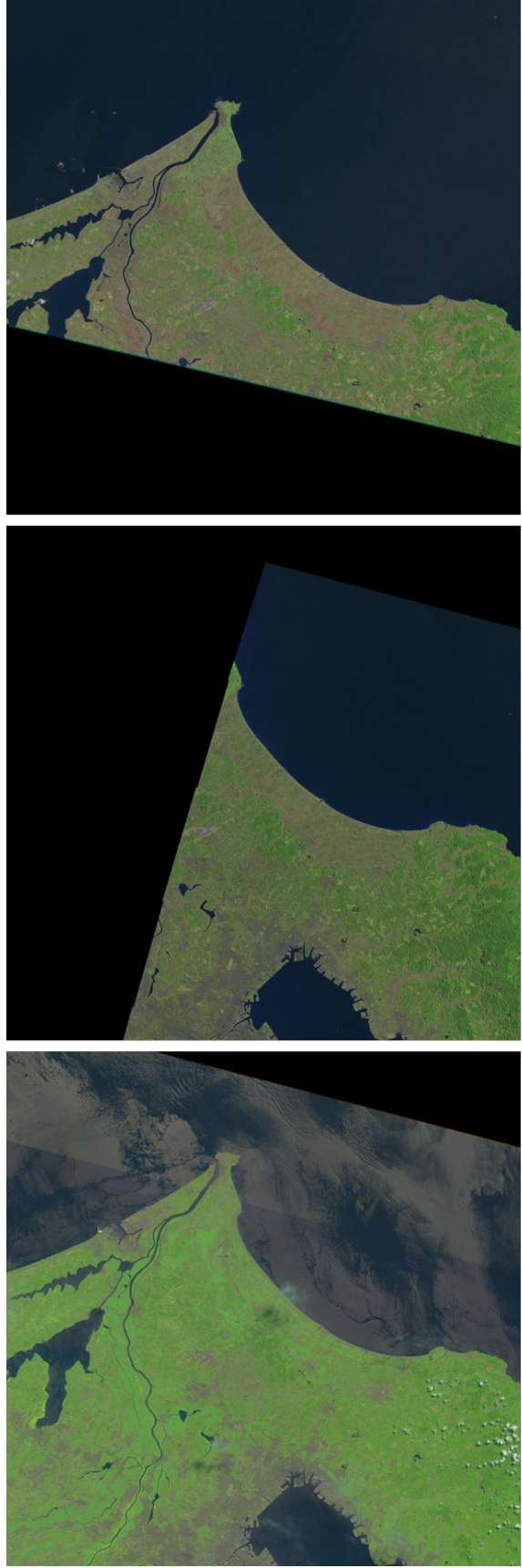


Figure 3.2: Proportional distribution of cultivated area size per farmer



2016-02-10

2015-12-05

2015-08-07

**Figure 3.3:** Sentinel 2A coverage (T54SVE) of the study area on various dates

## 3.2.2 Data acquisition and processing

### 3.2.2.1 MODIS Data

Two sets of MODIS surface reflectance datasets were acquired; MOD09GA and MOD09GQ. The MOD09GQ data set was used for extraction of the red (620-670 nm) and Near-infrared (841-876 nm) bands necessary for computation of NDVI. The MOD09GA dataset was necessary for quality assessment and generation of masks necessary for reconstruction of cloud-free daily NDVI images. The reflectance band quality scientific data set (SDS) in the MOD09GQ contains band quality assessment information including a bit parameter for cloud state. However, this parameter has not been populated since Version 3 of the MOD09GQ product and therefore can only be retrieved from the MOD09GA 1 km state SDS. Pre-processing of the MODIS data therefore involved extraction of the red and NIR surface reflectance bands and the 1 km state SDS band from MOD09GQ and MOD09GA HDF files respectively. The extracted bands were then reprojected to UTM Zone 54N, subset to cover the whole of Chiba prefecture, and in the case of the state 1 km SDS, after bit conversion and generation of QC masks, resampling to the nominal resolution of the MOD09GQ data set of 250m. After scaling the surface reflectance bands, NDVI was computed and the masks applied, resulting in daily NDVI images at 250m which had gaps due to masking of clouds and bad quality pixels. The entire process was carried out using custom written scripts using R (Version 3.4.4) in RStudio (Version 1.1.456) and is depicted in Figure 3.4.

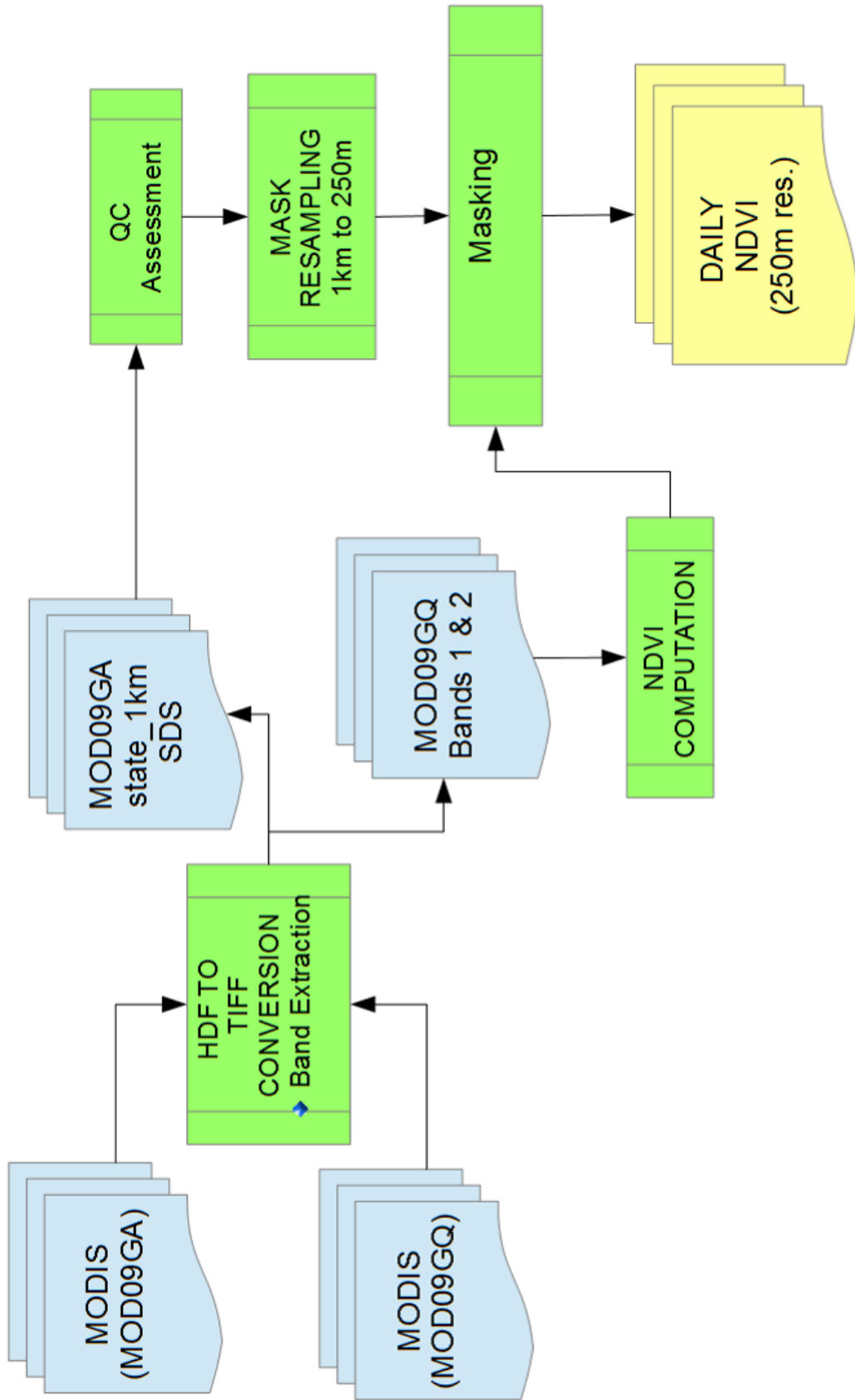
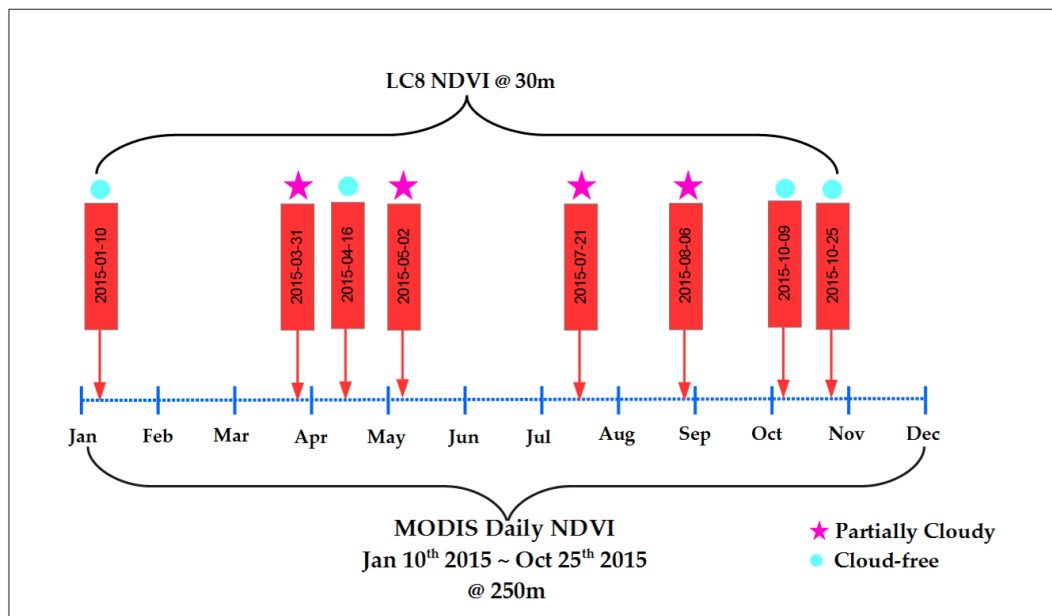


Figure 3.4: MOD09GA and MOD09GQ pre-processing workflow

### 3.2.2.2 Landsat Data

Landsat 8 Operational Land Imager (OLI) surface reflectance Level-2 images for the year 2015 were acquired for WRS path/row 107/035, which covers the study area. An initial threshold of less than 10 % cloud cover yielded four images within the year, with one image for winter (January 10th, 2015), one in spring (April 16th, 2015) and two in the fall (9th and 25th October, 2015). Adequate seasonal distribution was desired and therefore the threshold was decreased to 20 % cloud cover over land and 30 % in an entire scene. The revised threshold yielded 8 images with sufficient seasonal distribution. NDVI was then computed using the red (636-673 nm) and NIR (851-879 nm) bands. Figure 3.5 depicts the relative temporal distribution of the Landsat and MODIS images. In addition, the Maximum Value Composite NDVI (MVC-NDVI) between consecutive dates of the eight images acquired was computed.

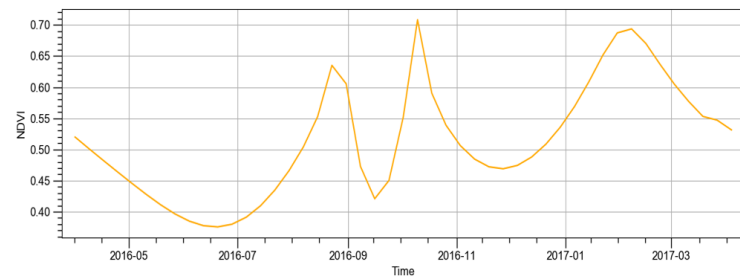




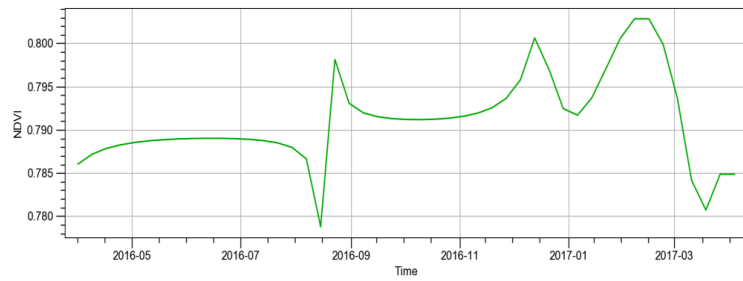
**Figure 3.5:** Relative temporal distribution of Landsat-8 OLI and MODIS NDVI images for the study epoch

### 3.2.2.3 MODIS-Landsat NDVI Fusion

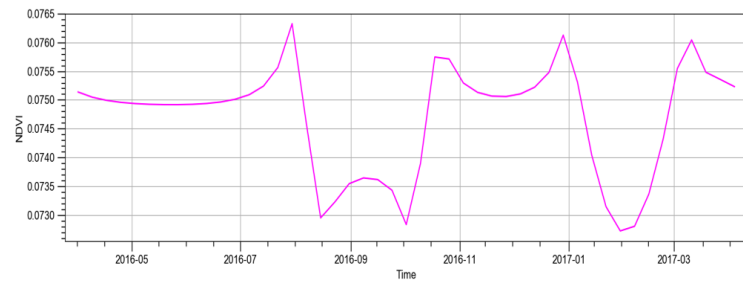
Only the most cloud-free images acquired using the first threshold ( $< 10\%$  cloud cover) were used in the fusion process. Spatio-temporal fusion via Index-then-Blend (IB) was implemented using the MODIS Daily 250m NDVI and Landsat 8 intermittent NDVI images as described in Zhu *et al.* (2010). The MODIS NDVI images were first resampled to 30m and cropped to match the extent of the Landsat 8 NDVI images using R (v3.4.4). Fusion was implemented in ENVI IDL (v4.8) using the open-source Enhanced Spatio-Temporal Adaptive Reflectance Fusion Model (ESTARFM), available from the Remote Sensing & Spatial Analysis Lab site. For a fusion block size of 500, it took an average of 40 minutes to fuse each MODIS NDVI image with reference to two Landsat images and their corresponding MODIS images. For computational efficiency, an 8-day interval was chosen. This, in addition to significantly reducing the processing time, gave credence to the decision to acquire and process the MODIS daily data, since it allowed for selection of a starting date matching the availability of Landsat images. To put a finer point on it, had the standard 8-day interval surface reflectance or MODIS NDVI product been chosen, there would have been no corresponding Landsat images for reference in the fusion process. Subsequent to the fusion process, the time series of synthetic Landsat images was smoothed and filtered to mitigate the effects of noise due to gaps in the original MODIS data. It should be noted that the decision to use the non-reconstructed i.e. non gap-filled, unsmoothed and unfiltered, MODIS images was arrived at after a previous experiment in which fully reconstructed MODIS NDVI images were used in the fusion process failed, resulting in anomalous NDVI temporal profiles as shown in Figure 3.6.



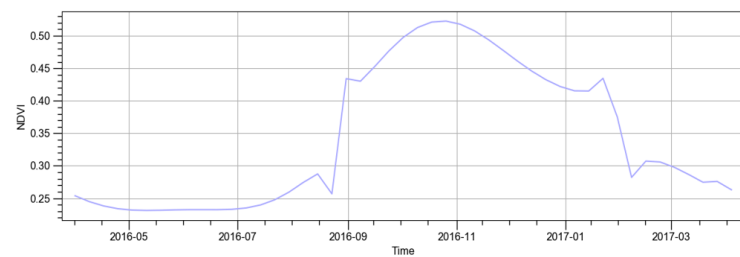
(a) Cropland



(b) Forest



(c) Urban



(d) Paddy

**Figure 3.6:** Anomalous NDVI time-series profiles for various land use/cover types after fusion using fully reconstructed MODIS images

## 3.3 Classification

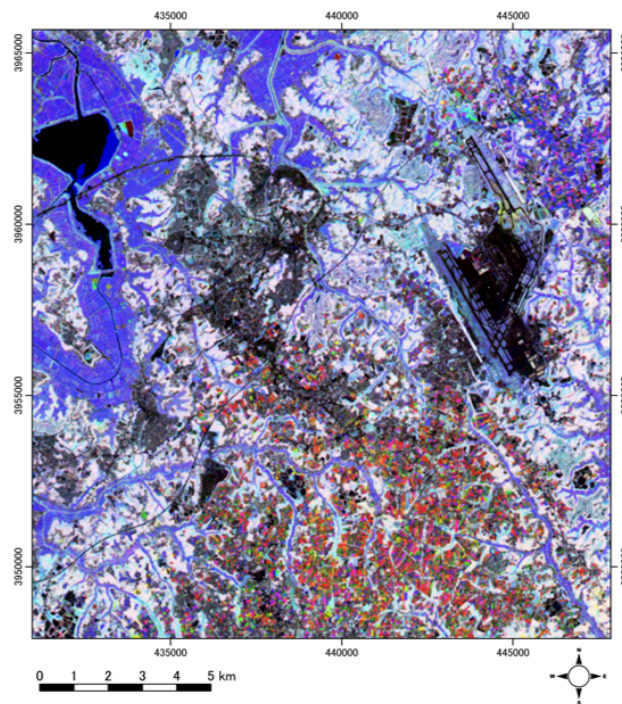
### 3.3.1 Training and Validation Samples

In this study, Random Forests (RF), an ensemble learning classifier was used for classification of the synthetic Landsat-like NDVI fusion image time series to:

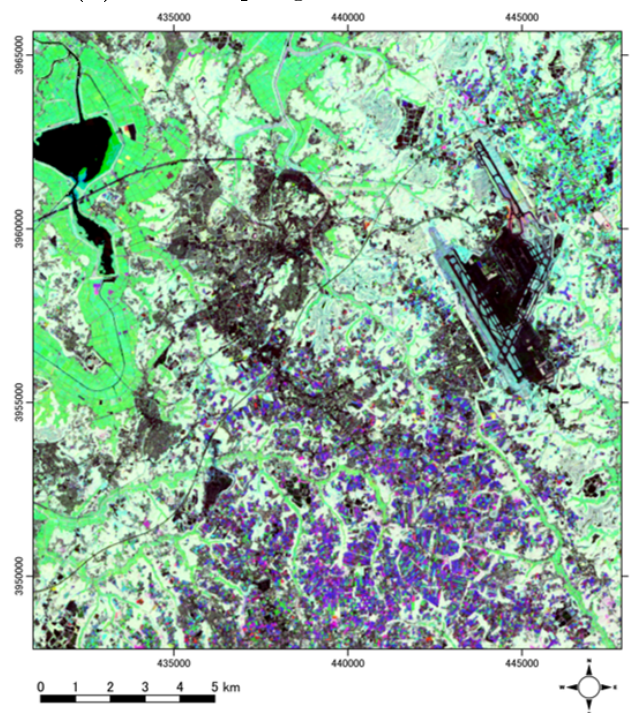
1. Generate the annual cropland extent map of the study area
2. Estimate cropping regimes, patterns or intensities of the identified croplands
3. Assess the applicability of the data set to distinction of a single known crop-type from other unknown crop types using a limited reference dataset.

RF classification was chosen because it has been found to have a high capacity for handling high data dimensionality such as is found in time series datasets (Kloiber *et al.*, 2015; Millard and Richardson, 2015). Key to any supervised classification process are the reference datasets necessary for training of the classification model and validation of the results. For the classification of cropland extent, two existing cropland datasets were assessed for viability as reference data sets. JAXA's High Resolution Land-Use and Land-Cover map of Japan (HRLULC Ver.18.03) is a 30m land cover map of Japan generated using multi-temporal, multi-source data. It includes the upland cropland and rice paddy field layers which were of particular interest in this study. However, since the data used in its production is not temporally specific and ranges from 2014 to 2016, it was decided to use this dataset for comparison of the results of this study.

In addition, the recently released Global Food Security-Support Analysis Data at 30m (GFSAD30) provides global cropland area data (Oliphant *et al.*, 2017). The Southeast and Northeast Asia dataset (GFSAD30SEACE) was acquired and assessed for suitability as a source of training and validation data in this study. The cropland extent in this dataset represents all cultivated land including paddy, irrigated and rainfed areas. As the discrimination between paddy rice fields and other croplands was an objective of this study, the GFSAD30SEACE dataset was used for validation of our result in terms of total cropland extent. In the absence of a reference dataset that was temporally specific to the year 2015, training and validation samples were generated using the Maximum Value Composite NDVI (MVC-NDVI) computed between consecutive NDVI images of the sparse Landsat image time series. In addition to minimizing the effects of cloud cover, the seasonal MVC-NDVI RGB composite stacks revealed inter-seasonal pixel-level NDVI changes that made it possible to determine seasonal behaviour of the major land cover types and set rules for distinguishing the major land cover classes and cropping patterns. The selection of sample data for the major classes was corroborated by the Google Earth (GE) image available for 9th October, 2015 as shown in Figure 3.7. Figure 3.7a shows the Winter-Spring-Summer composite while Figure 3.7b shows the Spring-Summer-Fall composite for 2015. The off-white regions in both Figures 3.7a and 3.7b depict dense vegetation such as forests which have high NDVI with minimal variation intra-annually. The black and gray regions are urban and water features which have low NDVI with minimal variation within the year. The Red, Blue and Green regions represent vegetation whose maximum NDVI corresponds with the seasonal order in the RGB composite. Figure 3.8 depicts the subset of the study region shown in Figures 3.7a and 3.7b as captured on Google Earth on 9<sup>th</sup> October 2015.



(a) Winter-Spring-Summer MVC-NDVI



(b) Spring-Summer-Fall MVC-NDVI

**Figure 3.7:** RGB composites of the seasonal Maximum Value Composite NDVI (MVC-NDVI) for a subset of the study area.



**Figure 3.8:** Google Earth image on 9<sup>th</sup> October 2015 for the same area subset shown in Figure 3.7

### 3.3.2 Crop-type Mapping Experiment

Classification of peanuts was tested using the time-series dataset and knowledge on location of cultivation. Peanuts are a popular crop in this region, grown for their commercial value with approximately 75% of Japan's domestic production being attributed to Chiba prefecture. From aerial and satellite images, it is impossible to distinguish with certainty, one crop (e.g. peanuts) from another (e.g. carrots) during the growing season, hence the need for *in situ* data such as field photos. As such, in order to know which crop was growing at a certain location at a given time, field photos or farm surveys are necessary, during the growing season in every year since farmers change crops cultivated from year to year, especially in the case of horticultural food crops. Given that acquisition of such information is time consuming and costly, creative means of inferring and deciphering such information from existing data are necessary. In this study, the post-harvest practice of *jiboshi* by peanut farmers in Japan, makes it possible to know on which fields peanuts had been growing within at least a month from the time of harvesting.

After harvest, peanut pods will typically have approximately 50% moisture which renders them prone to contamination with mycotoxins which are a food safety concern and may lead to major economic losses (Dickens, 1973; Allen, Sorenson and Peterson, 1971). Peanut farmers in Chiba prefecture will after harvest, leave the peanut plants and pods in inverted windrows which allow for air to circulate around the pod and for the moisture content to diminish significantly for about a week. Thereafter, the peanut plants and pods are piled into solitary heaps as shown in Figure 3.9a in a process referred to as *jiboshi* (drying on the ground) for about a month. These piles or heaps are



---

referred to as *bocchi* and are visible from GE images as shown in Figure 3.9b, thus allowing one to know that peanuts had been growing on that field or an adjacent one within at least a month of the acquisition of the image. A total of 378 Training and validation samples were collected within the study area for locations where *bocchi* were visible in the GE image for 9th October, 2015.



(a) Google Maps Street View of post-harvest peanut heaps known as *bocchi*



(b) Google Earth view of *bocchi* shown in 3.9a on 9<sup>th</sup> October, 2015

**Figure 3.9:** Google Maps Street View and Google Earth views of peanuts post-harvest practice on (9<sup>th</sup> October, 2015) used for identification of location cultivation (N35°37', E140°14)

# Chapter 4

## Results and Discussion

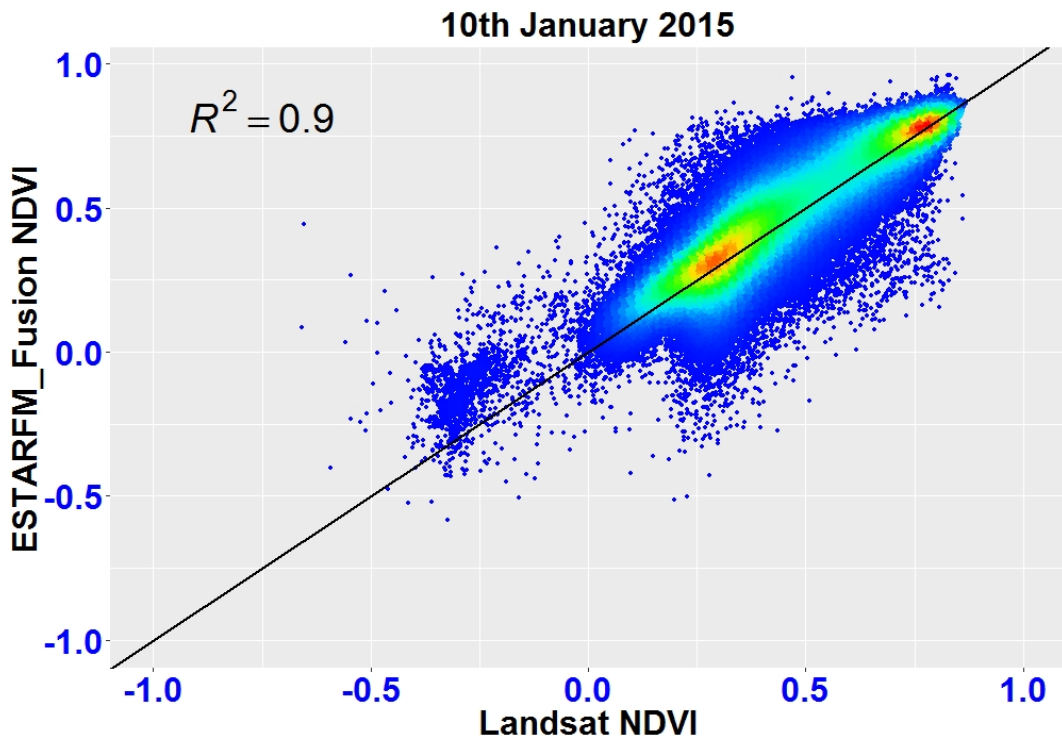
### 4.1 MODIS-Landsat Fusion

The performance of the fusion process in generating synthetic Landsat images was evaluated quantitatively and qualitatively. The quantitative assessment of the results was carried out via a correlation test of the ESTARFM Fusion NDVI images and the corresponding available observed Landsat NDVI images for the dates when cloud cover was less than 10%. A random sample of 2,000,000 pixels in each fusion NDVI image and its corresponding Landsat image was selected and scatterplots of fusion NDVI against observed NDVI generated in order to examine the association between the two. Overall, there was strong positive linear correlation with  $R^2 > 0.9$  for all dates as depicted in Figure 4.2.

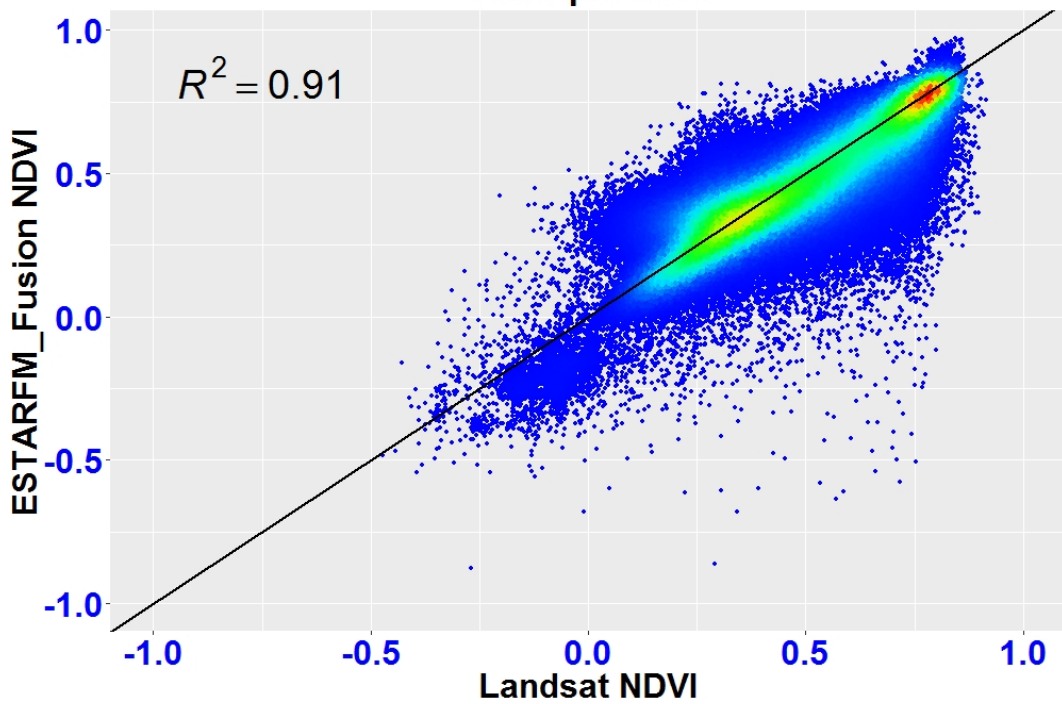
The highest correlation was found in the early fall images of October 9<sup>th</sup> and 25<sup>th</sup>, 0.95 and 0.96 respectively, while the winter (10<sup>th</sup> January) and early Spring (16<sup>th</sup> April) images had lower  $R^2$  values of 0.9 and 0.91 respectively. On examining the relative density distribution of NDVI in each image, we see that there are three main clusters in the January and April images,

( $-0.5 < \text{NDVI} < 0$ ), ( $0 < \text{NDVI} < 0.5$ ) and  $\text{NDVI} > 0.6$ . Further, majority of the outliers in these images, lie in the lower ranges ( $-0.75 < \text{NDVI} < 0$ ). In the subsequent October images, the trend appears to dissipate and a comet-like configuration with one cluster in the upper ranges,  $\text{NDVI} > 0.5$ , emerges. As NDVI is a measure of vegetation vigor, the higher association and number of clusters in the early fall images when vegetation is more vibrant compared to the Winter and early Spring images, may be attributed to seasonal variations and an indication of vegetation land cover density in a region. Further investigation of this phenomenon is necessary and could provide interesting insights into how to implement fusion for vegetation monitoring in studies of regions with disparate climates and land cover characteristics.

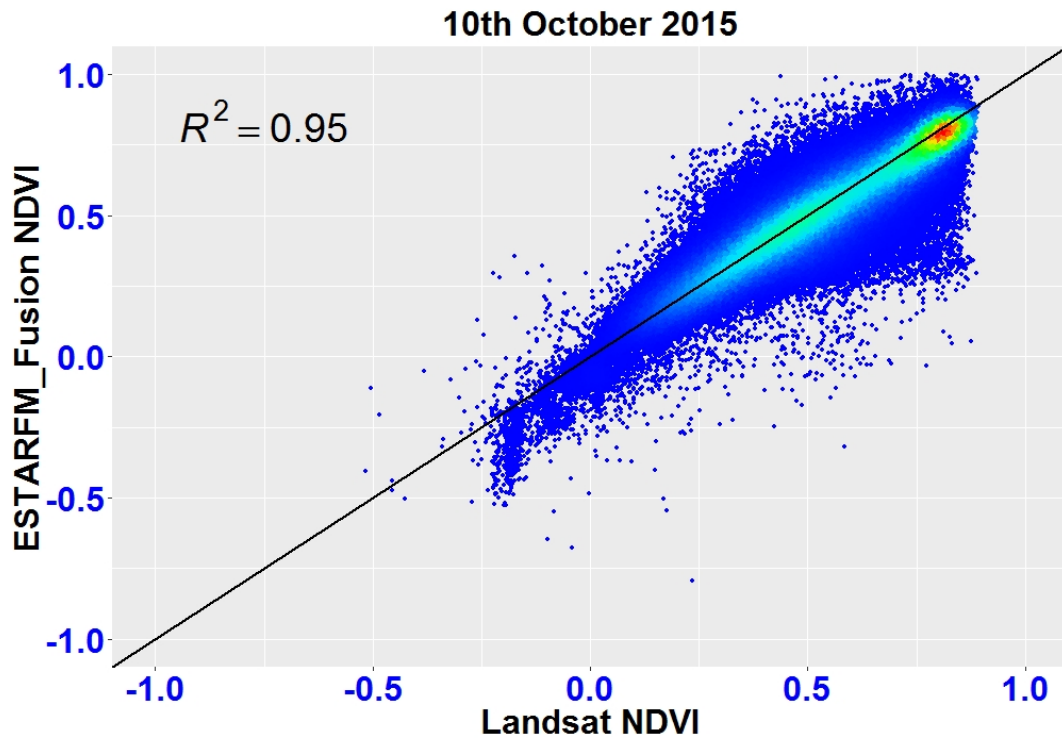
Figure 4.3 shows NDVI temporal evolution in the smoothed fusion series and the original Landsat 8 series, sampled from the main land cover classes in the study area in a qualitative assessment of the fusion result. Several points per land cover class were sampled and the mean NDVI across the study epoch in both the fusion NDVI and observed NDVI time series stacks extracted. The configurations or shapes of temporal profiles in both data sets were analogous though the amplitude in the observed NDVI stack was higher than in the fusion stack. This is expected since ESTARFM fusion model is a weighted function based model and it has been found that while these models adequately predict changes in attributes of land cover, they assume that the rate of change between the two reference periods is constant and may result in a muted prediction, (Zhu *et al.*, 2015; Liao *et al.*, 2017). The difference in NDVI amplitude between the fusion and observed time series stacks was not deemed to have negative implications on achieving the objectives of this study since we were interested in the attribute changes especially in the vegetation classes and these were well captured, based on the configurations of the profiles.



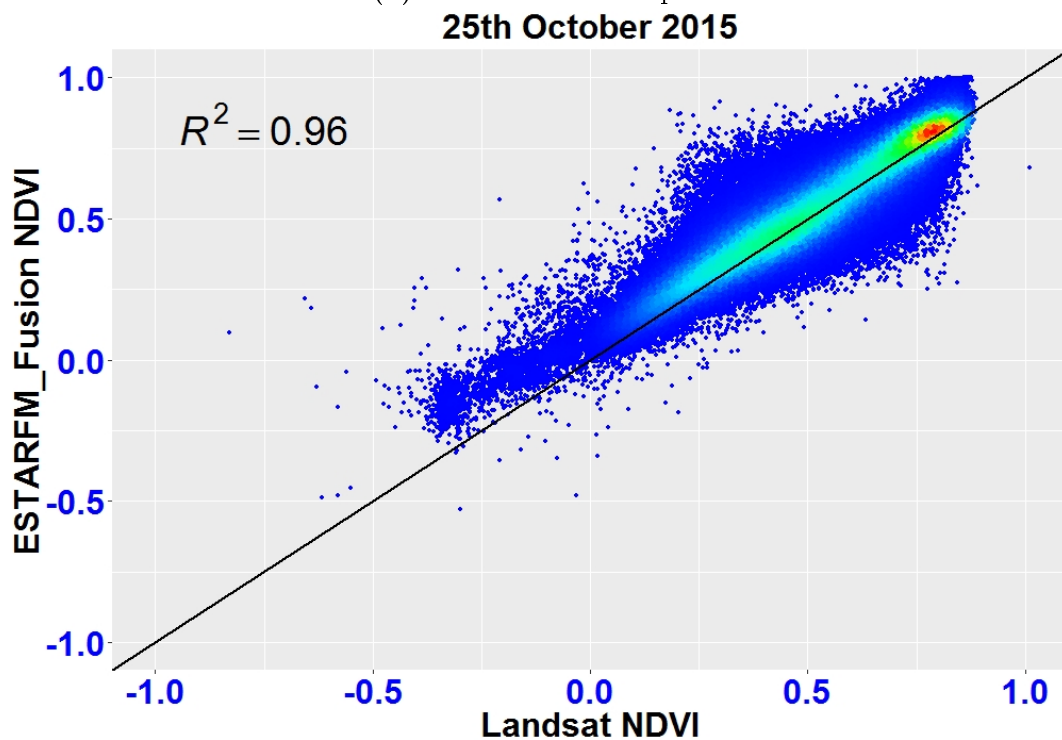
(a) 2015-01-10 Scatterplot  
**16th April 2015**



(b) 2015-04-16 Scatterplot

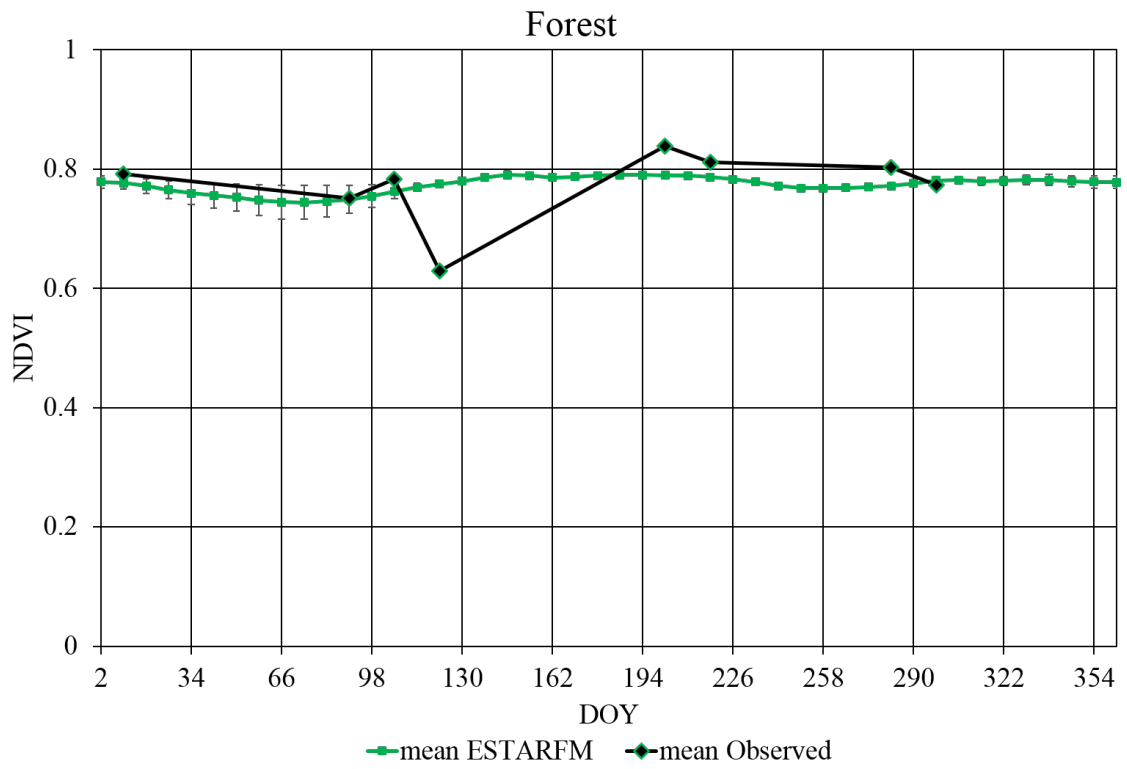


(a) 2015-10-09 Scatterplot

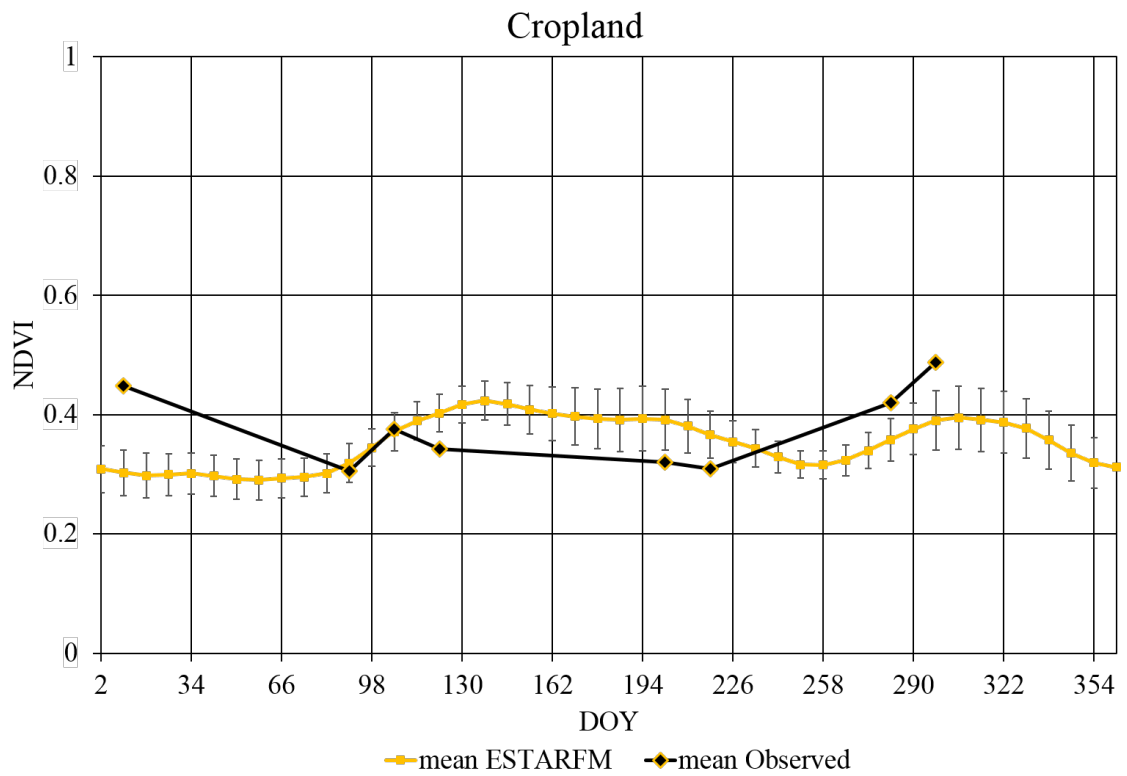


(b) 2015-10-25 Scatterplot

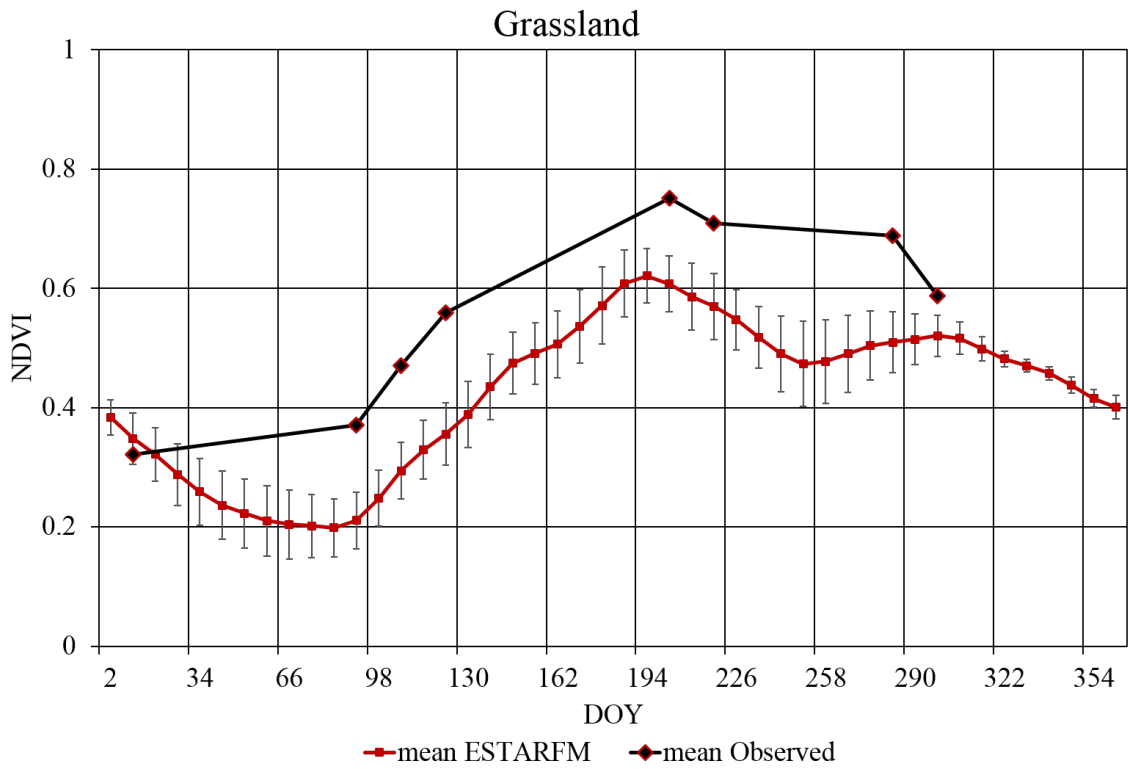
**Figure 4.2:** Scatterplots showing results of comparison of synthetic fusion NDVI images with original Landsat images



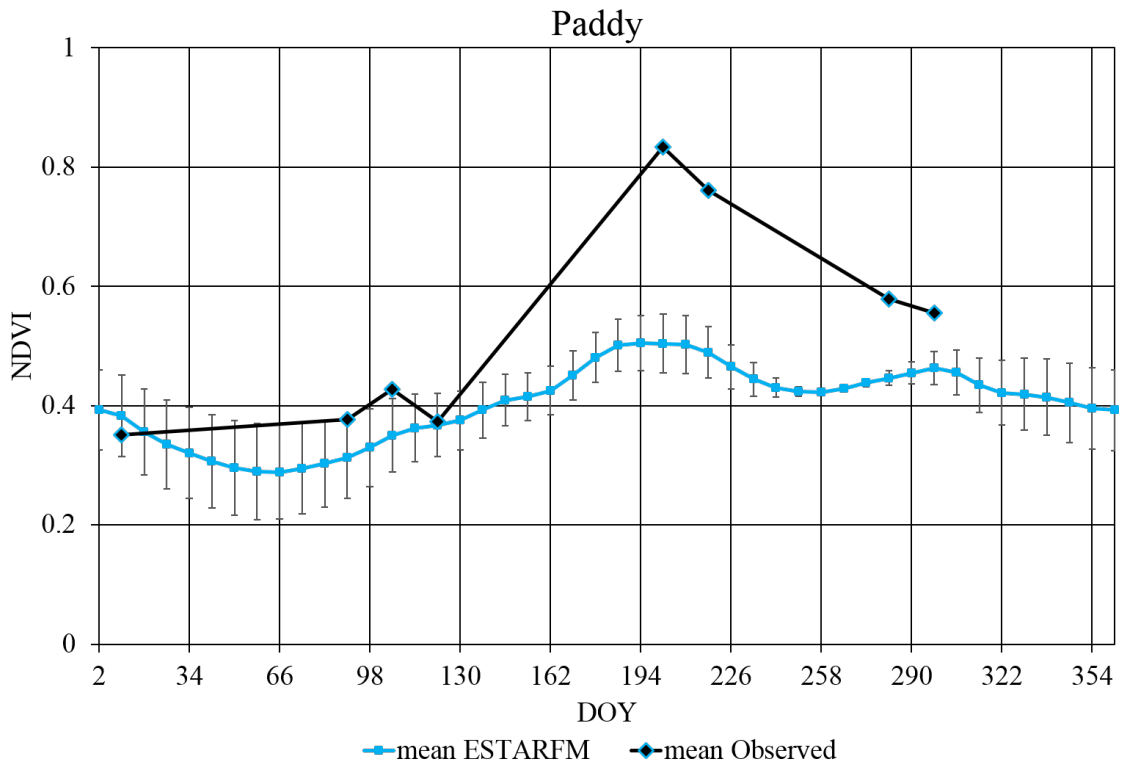
(a) Forest



(b) Cropland

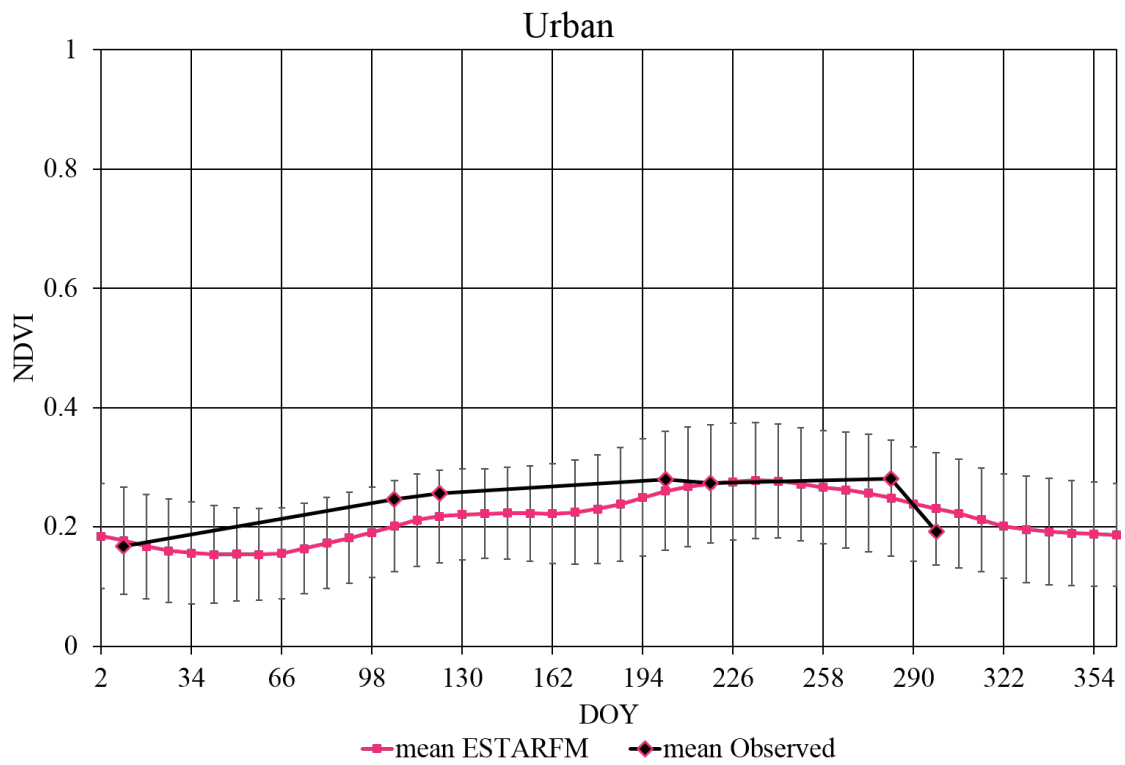


(c) Grassland

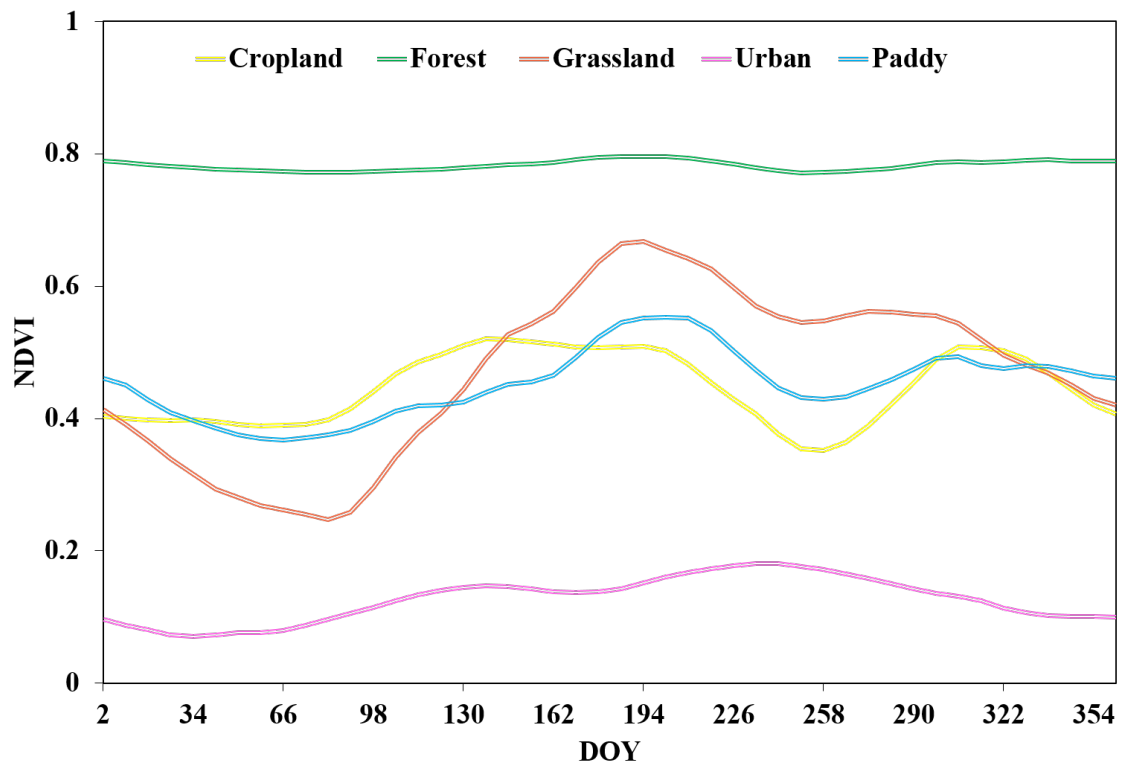


(d) Paddy





(e) Urban



(f) All land cover/use types fusion NDVI profiles

**Figure 4.3:** Comparison of synthetic and original Landsat NDVI time series profiles of major land cover types

## 4.2 Cropland identification and discrimination

Cropland extent in the context of this study was defined as all land used for crop cultivation excluding paddy fields. Figure 4.4 shows the results of land use/cover classification of the study area for the year of study with the main land use/cover classes being cropland, forest, grassland paddy, urban and water. The estimated area of croplands for the study area in 2015 was 85.5 Km<sup>2</sup> and is as depicted in Figure 4.5a. Table 4.1 shows the random forest classification error matrix.

An overall classification accuracy of 91.65% was achieved and the dominant land cover classes of forest, grassland, urban and water and paddy had the highest Producer's (PA) and User's accuracies (UA) of more than 90%. The cropland area estimation had the lowest, albeit acceptable, PA and UA of 79.8% and 86.4% respectively, given the size and heterogeneity of the cropland areas. Based on the classification result, cropland area accounts for just over 10% of the total land cover (13.7%) and is therefore not a dominant land use/cover class. As such, the classification accuracy was deemed to be sufficient. Further, the intra-annual temporal evolution of NDVI of the grassland, paddy and cropland land use/cover types as seen in Figure 4.3f shows the relative similarity between cropland profiles and paddy and grassland profiles. Vegetation along urban features such as roads and banks of water bodies was also misclassified as cropland and paddy. This study's result was compared to the Japan Aerospace Exploration Agency (JAXA) High Resolution Land Use Land Cover (HRLULC) map and the Global Food Security-Support Analysis Data 30m (GFSAD30) maps.

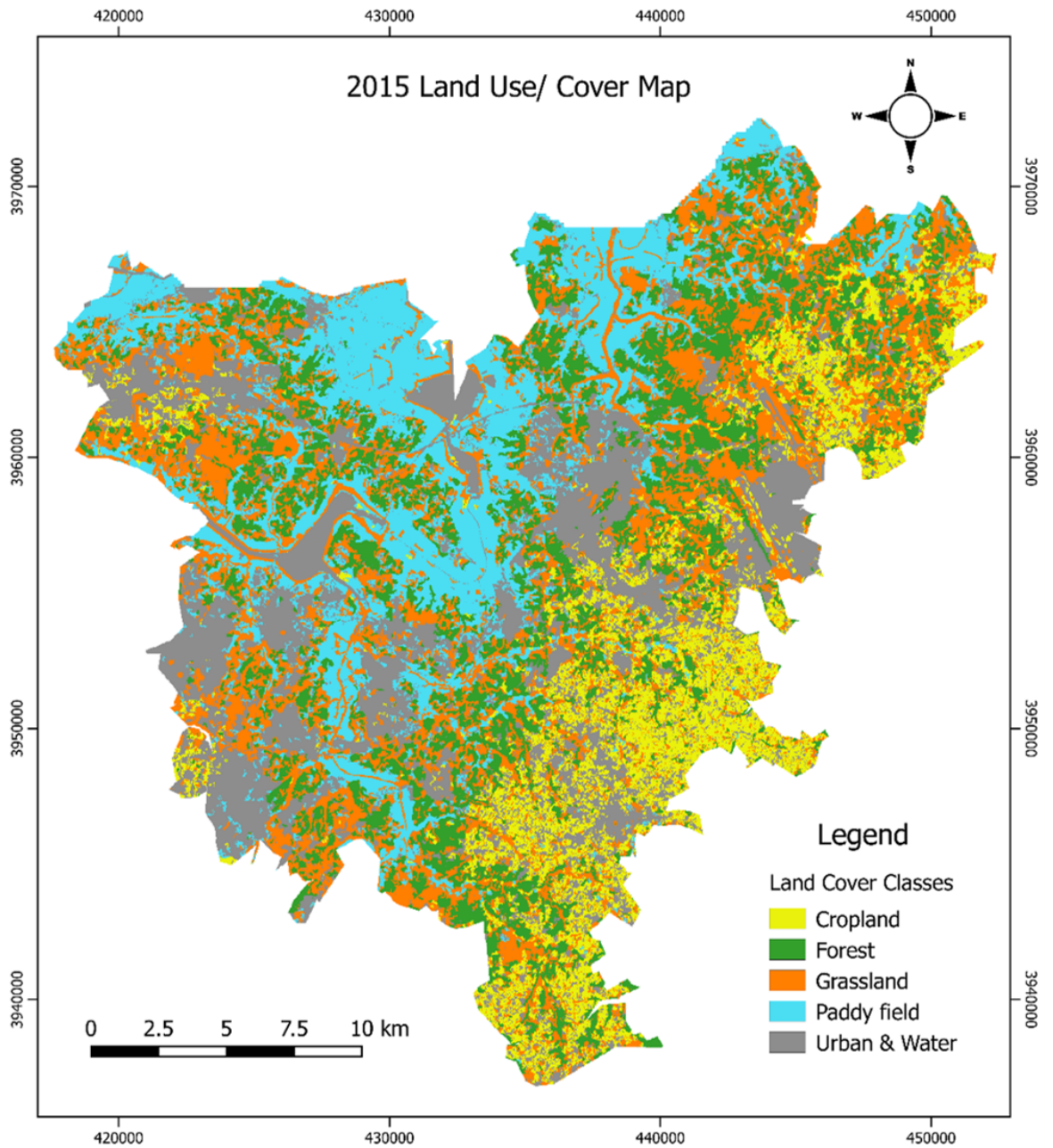


Figure 4.4: Land use/cover map of 2015 as mapped in this study

Table 4.1: Confusion matrix of cropland extent classification

	Cropland	Forest	Grassland	Paddy	Urban & Water	Total	UA (%)
Cropland	542	2	38	15	30	627	86.4
Forest	7	691	4	0	0	702	98.4
Grassland	38	0	638	27	0	703	90.8
Paddy	36	0	11	597	7	651	91.7
Urban & Water	56	0	0	12	640	708	90.4
Total	679	693	691	651	677	3391	
PA (%)	79.8	99.7	92.3	91.7	94.5		
OA (%)	91.7						
Kappa	0.9						

### 4.2.1 JAXA HRLULC map comparison

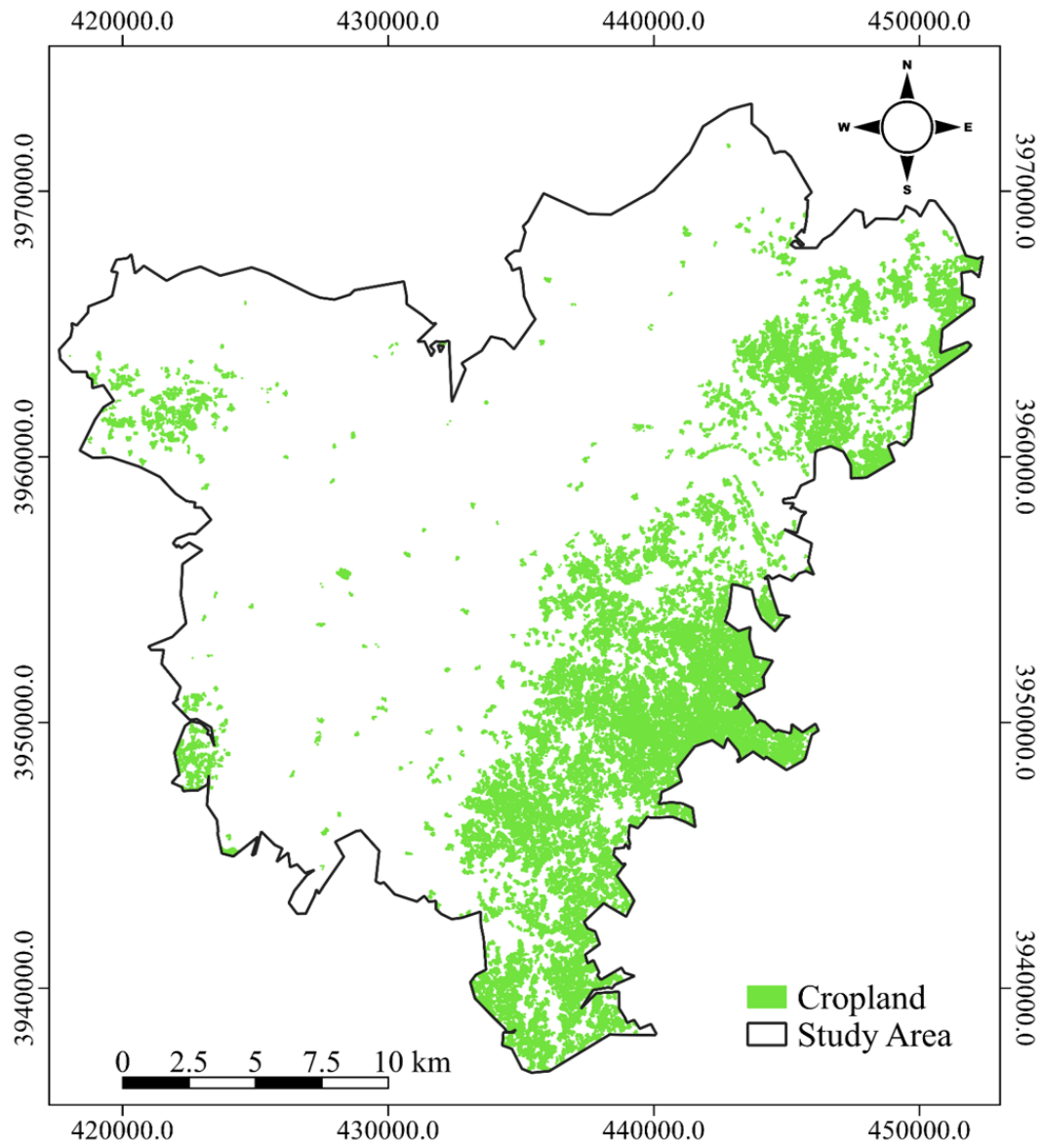
The cropland area according to the JAXA HRLULC map was approximately 367.9 Km<sup>2</sup> which is significantly higher than this study's estimate. In Sharma *et al.* (2016) disparities between the land use/cover map produced in that study, the JpLC-30m and the JAXA HRLULC (ver.14.02) were reported for all land cover classes including cropland. It should be noted that in this study, we compared our result to the more recently released JAXA HRLULC (ver.18.03) in which reported improvements from the earlier version (ver. 16.09) included an input data set that was more temporally specific (2014 to 2016) and visual interpretation of training and validation data. The input data for the JAXA HRLULC map included Landsat 8 images, ALOS-2/ PALSAR-2 25m 2015 mosaic dataset, ALOS PRISM Digital Surface Model (DSM) and auxiliary datasets from the Geographical Survey Institute (GSI), Open Street Map and Ministry of Agriculture, Forestry and Fisheries. Training data was acquired from the crowd-sourced field photo database, SACLAJ and ground survey information.

An overall classification accuracy of 81.6% is reported for the JAXA HRLULC map, with the highest PA and UA reported being that for the water class, 93.6% and 97.9% respectively. For the cropland class, the PA is 83.8 % and the UA is reported as 74.1%. Arguably, the task of national land use/cover mapping at the update rate demonstrated by JAXA is both arduous and formidable, requiring continuous improvement in data inputs and methods. These improvements require significant monetary and technical investment and the resulting product should be a reflection of this. It was therefore necessary to compare this study's result to this product, even though the production

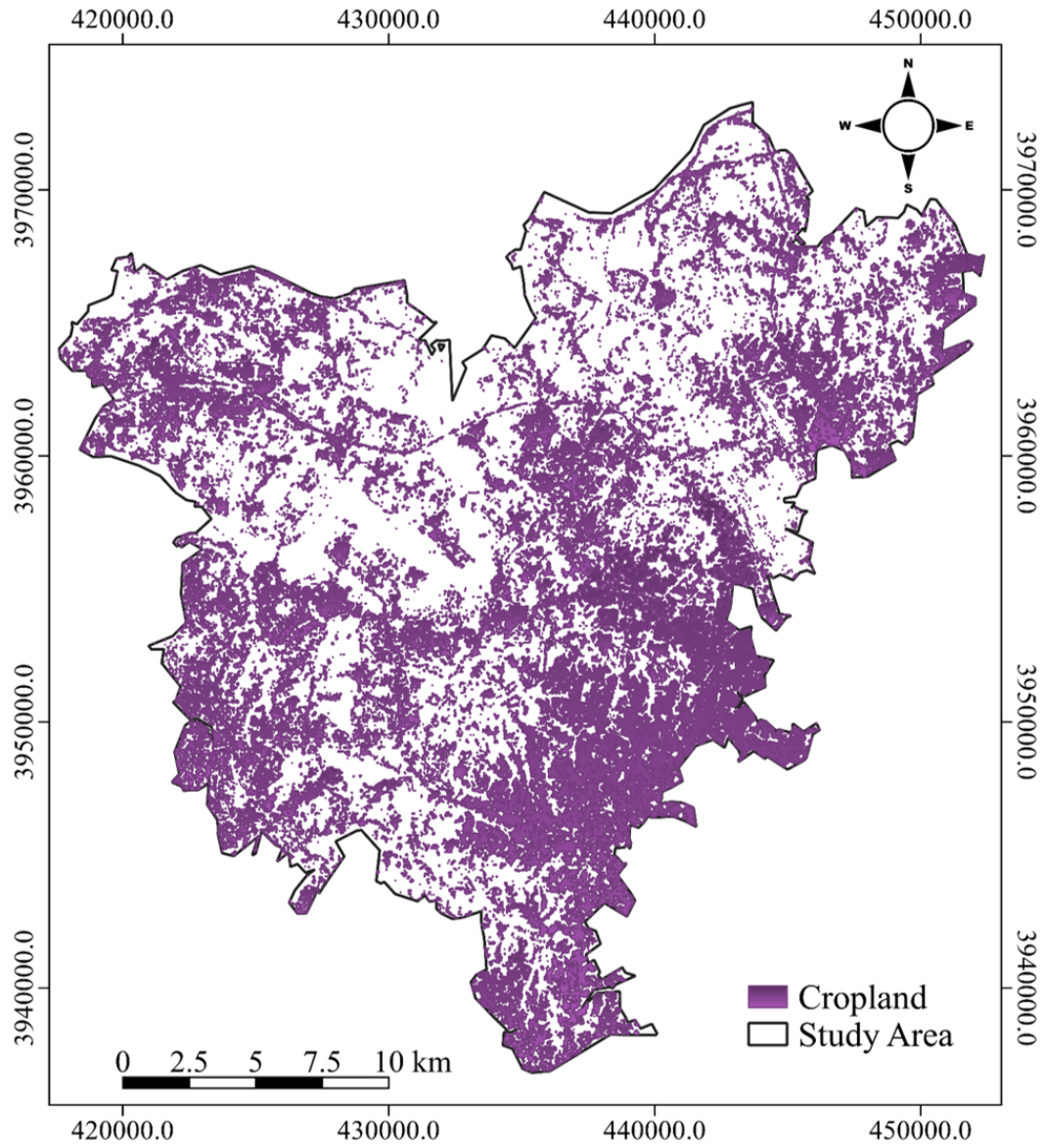
scale in this study was local, since the JAXA HRLULC is intended for use as a base map for various applications (JAXA, 2018). Figures 4.5a and 4.5b depict the cropland extent as estimated in this study and JAXA HRLULC map's cropland respectively.

### 4.2.2 GFSAD30m map comparison

The GFSAD30 product covering Japan and other Northeastern and Southeastern Asian countries is the GFSAD30mSEACE data set and was acquired since it is the only global cropland dataset disseminated at 30m. The GFSAD30 product represents cropland and non-cropland globally and therefore does not currently make a distinction between different types of croplands, though plans are afoot (Oliphant *et al.* (2017)). The cropland extent according to the GFSAD30 map is as shown in Figure 4.6 and the area is 129.4 Km<sup>2</sup>. Figure 4.7 is a spatial overlay of the GFSAD cropland and this study's cropland and paddy layers, showing that the former adequately captures the paddy fields and compares favorably with our result in that regard. However, upland croplands are underestimated in comparison to both this study's result and JAXA HRLULC, its limitations notwithstanding. Our result does overestimate paddy fields with a commission error of 2.3% and 4.15% as cropland and grassland respectively. However, this is almost balanced out by misclassification of some paddy fields as croplands. Using other metrics other than NDVI, for the same one-year data-set such as the NDWI index or shape and texture features may resolve this and enhance the accuracy of distinction between upland croplands and paddy fields.



(a) Cropland extent as estimated in this study for year 2015



(b) JAXA HRLULC cropland extent

**Figure 4.5:** Comparison of cropland extent of this study's result with JAXA HRLULC map



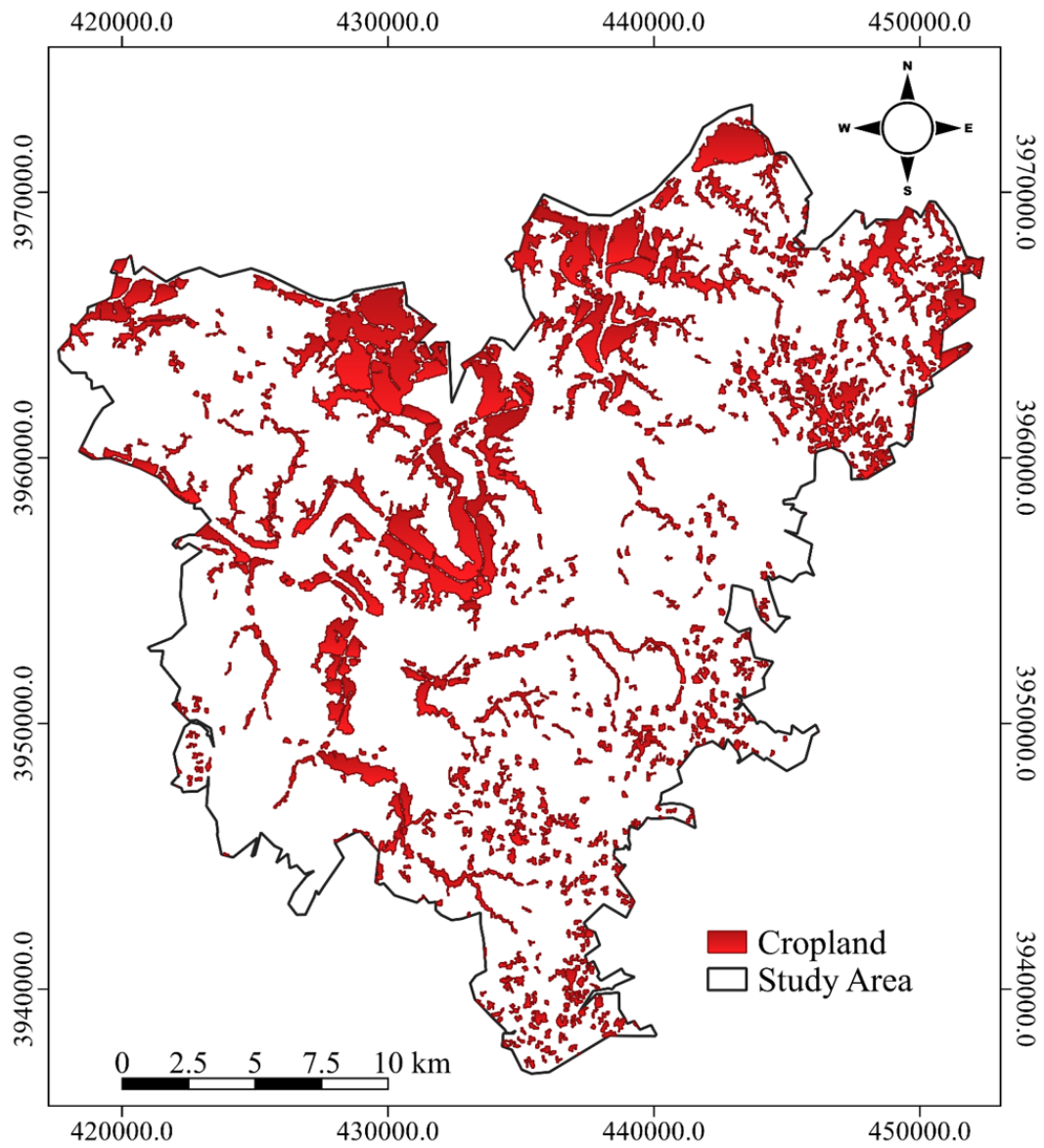


Figure 4.6: GFSAD30 cropland extent

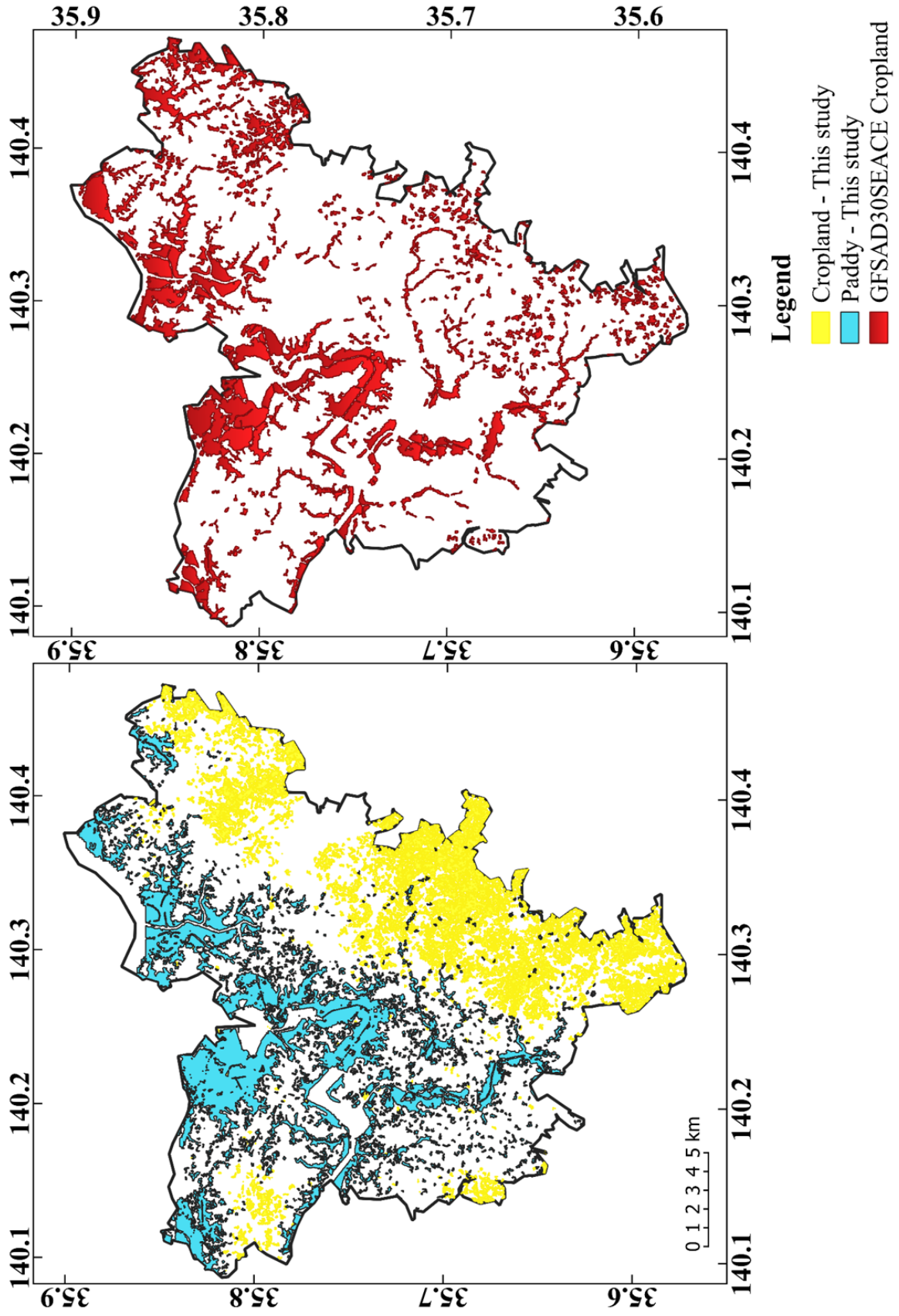


Figure 4.7: Comparison of this study's paddy and cropland extent with GFSAD30 cropland extent

This study demonstrates that using the simple yet robust NDVI with high temporal frequency, dynamic heterogeneous landscapes can be adequately mapped and monitored using data available within a year. From a policy development perspective, this aspect of our methodology is desirable as it allows for changes taking place in the landscape to be catalogued using the most recent data and disseminated with reasonable frequency and accuracy. Further, as demonstrated by the comparison of our result with the JAXA HRLULC and GFSAD30 maps, there is great value in local scale mapping efforts that can aid in the accurate production of national and global scale maps.

### 4.3 Estimation of cropping regimes

The estimation of cropping regimes, patterns or intensities within the year was based on two premises. The first being that, in this area while irrigation is available for most farmers and precipitation is stable thus favouring rainfed cultivation, farming of horticultural crops, which are the main products, is still dependent on seasonal market demand. Accordingly, while farmers are not restricted by availability of water, types of crops planted will still in effect be dictated by the season, hence indicating that cropping intensity can be as high as seasonal changes. The second premise was that in order to maximize returns on the land, since Chiba prefecture's climate is suitable for agriculture even in the winter, farmers may tend to plant as many different crops within a year, with the only restriction being the duration of growth per crop.



---

Table 4.2 shows the months when the market volume of some of Chiba prefecture's representative crop products is high. From this table, the seasonal nature of cultivation is apparent and while not exhaustive, it indicates that for most farmers, depending on the crop, the cropping intensity varies since for all crops apart from taro and daikon radish, market volume is high for more than two seasons in an year. Due to the sensitive nature of rice paddy fields, they are typically not used for cultivation of other crops after harvest within the year as this may upset the soils mineral balance. Consequently, paddy fields were expected to exhibit single cropping intensity. Figure 4.8 shows the map of estimated cropping patterns for the study area in 2015. The previously stated suppositions regarding cropping intensity *vis-a-vis* upland croplands and paddy fields hold true with a few exceptions.

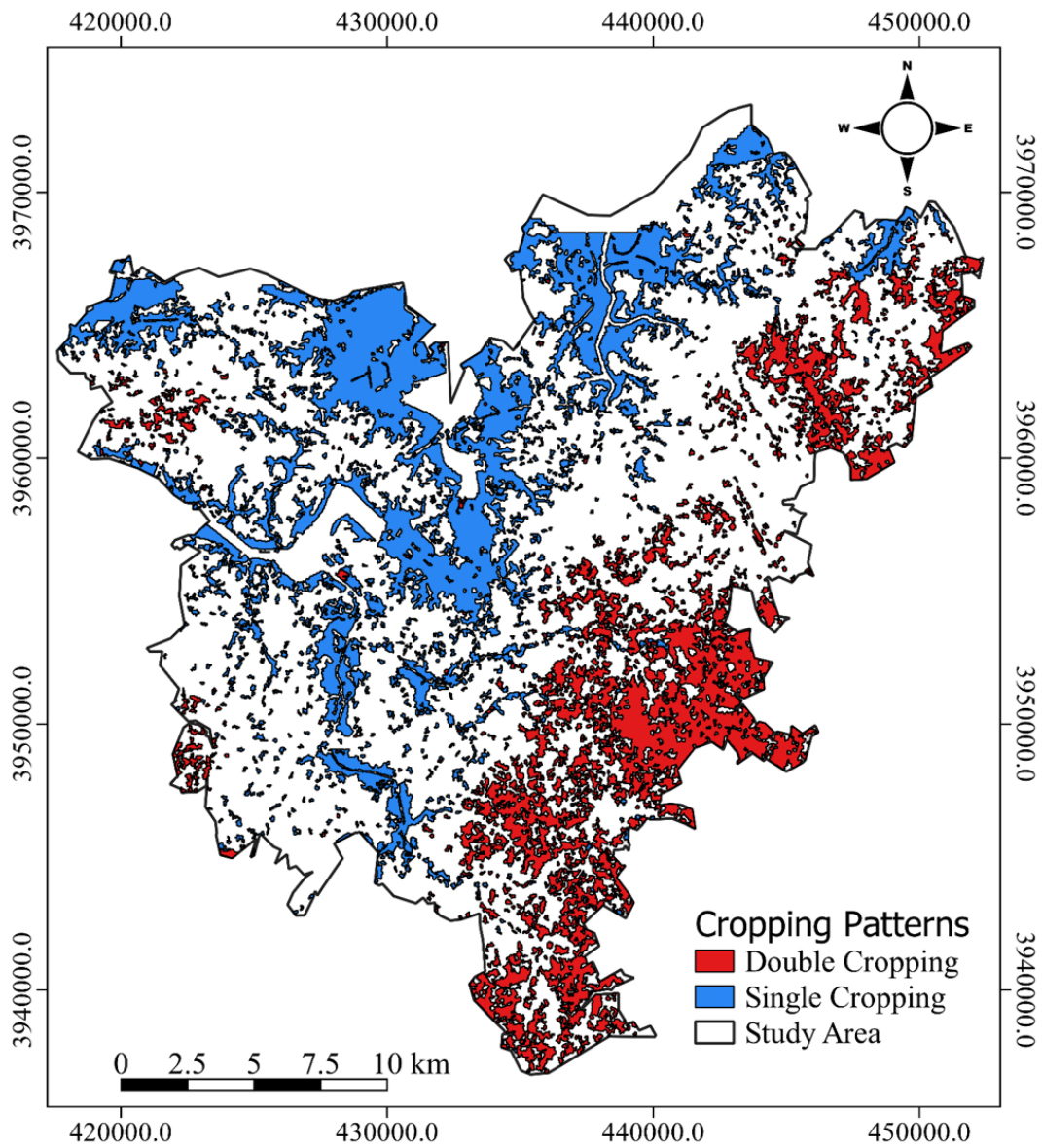


**Figure 4.8:** Cropping regimes estimated in this study for the year 2015

Cropping regimes estimation is essentially a change detection operation that is specific to crop cover and when implemented for all land cover types, it yields the land use/cover changes. Typically, land use/cover change evaluation is carried out for periods longer than one year due to the assumption that significant and permanent changes that have effects on the character of a location's land use/land cover take long. However, in urban and peri-urban landscapes, these changes can be effected intra-annually especially in vibrant economies, leading to rapid or even abrupt changes in the character and composition of land use/cover. A simple way of identifying these changes is through the use of bitemporal image analysis methods. However, as highlighted in Petitjean *at al.* (2010), changes do not commence at the same time, nor do they take place over the same period of time, necessitating more than two images since the number of possible combinations of change are limitless. In addition, there are other considerations impinging on the ability of classifiers to detect abrupt changes including; geometrical and spectral resolution, data acquisition frequency, atmospheric artefacts, application or user requirements and availability of or access to baseline *a priori* information and ground reference data, that must be taken into consideration. In this study, cropping regimes and intra-annual changes in land use/ cover were estimated by considering that annual NDVI evolution metrics in a dense time series provide a generalized feature space to the classification algorithm by capturing the salient features of phenological variation without reference to the time of the year as described in Schneider (2012). Changes from forest and grassland to mini-solar farms which are designated as urban land use/cover were detected after classification as shown in Figure 4.9. At the locations identified, the land cover was classified as urban in the land use/cover classification but classified as double cropping in the intra-annual change evaluation, indicating that there was a significant change

within the year. While the exact time of the change cannot be identified, comparison between GE images available for the 2015 and the previous year 2014 corroborate the occurrence of such a change event. Figure 4.10 shows a detailed representation at two (1 and 2) of the locations identified with respect to the Land Use/Cover and Cropping Regimes and Land Cover change maps generated in this study for 2015. Figure 4.11 shows that in the GE image of 2014, both locations 1 and 2 were grassland areas which were converted to solar farms, and therefore urban land cover, as seen in Figure 4.12.

## 4.4 Peanuts Mapping

Peanuts are an important crop for Chiba prefecture since approximately 75% of Japan's domestic supply of peanuts comes from here, (Japan Brand, n.d.; Ito, Aoki and Shimuzu, 2009). However, data on production of peanuts is sparse and no statistical data is available from the Ministry of Agriculture, Forestry and Fisheries. As dietary and nutrition trends change in Japan, the demand for peanuts as a snack and peanuts based products such as peanut butter is growing. Further, given the high quality of peanuts produced in Japan and the government's drive towards strategic development of Japan's agriculture for global supply as local food demand declines, it is important to have information on peanuts production, (MAFF, 2017). Given the scarcity of data, spatial reference data for classification of peanut production units was obtained via collection of samples for locations where the post-harvest practice of *jiboshi* was identified on the google earth image for October 9<sup>th</sup>, 2015, as explained in chapter 3. The overall classification accuracy of peanuts versus other crops was 67.1% with a producer's accuracy of 63.6% and user's accuracy of 71.4%. These accuracies were deemed to be satisfactory since the number of



---

reference data sample points was low (378) and random forest classification usually requires a large reference dataset in order to achieve high accuracies. Figure ?? shows the results of the classification of peanuts, while Table 4.3 shows the classification matrix. More needs to be done to accurately map peanuts but this study's result provides a starting point.

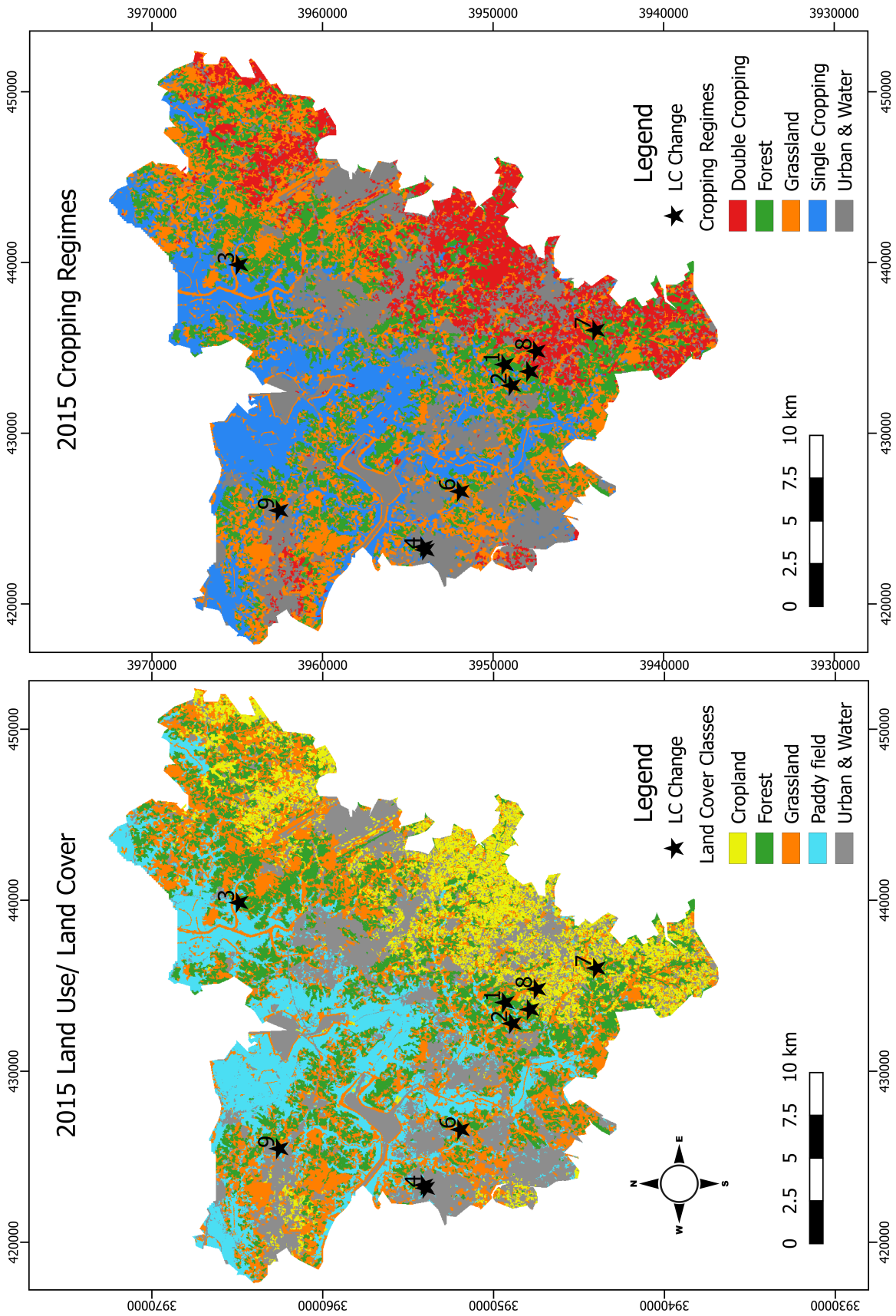


**Figure 4.9:** Locations where land cover change was detected in the Land Use/Cover Map and Cropping Regimes Estimation maps respectively

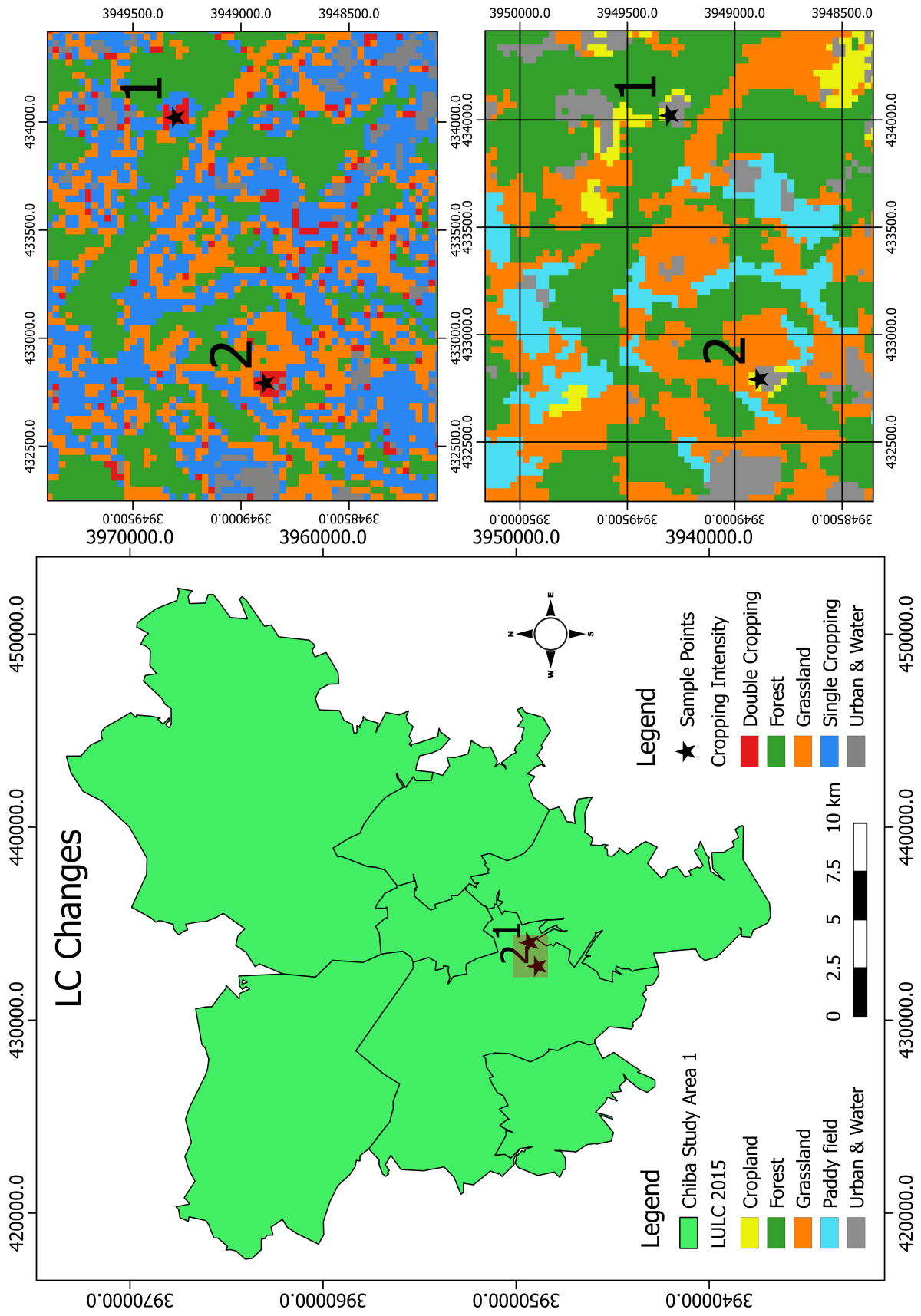


**Figure 4.10:** Detailed view of locations 1 and 2 where rapid conversion of land cover from 'Grassland' to 'Urban' was detected

2014



**Figure 4.11:** 2014 Google Earth image of locations 1 and 2 where rapid conversion of land cover from 'Grassland' to 'Urban' was detected

2015



**Figure 4.12:** 2015 Google Earth image of locations 1 and 2 where rapid conversion of land cover from 'Grassland' to 'Urban' was detected

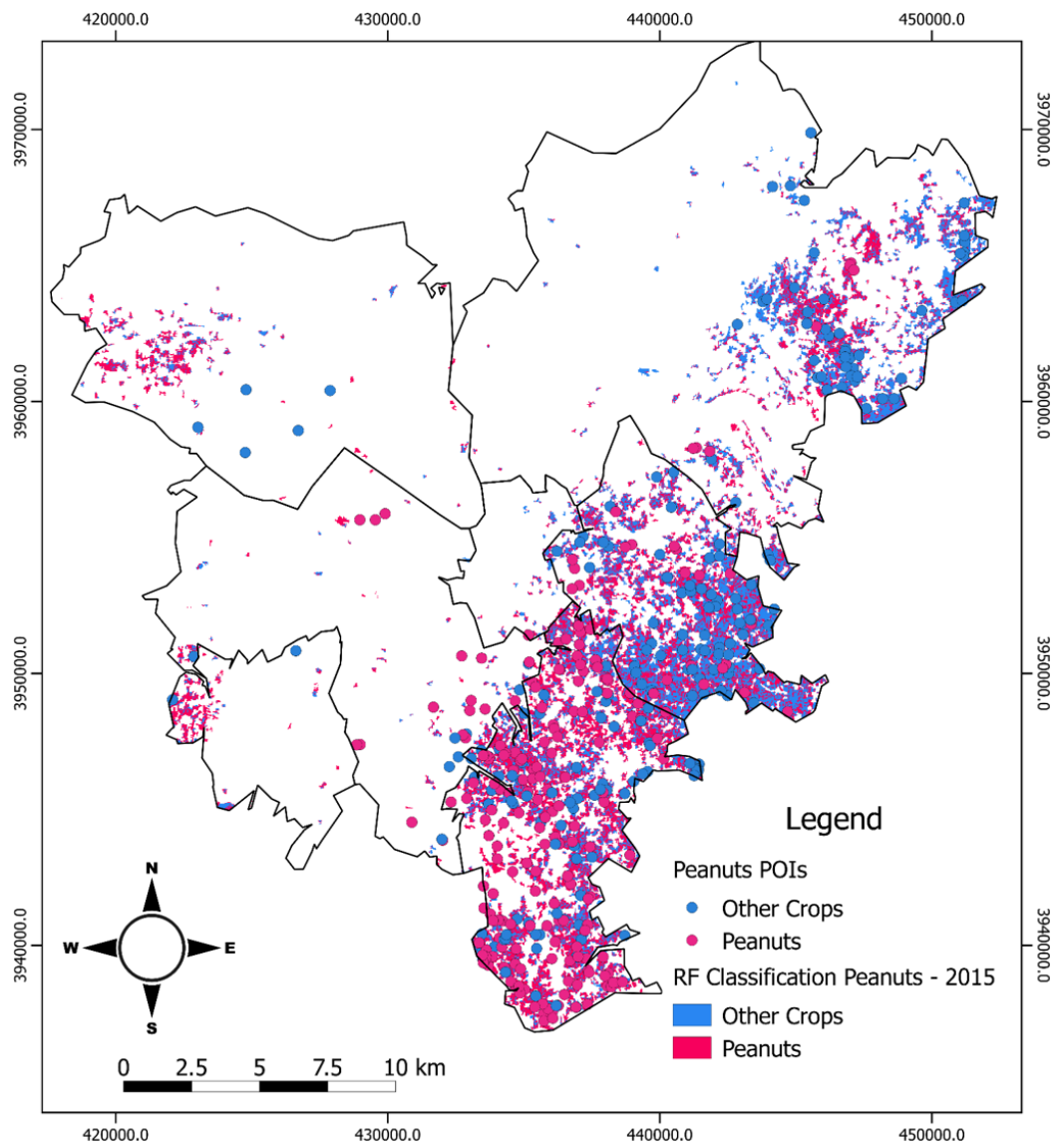


**Figure 4.13:** Distinction of peanuts cultivation from other crops within the study area for the year 2015

**Table 4.3:** Confusion matrix of peanuts classification

	Other Crops	Peanuts	Total	User Accuracy (U.A)
Other Crops	75	30	105	71.4
Peanuts	43	74	117	63.2
Total	118	104	222	
Producer Accuracy (P.A)	63.6	71.2		
Overall Accuracy (O.A)	67.1			

# Chapter 5

## Conclusions and Future Work

### 5.1 Conclusions

Cropland area estimation and distinction from other land cover types in heterogeneous landscapes can be challenging due to inadequate information especially in a dynamic landscape. However, it is imperative that this kind of information is available since it provides a basis for monitoring and managing agricultural production. While the field of remote sensing has in the recent years seen an increase in the number of sensors providing high and medium spatial resolution (10m – 30m) data, these sensors tend to have a lower temporal resolution. On the other hand, low spatial resolution datasets such as MODIS and NOAA-AVHRR (> 100m), have a higher temporal resolution due to their large spatial footprint. However, applications such as agriculture require continuous data in order to accurately estimate the phenological and biophysical properties. This is particularly true for croplands used for the cultivation of high value horticultural crops, which typically have short growing periods and whose numerous varieties result in spatially and temporally com-



plex dynamics. The mapping of these croplands thus requires data that has both high spatial and temporal resolution in order to adequately characterize these complex landscapes and discriminate from other land cover types and uses. This kind of data is currently unavailable due to technical and financial trade-offs that apply to construction of optical satellites in terms of spatial and temporal resolution. In view of these limitations, fusion methods have been developed with the aim of merging high spatial-low temporal resolution data with high temporal-low spatial resolution data.

The main objective of this study was to evaluate mapping and monitoring of urban and peri-urban agriculture in a complex landscape by exploiting multi-resolution spatio-temporal information. Towards the achievement of this goal, the specific objectives were:

1. To evaluate the application of fusion of multi-source satellite imagery to generation of synthetic high spatio-temporal resolution time series
2. To distinguish cropland from non-cropland and make a distinction between upland cropland and paddy rice fields with limited reference data
3. To extract temporal phenological metrics to enable cropping pattern or cropping intensity estimation in a limited reference data scenario
4. To test the applicability of empirical data, specifically post-harvest practices information, in distinguishing peanuts from other crops in the study area

In this study, we demonstrated that using intermittent moderate spatial resolution Landsat imagery and low spatial resolution daily MODIS surface reflectance imagery, information that can be used to distinguish croplands from

other land cover types can be retrieved. Fusion of the MODIS NDVI and Landsat NDVI images using the ESTARFM algorithm yielded reliable synthetic Landsat imagery with  $R^2 > 0.9$ . The use of daily MODIS data proved to be beneficial since the beginning of the synthetic image time series can be set with respect to the available reference Landsat images thus allowing for quantitative evaluation of the fusion time series. An Index-then-Blend (IB) approach was used in this study since the fusion process can be time consuming especially if implemented on a band-by-band basis. The results of this study indicate that for operation local scale agricultural monitoring, the classification of high spatio-temporal resolution time series can be easily implemented. This is further demonstrated by a test carried out on the application of the cropland mapping methodology developed in this study, on a cropland area with different socio-economic, geographical and climatic characteristics from this study's research area, presented in A.1.

The regular moderate resolution image time series with an 8-day interval proved to be adequate to the task of estimating cropland area and cropping patterns in a complex heterogeneous urban landscape. In addition, using knowledge of post-harvest practices of peanut farmers in the region, we were able to distinguish peanuts from other crops with an acceptable accuracy. The method used can be extended to crop type mapping provided that adequate ground truth or reference data is available. In a world that is increasingly being documented through amateur photography, various platforms for the mining and cataloguing of photographs shared on the internet for remote sensing product validation have emerged. The proliferation of crowd-sourced reference libraries such as the Site-based data for Assessment of Changing Landcover by JAXA (SACLAJ) and the Earth Observation and Modelling Facility's Field Photo will enable better construction of reference datasets for training and valida-

tion of classification models.

## 5.2 Contributions

This thesis makes novel contributions to the field of agricultural remote sensing for agricultural mapping and monitoring, especially in distinguishing croplands from other land cover types using intra-annual time series analysis.

The specific contributions of this research are summarised as follows:

1. We have classified land use and land cover using a temporally specific dataset and scalable analytical framework thus generating an annual land use/ cover map that can allow for operational annual land cover change monitoring.
2. We estimated annual cropland extent and reliably distinguished upland cropland from paddy rice as demonstrated via comparison with the existing national scale JAXA HRLULC.
3. We used a novel means of acquiring crop type information, specific to peanuts and based on post-harvest practices. We then tested the applicability of such data to peanuts classification and obtained satisfactory results.

## 5.3 Future Work

The research presented in this thesis will be extended in a variety of ways in the near future, including:

1. In this study, we used only the NDVI index as a predictor in a machine learning classification model. In future, we shall incorporate other indices using the same IB fusion approach and evaluate the performance.
2. This study was implemented at a local scale and while we recognize the importance of local datasets, it is hoped that the methodology can be scaled up to national and global scales. There are of course many factors that may restrict wholesale application of the method as-is but the overarching goal is to have a method that is easily operationalized. Using a simple index like NDVI has advantages with respect to inter- and trans-disciplinary cooperation. However, there are limitations that may arise as a result of data availability, computational resources and expertise.
3. The proliferation of crowd-sourced field photo libraries and the nearly universal coverage of Google Maps Street View provides an excellent opportunity for building the crop spectral library. We are currently evaluating this approach using the 2012 dataset for Chiba Prefecture and hope for positive results.

# Bibliography

- [1] S Abdikan, FB Sanli, M Ustuner, and F Calò. “Land cover mapping using Sentinel-1 SAR data”. In: *The International Archives of Photogrammetry, Remote Sensing and Spatial Information Sciences* 41 (2016), p. 757.
- [2] Rakesh Agrawal, Christos Faloutsos, and Arun Swami. “Efficient similarity search in sequence databases”. In: *International conference on foundations of data organization and algorithms*. Springer, Berlin, Heidelberg. 1993, pp. 69–84.
- [3] Adriana Allen. “Environmental planning and management of the peri-urban interface: perspectives on an emerging field”. In: *Environment and urbanization* 15.1 (2003), pp. 135–148.
- [4] WS Allen, JW Sorenson, and NK Person Jr. “Guide for Harvesting, Handling and Drying Peanuts.” In: *Leaflet/Texas Agricultural Extension Service; no. 1029*. (1971).
- [5] Luciano Alparone, Bruno Aiazzi, Stefano Baronti, and Andrea Garzelli. *Remote sensing image fusion*. Crc Press, 2015.
- [6] James Richard Anderson. *A land use and land cover classification system for use with remote sensor data*. Vol. 964. US Government Printing Office, 1976.

- [7] Kwasi Appeaning Addo. “Urban and peri-urban agriculture in developing countries studied using remote sensing and in situ methods”. In: *Remote Sensing* 2.2 (2010), pp. 497–513.
- [8] Dalila Attaf, Djamila Hamdadou, Sidahmed Benabderrahmane, and Aicha Lafrid. “Satellite Images Analysis with Symbolic Time Series: A Case Study of the Algerian Zone”. In: *arXiv preprint arXiv:1606.07784* (2016).
- [9] Gertrude Atukunda and Daniel Maxwell. “Farming in the city of Kampala: Issues for urban management”. In: *African Urban Quarterly* 11.2-3 (1996), pp. 264–275.
- [10] Clement Atzberger. “Advances in remote sensing of agriculture: Context description, existing operational monitoring systems and major information needs”. In: *Remote sensing* 5.2 (2013), pp. 949–981.
- [11] Etienne Bartholome and Allan S Belward. “GLC2000: a new approach to global land cover mapping from Earth observation data”. In: *International Journal of Remote Sensing* 26.9 (2005), pp. 1959–1977.
- [12] Mariana Belgiu and Ovidiu Csillik. “Sentinel-2 cropland mapping using pixel-based and object-based time-weighted dynamic time warping analysis”. In: *Remote sensing of environment* 204 (2018), pp. 509–523.
- [13] Chandrashekhara M Biradar, Prasad S Thenkabail, Praveen Noojipady, Yuanjie Li, Venkateswarlu Dheeravath, Hugh Turrall, Manohar Velpuri, Murali K Gumma, Obi Reddy P Gangalakunta, Xueliang L Cai, et al. “A global map of rainfed cropland areas (GMRCAs) at the end of last millennium using remote sensing”. In: *International journal of applied earth observation and geoinformation* 11.2 (2009), pp. 114–129.

- [14] JW Birch. “Rural Land Use and Location Theory: A Review”. In: *Economic Geography* 39.3 (1963), pp. 273–276.
- [15] S Bontemps, P Defourny, J Radoux, E Van Bogaert, C Lamarche, F Achard, P Mayaux, M Boettcher, C Brockmann, G Kirches, et al. “Consistent global land cover maps for climate modelling communities: current achievements of the ESA’s land cover CCI”. In: *Proceedings of the ESA Living Planet Symposium*. 2013, pp. 9–13.
- [16] Sophie Bontemps, Pierre Defourny, Eric V Bogaert, Olivier Arino, Vasileios Kalogirou, and Jose R Perez. *GLOBCOVER 2009 - Products description and validation report*. Tech. rep. Louvain-la-Neuve, Belgium: Université Catholique de Louvain and European Space Agency, 2011.
- [17] Sophie Bontemps, M Herold, L Kooistra, A Van Groenestijn, A Hartley, O Arino, Inès Moreau, and Pierre Defourny. “Revisiting land cover observation to address the needs of the climate modeling community.” In: *Biogeosciences* 9.6 (2012).
- [18] Goedele Van den Broeck and Miet Maertens. “Horticultural exports and food security in developing countries”. In: *Global food security* 10 (2016), pp. 11–20.
- [19] Kelly Bronson and Irena Knezevic. “Big Data in food and agriculture”. In: *Big Data & Society* 3.1 (2016), p. 2053951716648174.
- [20] Molly E Brown, Jorge E Pinzón, Kamel Didan, Jeffrey T Morisette, and Compton J Tucker. “Evaluation of the consistency of long-term NDVI time series derived from AVHRR, SPOT-vegetation, SeaWiFS, MODIS, and Landsat ETM+ sensors”. In: *IEEE Transactions on Geoscience and Remote Sensing* 44.7 (2006), pp. 1787–1793.

- [21] Toby N Carlson and David A Ripley. “On the relation between NDVI, fractional vegetation cover, and leaf area index”. In: *Remote sensing of Environment* 62.3 (1997), pp. 241–252.
- [22] Angela Katherine Castles. “A new identity for the peri-urban”. PhD thesis. University of Tasmania, 2014.
- [23] Kin-Pong Chan and Wai-Chee Fu. “Efficient time series matching by wavelets”. In: *icde*. IEEE. 1999, p. 126.
- [24] Bin Chen, Bo Huang, and Bing Xu. “Comparison of spatiotemporal fusion models: A review”. In: *Remote Sensing* 7.2 (2015), pp. 1798–1835.
- [25] Qing Cheng, Huanfeng Shen, Liangpei Zhang, and Zhenghong Peng. “Missing Information Reconstruction for Single Remote Sensing Images Using Structure-Preserving Global Optimization”. In: *IEEE Signal Processing Letters* 24.8 (2017), pp. 1163–1167.
- [26] Kenneth M Chomitz, Piet Buys, and Timothy S Thomas. *Quantifying the rural-urban gradient in Latin America and the Caribbean*. Vol. 3634. World Bank Publications, 2005.
- [27] Alexis Comber, Peter Fisher, and Richard Wadsworth. “What is land cover?” In: *Environment and Planning B: Planning and Design* 32.2 (2005), pp. 199–209.
- [28] William H Cooper, J Michael Donnelly, and Renée Johnson. “Japan’s 2011 earthquake and tsunami: economic effects and implications for the United States”. In: *Congressional research service* (2011).
- [29] Mihai Datcu, Klaus Seidel, Andrea Pelizzari, Michael Schroeder, Hubert Rehrauer, Gintautas Palubinskas, and Marc Walessa. “Image information mining and remote sensing data interpretation”. In: *Geoscience and*



- Remote Sensing Symposium, 2000. Proceedings. IGARSS 2000. IEEE 2000 International*. Vol. 7. IEEE. 2000, pp. 3057–3059.
- [30] RS DeFries and JRG Townshend. “NDVI-derived land cover classifications at a global scale”. In: *International Journal of Remote Sensing* 15.17 (1994), pp. 3567–3586.
- [31] Nicolas Delbart, Vaudour Emmanuelle, Maignan Fabienne, Ottlé Catherine, and Gilliot Jean-Marc. “Combining optical remote sensing, agricultural statistics and field observations for culture recognition over a peri-urban region”. In: *EGU General Assembly Conference Abstracts*. Vol. 19. 2017, p. 3585.
- [32] Antonio Di Gregorio. *Land cover classification system: classification concepts and user manual: LCCS*. Vol. 8. Food & Agriculture Org., 2005.
- [33] Donegan E. Finegold Y. Latham J. Jonckheere I. Di Gregorio A. Henry M. and Cumani R. *Land Cover Classification System: Software Version 3*. 2016. URL: <http://www.fao.org/3/a-i5232e.pdf>.
- [34] JW Dickens. “Peanut curing and post-harvest physiology”. In: *Peanuts Culture and Uses* (1973).
- [35] Ntwali Didier. “Comparison of spatial and temporal cloud coverage derived from CloudSat, CERES, ISCCP and their relationship with precipitation over Africa”. In: *Am J Remote Sens* 3.2 (2015), pp. 17–28.
- [36] Jean-Paul Donnay, Mike J Barnsley, and Paul A Longley. *Remote sensing and urban analysis: GISDATA 9*. CRC Press, 2014.
- [37] Peijun Du, Alim Samat, Björn Waske, Sicong Liu, and Zhenhong Li. “Random forest and rotation forest for fully polarized SAR image clas-

- sification using polarimetric and spatial features”. In: *ISPRS Journal of Photogrammetry and Remote Sensing* 105 (2015), pp. 38–53.
- [38] John S Duffield and Brian Woodall. “Japan’s new basic energy plan”. In: *Energy Policy* 39.6 (2011), pp. 3741–3749.
- [39] Christine Eigenbrod and Nazim Gruda. “Urban vegetable for food security in cities. A review”. In: *Agronomy for Sustainable Development* 35.2 (2015), pp. 483–498.
- [40] Erle C Ellis, Jed O Kaplan, Dorian Q Fuller, Steve Vavrus, Kees Klein Goldewijk, and Peter H Verburg. “Used planet: A global history”. In: *Proceedings of the National Academy of Sciences* (2013), p. 201217241.
- [41] Irina V Emelyanova, Tim R McVicar, Thomas G Van Niel, Ling Tao Li, and Albert IJM van Dijk. “Assessing the accuracy of blending Landsat–MODIS surface reflectances in two landscapes with contrasting spatial and temporal dynamics: A framework for algorithm selection”. In: *Remote Sensing of Environment* 133 (2013), pp. 193–209.
- [42] Kirsten L Findell, Elena Shevliakova, PCD Milly, and Ronald J Stouffer. “Modeled impact of anthropogenic land cover change on climate”. In: *Journal of Climate* 20.14 (2007), pp. 3621–3634.
- [43] DWJ Foeken and Alice Mboganie-Mwangi. *Increasing food security through urban farming in Nairobi*. DSE, Feldafing, 2000.
- [44] Giles M Foody. “Thematic map comparison”. In: *Photogrammetric Engineering & Remote Sensing* 70.5 (2004), pp. 627–633.
- [45] Gerald Forkuor and Olufunke Cofie. “Dynamics of land-use and land-cover change in Freetown, Sierra Leone and its effects on urban and peri-urban agriculture—a remote sensing approach”. In: *International Journal of Remote Sensing* 32.4 (2011), pp. 1017–1037.

- [46] Steffen Fritz, Ian McCallum, Christian Schill, Christoph Perger, Linda See, Dmitry Schepaschenko, Marijn Van der Velde, Florian Kraxner, and Michael Obersteiner. “Geo-Wiki: An online platform for improving global land cover”. In: *Environmental Modelling & Software* 31 (2012), pp. 110–123.
- [47] Feng Gao, William P Kustas, and Martha C Anderson. “A data mining approach for sharpening thermal satellite imagery over land”. In: *Remote Sensing* 4.11 (2012), pp. 3287–3319.
- [48] Feng Gao, Jeff Masek, Matt Schwaller, and Forrest Hall. “On the blending of the Landsat and MODIS surface reflectance: Predicting daily Landsat surface reflectance”. In: *IEEE Transactions on Geoscience and Remote sensing* 44.8 (2006), pp. 2207–2218.
- [49] Hassan Ghassemian. “A review of remote sensing image fusion methods”. In: *Information Fusion* 32 (2016), pp. 75–89.
- [50] Cristina Gómez, Joanne C White, and Michael A Wulder. “Optical remotely sensed time series data for land cover classification: A review”. In: *ISPRS Journal of Photogrammetry and Remote Sensing* 116 (2016), pp. 55–72.
- [51] George Grekousis, Giorgos Mountrakis, and Marinos Kavouras. “An overview of 21 global and 43 regional land-cover mapping products”. In: *International Journal of Remote Sensing* 36.21 (2015), pp. 5309–5335.
- [52] Åsa Gren and Erik Andersson. “Being efficient and green by rethinking the urban-rural divide—Combining urban expansion and food production by integrating an ecosystem service perspective into urban planning”. In: *Sustainable cities and society* 40 (2018), pp. 75–82.

- [53] Barry Haack and Ron Mahabir. “Relative value of radar and optical data for land cover/use mapping: Peru example”. In: *International Journal of Image and Data Fusion* 9.1 (2018), pp. 1–20.
- [54] Jiawei Han, Jian Pei, and Micheline Kamber. *Data mining: concepts and techniques*. Elsevier, 2011.
- [55] Pengyu Hao, Yulin Zhan, Li Wang, Zheng Niu, and Muhammad Shakir. “Feature selection of time series MODIS data for early crop classification using random forest: A case study in Kansas, USA”. In: *Remote Sensing* 7.5 (2015), pp. 5347–5369.
- [56] Onosato Masahiko Hori Masahiro Shiomi Kei Hashimoto Hidetoshiro Tadashi Takeo. “Development of High Accuracy Land Cover Classification Method Using Multiple Period Optical Observation Data”. In: *Journal of Japan Remote Sensing Society* 34.2 (2014), pp. 102–112.
- [57] Masatsugu Hayashi and Larry Hughes. “The policy responses to the Fukushima nuclear accident and their effect on Japanese energy security”. In: *Energy Policy* 59 (2013), pp. 86–101.
- [58] Khaled Hazaymeh and Quazi K Hassan. “Spatiotemporal image-fusion model for enhancing the temporal resolution of Landsat-8 surface reflectance images using MODIS images”. In: *Journal of Applied Remote Sensing* 9.1 (2015), p. 096095.
- [59] Konrad Hentze, Frank Thonfeld, and Gunter Menz. “Evaluating crop area mapping from MODIS time-series as an assessment tool for Zimbabwe’s “fast track land reform programme””. In: *PloS one* 11.6 (2016), e0156630.

- [60] Txomin Hermosilla, Michael A Wulder, Joanne C White, Nicholas C Coops, and Geordie W Hobart. “An integrated Landsat time series protocol for change detection and generation of annual gap-free surface reflectance composites”. In: *Remote Sensing of Environment* 158 (2015), pp. 220–234.
- [61] Shuji Hisano. “Food security politics and alternative agri-food initiatives in Japan”. In: *Kyoto University Graduate School of Economics* (2015).
- [62] Richard A Houghton, Jo I House, Julia Pongratz, Guido R Van Der Werf, Ruth S DeFries, Mathew C Hansen, C Le Quéré, and Navin Ramankutty. “Carbon emissions from land use and land-cover change”. In: *Biogeosciences* 9.12 (2012), pp. 5125–5142.
- [63] David L Iaquina, Axel W Drescher, et al. “Defining the peri-urban: rural-urban linkages and institutional connections”. In: *Land reform* 2 (2000), pp. 8–27.
- [64] Toshichika Iizumi and Navin Ramankutty. “How do weather and climate influence cropping area and intensity?” In: *Global Food Security* 4 (2015), pp. 46–50.
- [65] Markus Immitzer, Francesco Vuolo, and Clement Atzberger. “First experience with Sentinel-2 data for crop and tree species classifications in central Europe”. In: *Remote Sensing* 8.3 (2016), p. 166.
- [66] Jordi Inglada, Marcela Arias, Benjamin Tardy, Olivier Hagolle, Silvia Valero, David Morin, Gérard Dedieu, Guadalupe Sepulcre, Sophie Bontemp, Pierre Defourny, et al. “Assessment of an operational system for crop type map production using high temporal and spatial resolution

- satellite optical imagery”. In: *Remote Sensing* 7.9 (2015), pp. 12356–12379.
- [67] JAXA. *High Resolution Land Use and Land Cover Map Products*. Sept. 2018. URL: [https://www.eorc.jaxa.jp/ALOS/en/lulc/data/index.htm#vietnam\\_v18.09](https://www.eorc.jaxa.jp/ALOS/en/lulc/data/index.htm#vietnam_v18.09).
- [68] Gao Jie. “Data Mining from Remote Sensing Snow and Vegetation Product”. In: *Advances in Data Mining Knowledge Discovery and Applications*. InTech, 2012.
- [69] Renée Johnson. “Japan’s 2011 earthquake and tsunami: Food and agriculture implications”. In: *Current Politics and Economics of Northern and Western Asia* 20.4 (2011), p. 651.
- [70] Andreea Julea, Nicolas Méger, Philippe Bolon, Christophe Rigotti, Marie-Pierre Doin, Cécile Lasserre, Emmanuel Trouvé, and Vasile N Lazarescu. “Unsupervised spatiotemporal mining of satellite image time series using grouped frequent sequential patterns”. In: *IEEE Transactions on Geoscience and Remote Sensing* 49.4 (2011), pp. 1417–1430.
- [71] Yves Julien and José A Sobrino. “Comparison of cloud-reconstruction methods for time series of composite NDVI data”. In: *Remote Sensing of Environment* 114.3 (2010), pp. 618–625.
- [72] ZD Kalensky. “AFRICOVER land cover database and map of Africa”. In: *Canadian journal of remote sensing* 24.3 (1998), pp. 292–297.
- [73] Jed O Kaplan, Kristen M Krumhardt, Erle C Ellis, William F Rudiman, Carsten Lemmen, and Kees Klein Goldewijk. “Holocene carbon emissions as a result of anthropogenic land cover change”. In: *The Holocene* 21.5 (2011), pp. 775–791.

- [74] Rajmita Kar, GP Obi Reddy, Nirmal Kumar, and SK Singh. “Monitoring spatio-temporal dynamics of urban and peri-urban landscape using remote sensing and GIS—A case study from Central India”. In: *The Egyptian Journal of Remote Sensing and Space Science* (2018).
- [75] BK Kenduiywo, D Bargiel, and U Soergel. “Spatial-temporal conditional random fields crop classification from TerraSAR-X Images.” In: *ISPRS Annals of Photogrammetry, Remote Sensing & Spatial Information Sciences* 2 (2015).
- [76] Eamonn J Keogh and Michael J Pazzani. “Scaling up dynamic time warping for datamining applications”. In: *Proceedings of the sixth ACM SIGKDD international conference on Knowledge discovery and data mining*. ACM. 2000, pp. 285–289.
- [77] Jeremy T Kerr and Marsha Ostrovsky. “From space to species: ecological applications for remote sensing”. In: *Trends in ecology & evolution* 18.6 (2003), pp. 299–305.
- [78] Kees Klein Goldewijk, Arthur Beusen, Gerard Van Drecht, and Martine De Vos. “The HYDE 3.1 spatially explicit database of human-induced global land-use change over the past 12,000 years”. In: *Global Ecology and Biogeography* 20.1 (2011), pp. 73–86.
- [79] Steven M Kloiber, Robb D Macleod, Aaron J Smith, Joseph F Knight, and Brian J Huberty. “A semi-automated, multi-source data fusion update of a wetland inventory for east-central Minnesota, USA”. In: *Wetlands* 35.2 (2015), pp. 335–348.
- [80] Nataliia Kussul, Andrii Shelestov, Mykola Lavreniuk, Alexei Novikov, and Bohdan Yailymov. “Fusion Of Sentinel-1A And Sentinel-1B Data To Discover Of Crop Planting And Crop Phenology Phases”. In: (2017).

- [81] Celine Lamarche, Sophie Bontemps, Astrid Verhegghen, Jullien Radoux, Eric Vanbogaert, Vasileios Kalogirou, Frank Martin Seifert, Olivier Arino, and Pierre Defourny. “Characterizing The Surface Dynamics For Land Cover Mapping: Current Achievements Of The ESA CCI Land Cover”. In: *ESA Special Publication 72279* (2013).
- [82] Marie-Julie Lambert, François Waldner, and Pierre Defourny. “Crop-land mapping over Sahelian and Sudanian agrosystems: A knowledge-based approach using PROBA-V time series at 100-m”. In: *Remote Sensing* 8.3 (2016), p. 232.
- [83] Valentine Lebourgeois, Stéphane Dupuy, Élodie Vintrou, Maël Ameline, Suzanne Butler, and Agnès Bégué. “A combined random forest and OBIA classification scheme for mapping smallholder agriculture at different nomenclature levels using multisource data (simulated Sentinel-2 time series, VHRS and DEM)”. In: *Remote Sensing* 9.3 (2017), p. 259.
- [84] Diana Lee-Smith and Pyar Ali Memon. *Kenya. Urban agriculture in Kenya*. 1994.
- [85] Antoine Lefebvre. *Feasibility study about the mapping and monitoring of green linear features based on VHR*. Tech. rep. Systèmes d’Information à Référence Spatiale (SIRS), 2014. URL: <https://land.copernicus.eu/user-corner/technical-library/study-lead-by-sirs>.
- [86] Erika Lepers, Eric F Lambin, Anthony C Janetos, Ruth DeFries, Frédéric Achard, Navin Ramankutty, and Robert J Scholes. “A synthesis of information on rapid land-cover change for the period 1981–2000”. In: *AIBS Bulletin* 55.2 (2005), pp. 115–124.



- [87] Le Li, Yaolong Zhao, Yingchun Fu, Yaozhong Pan, Le Yu, and Qinchuan Xin. “High resolution mapping of cropping cycles by fusion of landsat and MODIS data”. In: *Remote Sensing* 9.12 (2017), p. 1232.
- [88] Chunhua Liao, Jinfei Wang, Ian Pritchard, Jianguo Liu, and Jiali Shang. “A spatio-temporal data fusion model for generating NDVI time series in heterogeneous regions”. In: *Remote Sensing* 9.11 (2017), p. 1125.
- [89] Martin Liggins II, David Hall, and James Llinas. *Handbook of multi-sensor data fusion: theory and practice*. CRC press, 2017.
- [90] Thomas Lillesand, Ralph W Kiefer, and Jonathan Chipman. *Remote sensing and image interpretation*. John Wiley & Sons, 2014.
- [91] Jessica Lin, Eamonn Keogh, Li Wei, and Stefano Lonardi. “Experiencing SAX: a novel symbolic representation of time series”. In: *Data Mining and knowledge discovery* 15.2 (2007), pp. 107–144.
- [92] David B Lobell and Gregory P Asner. “Cropland distributions from temporal unmixing of MODIS data”. In: *Remote Sensing of Environment* 93.3 (2004), pp. 412–422.
- [93] F Löw, U Michel, S Dech, and C Conrad. “Impact of feature selection on the accuracy and spatial uncertainty of per-field crop classification using support vector machines”. In: *ISPRS journal of photogrammetry and remote sensing* 85 (2013), pp. 102–119.
- [94] Shuaib Lwasa, Frank Mugagga, Bolanle Wahab, David Simon, John Connors, and Corrie Griffith. “Urban and peri-urban agriculture and forestry: Transcending poverty alleviation to climate change mitigation and adaptation”. In: *Urban Climate* 7 (2014), pp. 92–106.

- [95] M Mattingly and A Allen. *Living Between Urban and Rural Areas: Guidelines for Strategic Environment Planning and Management of the Peri-Urban Interface*. 2001.
- [96] Nicolas Matton, Guadalupe Sepulcre Canto, François Waldner, Silvia Valero, David Morin, Jordi Inglada, Marcela Arias, Sophie Bontemps, Benjamin Koetz, and Pierre Defourny. “An automated method for annual cropland mapping along the season for various globally-distributed agrosystems using high spatial and temporal resolution time series”. In: *Remote Sensing* 7.10 (2015), pp. 13208–13232.
- [97] Beacon Mbiba and Marie Huchzermeyer. “Contentious development: peri-urban studies in sub-Saharan Africa”. In: *Progress in Development Studies* 2.2 (2002), pp. 113–131.
- [98] Roger M McCoy. *Field methods in remote sensing*. Guilford Press, 2005.
- [99] Duncan McGregor and David Simon. *The peri-urban interface: Approaches to sustainable natural and human resource use*. Routledge, 2012.
- [100] Koreen Millard and Murray Richardson. “On the importance of training data sample selection in random forest image classification: A case study in peatland ecosystem mapping”. In: *Remote sensing* 7.7 (2015), pp. 8489–8515.
- [101] John Monteith and Mike Unsworth. *Principles of environmental physics*. Academic Press, 2007.
- [102] Brice Mora, Nandin-Erdene Tsendbazar, Martin Herold, and Olivier Arino. “Global land cover mapping: Current status and future trends”. In: *Land Use and Land Cover Mapping in Europe*. Springer, 2014, pp. 11–30.

- [103] Luc JA Mougeot. “Urban agriculture: Definition, presence, potentials and risks, and policy challenges”. In: *Cities feeding people series; rept.* 31 (2000).
- [104] Bouchra Nechad, Aida Alvera-Azcaràte, Kevin Ruddick, and Naomi Greenwood. “Reconstruction of MODIS total suspended matter time series maps by DINEOF and validation with autonomous platform data”. In: *Ocean Dynamics* 61.8 (2011), pp. 1205–1214.
- [105] Okada Norio, Tao Ye, Yoshio Kajitani, Peijun Shi, and Hirokazu Tatano. “The 2011 eastern Japan great earthquake disaster: Overview and comments”. In: *International Journal of Disaster Risk Science* 2.1 (2011), pp. 34–42.
- [106] Davide Notti, Fabiana Calò, Francesca Cigna, Michele Manunta, Gerardo Herrera, Matteo Berti, Claudia Meisina, Deodato Tapete, and Francesco Zucca. “A user-oriented methodology for DInSAR time series analysis and interpretation: Landslides and subsidence case studies”. In: *Pure and Applied Geophysics* 172.11 (2015), pp. 3081–3105.
- [107] I Wayan Nuarsa, Fumihiko Nishio, and Chiharu Hongo. “Spectral Characteristics and Mapping of Rice Plants Using Multi-Temporal Landsat Data”. In: *Journal of Agricultural Science* 3.1 (2011).
- [108] A. J. Oliphant, P. S. Thenkabail, P. Teluguntla, J. Xiong, R. G. Congalton, K. Yadav, R. Massey, M. K. Gumma, and C. Smith. “NASA Making Earth System Data Records for Use in Research Environments (MEaSUREs) Global Food Security-support Analysis Data (GFSAD) Cropland Extent 2015 Southeast Asia 30 m V001”. In: *NASA EOSDIS Land Processes DAAC* (2017).

- [109] Ina Opitz, Regine Berges, Annette Piorr, and Thomas Krikser. “Contributing to food security in urban areas: Differences between urban agriculture and peri-urban agriculture in the Global North”. In: *Agriculture and Human Values* 33.2 (2016), pp. 341–358.
- [110] Francesco Orsini, Daniela Gasperi, Livia Marchetti, Chiara Piovene, Stefano Draghetti, Solange Ramazzotti, Giovanni Bazzocchi, and Giorgio Gianquinto. “Exploring the production capacity of rooftop gardens (RTGs) in urban agriculture: the potential impact on food and nutrition security, biodiversity and other ecosystem services in the city of Bologna”. In: *Food Security* 6.6 (2014), pp. 781–792.
- [111] Jong-Geol PARK, Ryutaro TATEISHI, and Masayuki MATSUOKA. “A proposal of the Temporal Window Operation (TWO) method to remove high-frequency noises in AVHRR NDVI time series data”. In: *Journal of the Japan Society of Photogrammetry and Remote Sensing* 38.5 (1999), pp. 36–47.
- [112] Janila Pasupuleti, SN Nigam, Manish K Pandey, P Nagesh, and Rajeev K Varshney. “Groundnut improvement: use of genetic and genomic tools”. In: *Frontiers in plant science* 4 (2013), p. 23.
- [113] François Petitjean, Pierre Gançarski, Florent Masegla, and Germain Forestier. “Analysing satellite image time series by means of pattern mining”. In: *International Conference on Intelligent Data Engineering and Automated Learning*. Springer. 2010, pp. 45–52.
- [114] Christine Pohl and John van Genderen. “Structuring contemporary remote sensing image fusion”. In: *International Journal of Image and Data Fusion* 6.1 (2015), pp. 3–21.

- [115] Christine Pohl and John Van Genderen. *Remote sensing image fusion: A practical guide*. Crc Press, 2016.
- [116] Cle Pohl and John L Van Genderen. “Review article multisensor image fusion in remote sensing: concepts, methods and applications”. In: *International journal of remote sensing* 19.5 (1998), pp. 823–854.
- [117] Julia Pongratz, Christian Reick, Thomas Raddatz, and Martin Claussen. “A reconstruction of global agricultural areas and land cover for the last millennium”. In: *Global Biogeochemical Cycles* 22.3 (2008).
- [118] John R Porter, Robert Dyball, David Dumaresq, Lisa Deutsch, and Hiroataka Matsuda. “Feeding capitals: Urban food security and self-provisioning in Canberra, Copenhagen and Tokyo”. In: *Global food security* 3.1 (2014), pp. 1–7.
- [119] Niraj Priyadarshi, VM Chowdary, YK Srivastava, Iswar Chandra Das, and Chandra Shekhar Jha. “Reconstruction of time series MODIS EVI data using de-noising algorithms”. In: *Geocarto International* 33.10 (2018), pp. 1095–1113.
- [120] Navin Ramankutty and Jonathan A Foley. “Characterizing patterns of global land use: An analysis of global croplands data”. In: *Global Biogeochemical Cycles* 12.4 (1998), pp. 667–685.
- [121] Navin Ramankutty and Jonathan A Foley. “Estimating historical changes in global land cover: Croplands from 1700 to 1992”. In: *Global biogeochemical cycles* 13.4 (1999), pp. 997–1027.
- [122] Fabrizio Ramoino, Florin Tutunaru, Fabrizio Pera, and Olivier Arino. “Ten-Meter Sentinel-2A Cloud-Free Composite—Southern Africa 2016”. In: *Remote Sensing* 9.7 (2017), p. 652.

- [123] John Alan Richards. *Remote sensing digital image analysis: an introduction*. 5th. Heidelberg: Springer, 2013.
- [124] John Rogan and DongMei Chen. “Remote sensing technology for mapping and monitoring land-cover and land-use change”. In: *Progress in planning* 61.4 (2004), pp. 301–325.
- [125] Maria Esther Sanz Sanz, Davide Martinetti, and Claude Napoleone. “Operational modelling of peri-urban farmland for food planning in Mediterranean region”. In: *8. Annual Conference of the AESOP Sustainable Food Planning group*. 2017, 159–p.
- [126] Michael Schmitt, Florence Tupin, and Xiao Xiang Zhu. “Fusion of SAR and optical remote sensing data—Challenges and recent trends”. In: *Geoscience and Remote Sensing Symposium (IGARSS), 2017 IEEE International*. IEEE. 2017, pp. 5458–5461.
- [127] Michael Schmitt and Xiao Xiang Zhu. “Data fusion and remote sensing: An ever-growing relationship”. In: *IEEE Geoscience and Remote Sensing Magazine* 4.4 (2016), pp. 6–23.
- [128] Annemarie Schneider. “Monitoring land cover change in urban and peri-urban areas using dense time stacks of Landsat satellite data and a data mining approach”. In: *Remote Sensing of Environment* 124 (2012), pp. 689–704.
- [129] Annemarie Schneider and Curtis E Woodcock. “Compact, dispersed, fragmented, extensive? A comparison of urban growth in twenty-five global cities using remotely sensed data, pattern metrics and census information”. In: *Urban Studies* 45.3 (2008), pp. 659–692.
- [130] Robert A Schowengerdt. *Remote sensing: models and methods for image processing*. Elsevier, 2006.

- [131] Linda See, Steffen Fritz, Liangzhi You, Navin Ramankutty, Mario Hertero, Chris Justice, Inbal Becker-Reshef, Philip Thornton, Karlheinz Erb, Peng Gong, et al. “Improved global cropland data as an essential ingredient for food security”. In: *Global Food Security* 4 (2015), pp. 37–45.
- [132] Yang Shao, Ross S Lunetta, Jayantha Ediriwickrema, and John Liames. “Mapping cropland and major crop types across the Great Lakes Basin using MODIS-NDVI data”. In: *Photogrammetric Engineering & Remote Sensing* 76.1 (2010), pp. 73–84.
- [133] Huanfeng Shen, Xinghua Li, Qing Cheng, Chao Zeng, Gang Yang, Huifang Li, and Liangpei Zhang. “Missing information reconstruction of remote sensing data: A technical review”. In: *IEEE Geoscience and Remote Sensing Magazine* 3.3 (2015), pp. 61–85.
- [134] Michal Shimoni, Juanfran Lopez, Y Forget, Eléonore Wolff, C Michelier, Taïs Grippa, Catherine Linard, and M Gilbert. “An urban expansion model for African cities using fused multi temporal optical and SAR data”. In: *2015 IEEE International Geoscience and Remote Sensing Symposium (IGARSS)*. IEEE. 2015, pp. 1159–1162.
- [135] Bipasha Paul Shukla, PK Pal, and PC Joshi. “A novel approach for selective reconstruction of cloud-contaminated satellite images”. In: *Journal of Atmospheric and Oceanic Technology* 28.8 (2011), pp. 1028–1035.
- [136] Marcelino Pereira S Silva, Gilberto Câmara, Ricardo Cartaxo M Souza, Dalton M Valeriano, and Maria Isabel Sobral Escada. “Mining patterns of change in remote sensing image databases”. In: *Data Mining, Fifth IEEE International Conference on*. IEEE. 2005, 8–pp.

- [137] David Simon. “Urban environments: issues on the peri-urban fringe”. In: *Annual review of environment and resources* 33 (2008), pp. 167–185.
- [138] David Simon and Friedrich Schiemer. “Crossing boundaries: complex systems, transdisciplinarity and applied impact agendas”. In: *Current Opinion in Environmental Sustainability* 12 (2015), pp. 6–11.
- [139] Anne HS Solberg. “Data fusion for remote sensing applications”. In: *Signal and image processing for remote sensing* (2006), pp. 249–271.
- [140] Qian Song, Qiong Hu, Qingbo Zhou, Ciara Hovis, Mingtao Xiang, Hua-jun Tang, and Wenbin Wu. “In-Season Crop Mapping with GF-1/WFV Data by Combining Object-Based Image Analysis and Random Forest”. In: *Remote Sensing* 9.11 (2017), p. 1184.
- [141] Wei Song, Bryan C Pijanowski, and Amin Tayyebi. “Urban expansion and its consumption of high-quality farmland in Beijing, China”. In: *Ecological indicators* 54 (2015), pp. 60–70.
- [142] Rei Sonobe, Hiroshi Tani, Xiufeng Wang, Nobuyuki Kobayashi, and Hideki Shimamura. “Random forest classification of crop type using multi-temporal TerraSAR-X dual-polarimetric data”. In: *Remote Sensing Letters* 5.2 (2014), pp. 157–164.
- [143] Sean Sweeney, Tatyana Ruseva, Lyndon Estes, and Tom Evans. “Mapping cropland in smallholder-dominated savannas: integrating remote sensing techniques and probabilistic modeling”. In: *Remote Sensing* 7.11 (2015), pp. 15295–15317.
- [144] Cecilia Tacoli. “Rural-urban interactions: a guide to the literature”. In: *Environment and urbanization* 10.1 (1998), pp. 147–166.



- [145] Masuo Takahashi, Kenlo Nishida Nasahara, Takeo Tadono, Tomohiro Watanabe, Masanori Dotsu, Toshiro Sugimura, and Nobuhiro Tomiyama. “JAXA high resolution land-use and land-cover map of Japan”. In: *Geoscience and Remote Sensing Symposium (IGARSS), 2013 IEEE International*. IEEE. 2013, pp. 2384–2387.
- [146] Kenichi Tatsumi, Yosuke Yamashiki, Miguel Angel Canales Torres, and Cayo Leonidas Ramos Taipe. “Crop classification of upland fields using Random forest of time-series Landsat 7 ETM+ data”. In: *Computers and Electronics in Agriculture* 115 (2015), pp. 171–179.
- [147] Pardhasaradhi G Teluguntla, Prasad S Thenkabail, Jun Xiong, Murali Krishna Gumma, Chandra Giri, Cristina Milesi, Mutlu Ozdogan, Russ Congalton, James Tilton, Temuulen Tsagaan Sankey, et al. “Global cropland area database (GCAD) derived from remote sensing in support of food security in the twenty-first century: current achievements and future possibilities”. In: *Land resources: monitoring, modelling, and mapping, Taylor & Francis, Boca Raton, Florida, available at: <http://pubs.er.usgs.gov/publication/70117684>* (2015).
- [148] Rajesh Bahadur Thapa and Yuji Murayama. “Land evaluation for peri-urban agriculture using analytical hierarchical process and geographic information system techniques: A case study of Hanoi”. In: *Land use policy* 25.2 (2008), pp. 225–239.
- [149] AL Thebo, Pay Drechsel, and EF Lambin. “Global assessment of urban and peri-urban agriculture: irrigated and rainfed croplands”. In: *Environmental Research Letters* 9.11 (2014), p. 114002.

- [150] Alexander Thornton. “Beyond the metropolis: Small town case studies of urban and peri-urban agriculture in South Africa”. In: *Urban forum*. Vol. 19. 3. Springer. 2008, p. 243.
- [151] Joy Tivy. *Agricultural ecology*. Routledge, 2014.
- [152] L Toma, AP Barnes, L-A Sutherland, S Thomson, F Burnett, and K Mathews. “Impact of information transfer on farmers’ uptake of innovative crop technologies: a structural equation model applied to survey data”. In: *The Journal of Technology Transfer* (2016), pp. 1–18.
- [153] Nathan Torbick, Xiaodong Huang, Beth Ziniti, David Johnson, Jeff Masek, and Michele Reba. “Fusion of Moderate Resolution Earth Observations for Operational Crop Type Mapping”. In: *Remote Sensing* 10.7 (2018), p. 1058.
- [154] Compton J Tucker, Jorge E Pinzon, Molly E Brown, Daniel A Slayback, Edwin W Pak, Robert Mahoney, Eric F Vermote, and Nazmi El Saleous. “An extended AVHRR 8-km NDVI dataset compatible with MODIS and SPOT vegetation NDVI data”. In: *International Journal of Remote Sensing* 26.20 (2005), pp. 4485–4498.
- [155] Kristof Van Tricht, Anne Gobin, Sven Gilliams, and Isabelle Piccard. “Synergistic use of radar Sentinel-1 and optical Sentinel-2 imagery for crop mapping: a case study for Belgium”. In: *Remote Sensing* 10.10 (2018), p. 1642.
- [156] Murali T Variath and P Janila. “Economic and Academic Importance of Peanut”. In: *The Peanut Genome*. Springer, 2017, pp. 7–26.
- [157] S Velickov, DP Solomatine, X Yu, and RK Price. “Application of data mining techniques for remote sensing image analysis”. In: *Proc. 4th Int. Conference on Hydroinformatics, USA*. 2000.

- [158] Michel Verleysen and Damien François. “The curse of dimensionality in data mining and time series prediction”. In: *International Work-Conference on Artificial Neural Networks*. Springer. 2005, pp. 758–770.
- [159] Diego Vidaurre, Iead Rezek, Samuel L Harrison, Stephen S Smith, and Mark Woolrich. “Dimensionality reduction for time series data”. In: *arXiv preprint arXiv:1406.3711* (2014).
- [160] Gemine Vivone, Rocco Restaino, Mauro Dalla Mura, Giorgio Licciardi, and Jocelyn Chanussot. “Contrast and error-based fusion schemes for multispectral image pansharpening”. In: *IEEE Geoscience and Remote Sensing Letters* 11.5 (2014), pp. 930–934.
- [161] MFA Vogels, Steven M De Jong, Geert Sterk, and Elisabeth A Addink. “Agricultural cropland mapping using black-and-white aerial photography, object-based image analysis and random forests”. In: *International Journal of Applied Earth Observation and Geoinformation* 54 (2017), pp. 114–123.
- [162] François Waldner, Steffen Fritz, Antonio Di Gregorio, and Pierre Defourny. “Mapping priorities to focus cropland mapping activities: Fitness assessment of existing global, regional and national cropland maps”. In: *Remote Sensing* 7.6 (2015), pp. 7959–7986.
- [163] François Waldner, Diego De Aballeyra, Santiago R Verón, Miao Zhang, Bingfang Wu, Dmitry Plotnikov, Sergey Bartalev, Mykola Lavreniuk, Sergii Skakun, and Nataliia Kussul. “Towards a set of agrosystem-specific cropland mapping methods to address the global cropland diversity”. In: *International Journal of Remote Sensing* 37.14 (2016), pp. 3196–3231.

- [164] Li'ai Wang, Xudong Zhou, Xinkai Zhu, Zhaodi Dong, and Wenshan Guo. "Estimation of biomass in wheat using random forest regression algorithm and remote sensing data". In: *The Crop Journal* 4.3 (2016), pp. 212–219.
- [165] Qunming Wang and Peter M Atkinson. "Spatio-temporal fusion for daily sentinel-2 images". In: *Remote Sensing of Environment* 204 (2018), pp. 31–42.
- [166] Anna WATANABE. "Agricultural impact of the nuclear accidents in Fukushima: the case of Ibaraki Prefecture". In: *DISASTER, INFRASTRUCTURE AND SOCIETY: Learning from the 2011 Earthquake in Japan Disaster foundation - Thinking from the Great East Japan Earthquake* 1 (2011), pp. 291–298.
- [167] Jennifer D Watts, Scott L Powell, Rick L Lawrence, and Thomas Hilker. "Improved classification of conservation tillage adoption using high temporal and synthetic satellite imagery". In: *Remote Sensing of Environment* 115.1 (2011), pp. 66–75.
- [168] Wei Wei, Wenbin Wu, Zhengguo Li, Peng Yang, and Qingbo Zhou. "Selecting the optimal NDVI time-series reconstruction technique for crop phenology detection". In: *Intelligent Automation & Soft Computing* 22.2 (2016), pp. 237–247.
- [169] Mingquan Wu, Chenghai Yang, Xiaoyu Song, Wesley Clint Hoffmann, Wenjiang Huang, Zheng Niu, Changyao Wang, Wang Li, and Bo Yu. "Monitoring cotton root rot by synthetic Sentinel-2 NDVI time series using improved spatial and temporal data fusion". In: *Scientific reports* 8.1 (2018), p. 2016.

- [170] Mingquan Wu, Xiaoyang Zhang, Wenjiang Huang, Zheng Niu, Changyao Wang, Wang Li, and Pengyu Hao. “Reconstruction of daily 30 m data from HJ CCD, GF-1 WFV, Landsat, and MODIS data for crop monitoring”. In: *Remote Sensing* 7.12 (2015), pp. 16293–16314.
- [171] Xiangming Xiao, Pavel Dorovskoy, Chandrashekhara Biradar, and Eli Bridge. “A library of georeferenced photos from the field”. In: *Eos, Transactions American Geophysical Union* 92.49 (2011), pp. 453–454.
- [172] Yichun Xie, Zongyao Sha, and Mei Yu. “Remote sensing imagery in vegetation mapping: a review”. In: *Journal of plant ecology* 1.1 (2008), pp. 9–23.
- [173] Tao Yang and Bill Hillier. “The fuzzy boundary: the spatial definition of urban areas”. In: *Proceedings, 6th International Space Syntax Symposium, İstanbul, 2007*. Istanbul Technical University. 2007, pp. 091–01.
- [174] Naoto Yokoya. “Texture-Guided Multisensor Superresolution for Remotely Sensed Images”. In: *Remote Sensing* 9.4 (2017), p. 316.
- [175] JAMES H Young, NK Person, JAMES O Donald, WILLIAM D Mayfield, HE Pattee, and CT Young. “Harvesting, curing, and energy utilization”. In: *Peanut Science and Technology. Yoakum, TX: American Peanut Research and Education Society* (1982), pp. 458–487.
- [176] Nicholas E Young, Ryan S Anderson, Stephen M Chignell, Anthony G Vorster, Rick Lawrence, and Paul H Evangelista. “A survival guide to Landsat preprocessing”. In: *Ecology* 98.4 (2017), pp. 920–932.
- [177] Ingo Zasada. “Multifunctional peri-urban agriculture—A review of societal demands and the provision of goods and services by farming”. In: *Land use policy* 28.4 (2011), pp. 639–648.

- [178] Ingo Zasada. “Peri-urban agriculture and multifunctionality: urban influence, farm adaptation behaviour and development perspectives”. PhD thesis. Technische Universität München, 2012.
- [179] Yongquan Zhao, Bo Huang, and Huihui Song. “A robust adaptive spatial and temporal image fusion model for complex land surface changes”. In: *Remote Sensing of Environment* 208 (2018), pp. 42–62.
- [180] Xiaolin Zhu, Eileen H Helmer, Feng Gao, Desheng Liu, Jin Chen, and Michael A Lefsky. “A flexible spatiotemporal method for fusing satellite images with different resolutions”. In: *Remote sensing of environment* 172 (2016), pp. 165–177.
- [181] Xiaolin Zhu, Jin Chen, Feng Gao, Xuehong Chen, and Jeffrey G Masek. “An enhanced spatial and temporal adaptive reflectance fusion model for complex heterogeneous regions”. In: *Remote Sensing of Environment* 114.11 (2010), pp. 2610–2623.
- [182] Xiaolin Zhu, Fangyi Cai, Jiaqi Tian, and Trecia Williams. “Spatiotemporal fusion of multisource remote sensing data: literature survey, taxonomy, principles, applications, and future directions”. In: *Remote Sensing* 10.4 (2018), p. 527.
- [183] Zhe Zhu, Curtis E Woodcock, John Rogan, and Josef Kellndorfer. “Assessment of spectral, polarimetric, temporal, and spatial dimensions for urban and peri-urban land cover classification using Landsat and SAR data”. In: *Remote Sensing of Environment* 117 (2012), pp. 72–82.
- [184] Hania Zlotnik. “World urbanization: trends and prospects”. In: *New Forms of Urbanization*. Routledge, 2017, pp. 43–64.

# Appendix

## A.1 Methodology Test Case: Kenya

### A.1.1 Introduction

It is estimated that approximately 40% of the total African population reside in urban areas and this proportion is set to grow due to major demographic and economic changes occurring in the region (Lwasa *et al.*, 2014; Zlotnik, 2017). According to Lee-Smith and Memon (1994), urban agriculture in Kenya is vital to the livelihoods of urban residents and more than two-thirds of urban farmers rely on subsistence farming which is characterized by poor investment and high intensity in small towns. High agricultural potential regions of Kenya, which are also densely populated, are located mainly around the central and western parts of the country as shown in Figure A.1.1 .

Mapping and monitoring of agriculture in Kenya, as in other parts of Africa, is not a continuous exercise due to low investment in research and development for smallholder subsistence farming and the resource intensive nature of such activities if conventional data collection methods are used ( Lee-Smith and Memon, 1994). Moreover, there are numerous challenges to agricultural production including floods, droughts, soil degradation, and pests and diseases,

all of which create an urgent need for continuous mapping and monitoring (Lwasa *et al.*, 2014). This therefore makes remote sensing particularly propitious since it provides repetitive, synoptic views of the earth and can provide a basis for reliable cropland mapping especially in the sub-Saharan savanna landscape (Sweeney *et al.*, 2015).

The application of fusion of multi-sensor optical remote sensing datasets towards agricultural mapping and monitoring has been demonstrated in this thesis, with respect to a study area in Japan which is located in the northern hemisphere. Whilst cloud cover is a major challenge for all optical remote sensing datasets, studies have shown that high spatial cloud cover is more frequent around the equator, due to stronger convection compared to other regions (Didier, 2015). Figure A.1.2 shows the relative spatial and temporal variations in the monthly percentage cloud cover for three regions in Africa. Precipitation is positively correlated with cloud cover and therefore, in the west African region, the rainy season is in June, July and August (JJA), in December, January and February (DJF) for south Africa and in both March, April and May (MAM) and September, October and November (SON) for east Africa (Didier, 2015). As most crop production in Africa is rainfed, the rainy seasons are crucial for agricultural monitoring. However, due to the high cloud cover, utilization of optical satellite imagery is severely limited.

Apart from cloud cover, an additional challenge with regards to missing data is prevalent in daily MODIS data over equatorial regions as shown in Figure A.1.3, due to daily variations in the satellites orbital path and geometry (Li *et al.*, 2017). This information can be reconstructed via composites such as the 8-day composite surface reflectance product. However, as shown in this thesis, the use of daily data for spatio-temporal fusion provides more reliable



synthetic data sets since the time series can be set to fully coincide with the available landsat images. For Kenya, this data gap is approximately 200 km and varies with time.

Evaluation of applicability of the methodology presented in this thesis within this area thus validates the operational framework for disparate geographical regions. Landsat and MODIS surface reflectance data covering the region depicted in Figure A.1.4 , with a relative distribution as shown in Figure A.1.5 , were acquired for the year 2016. Processing and analysis of the data was implemented as described in Chapter3 of this thesis. The next subsection presents the preliminary results of processing and analysis for the test study site in Kenya.

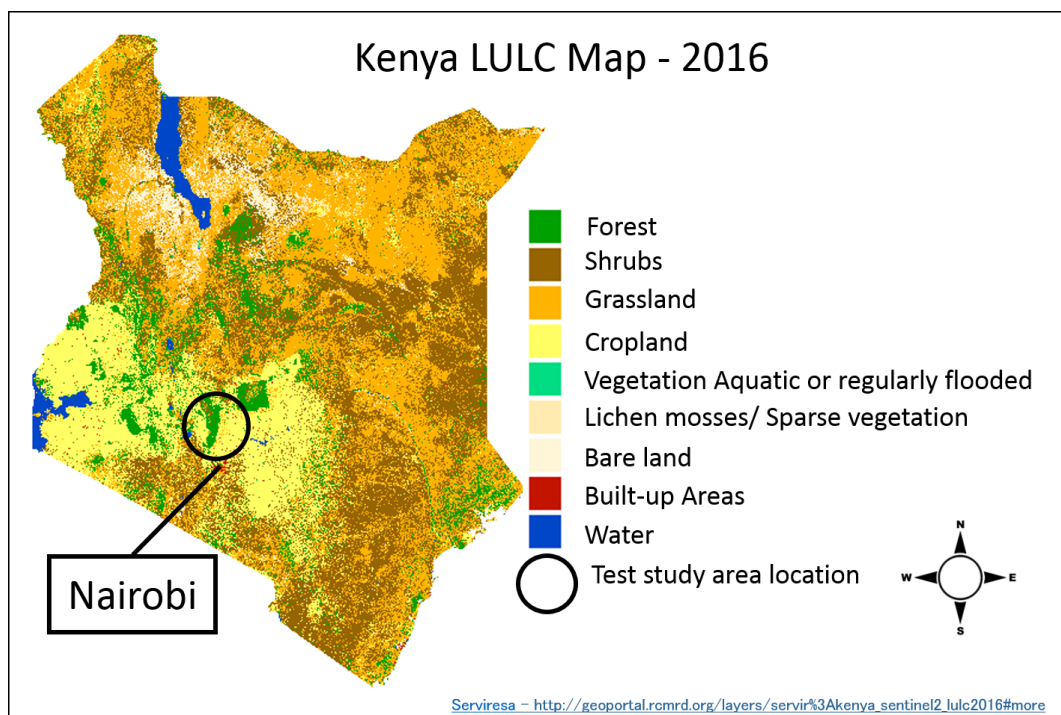


**Figure A.1.1** : The European Space Agency Climate Change Initiative (ESA CCI) Land use/ cover map of Kenya for 2016

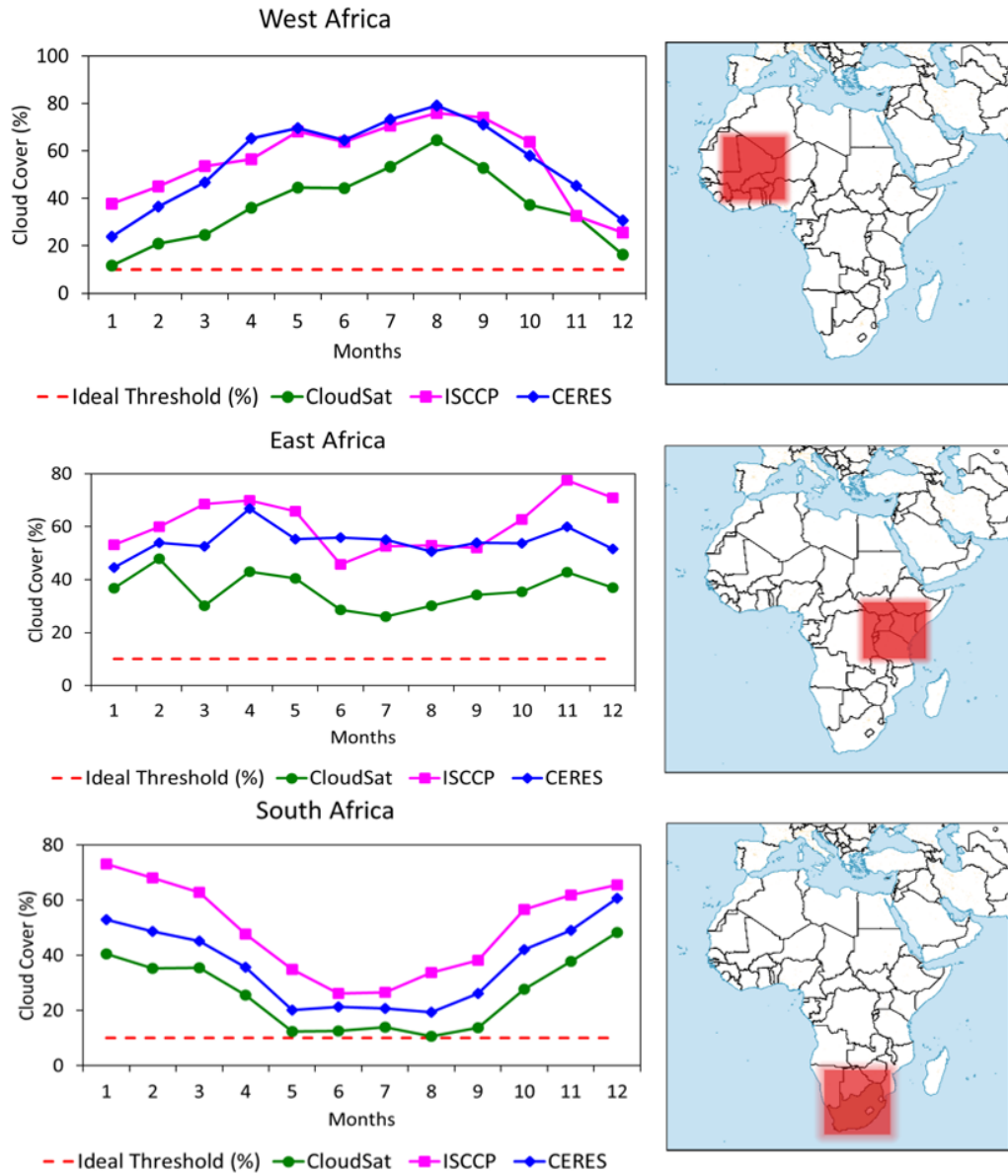
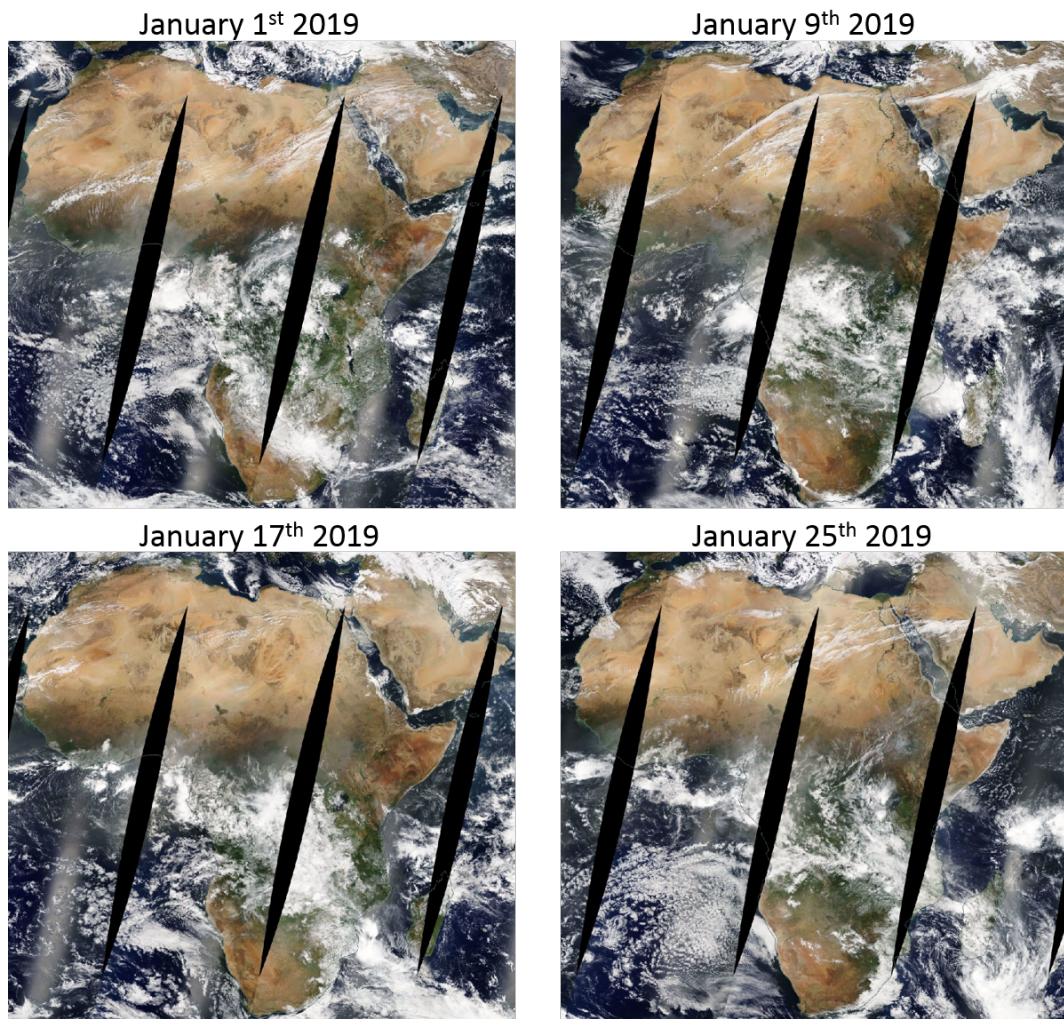


Figure A.1.2 : Percentage monthly total cloud cover in the west, east and southern Africa regions



**Figure A.1.3** : MODIS Terra daily corrected surface reflectance data for January 2019

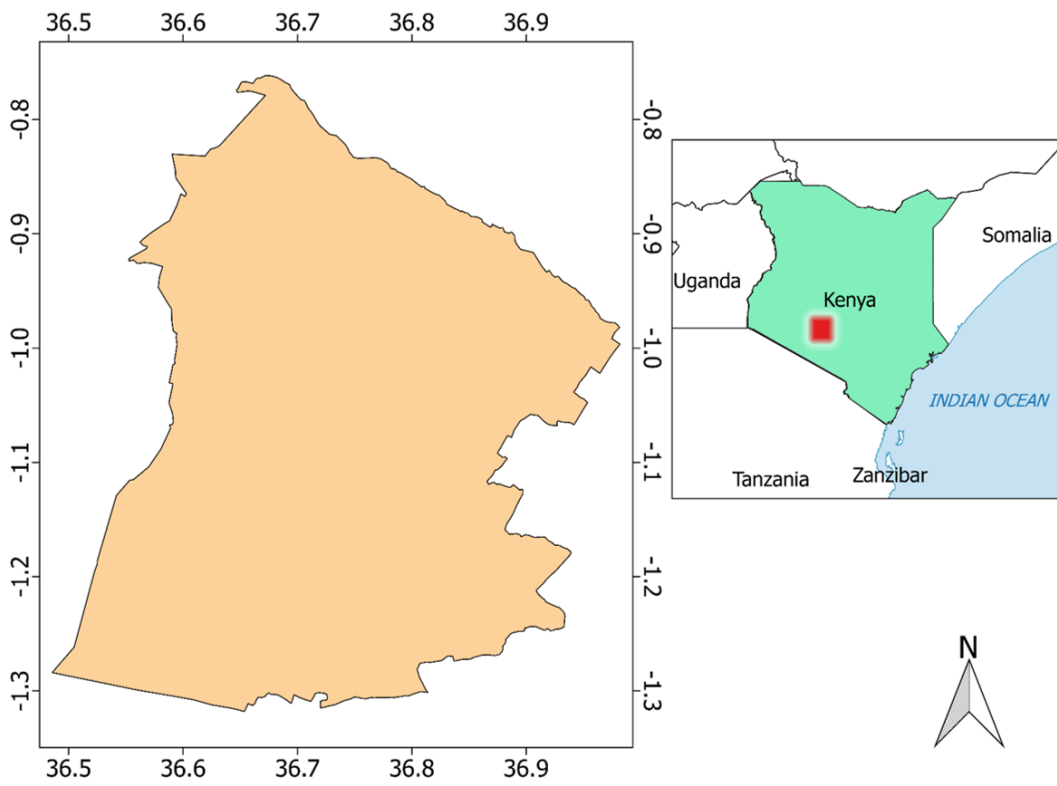
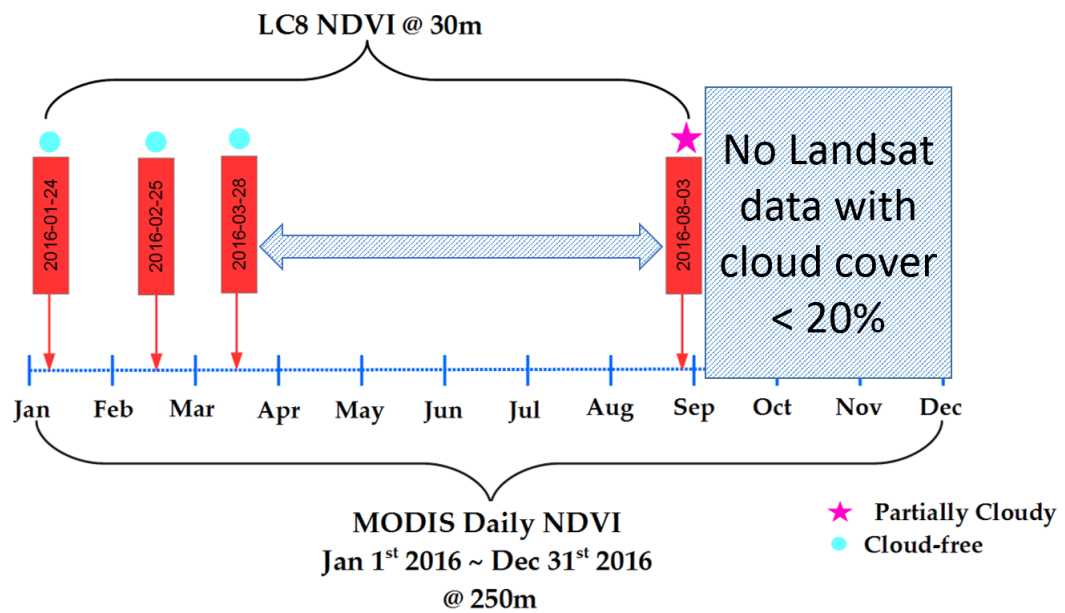


Figure A.1.4 : The test study area in Kenya located in the central highlands



**Figure A.1.5 :** Relative temporal distribution of Landsat and MODIS surface reflectance images acquired for the year 2016 for the Kenyan test study area

## A.1.2 Results of preliminary processing and analysis

### A.1.2.1 Spatio-temporal fusion

Spatio-temporal fusion of the daily MODIS and intermittent Landsat NDVI images was carried out with the four available Landsat images as the reference image pairs. The results of the quantitative assessment of the synthetic images generated by fusion, which also coincide with the reference image pairs are as shown in Figure A.1.6 . The January, February and March synthetic NDVI images have strong positive correlations with the observed Landsat NDVI images. However, the August synthetic image had a marginally positive correlation since the images used as reference pairs in its generation were those of February and March.

The results support the observations made in this thesis, that for generation of good synthetic images via spatio-temporal fusion, it is ideal to have reference image pairs that are temporally close to the prediction date. In this regard, it is the recommendation of this study that spatio-temporal fusion of images in this region should be carried out in a manner that maximizes the chances of acquiring cloud-free Landsat images. As such, a calendar year would not be ideal since the later part of the year, and especially during the planting and growing season, total percentage cloud cover tends to be high, as shown in Figure A.1.2 . Additional evaluation will be carried out using different configurations of annual data e.g. April-to-April using multi-year datasets.

### A.1.2.2 Land Use/Cover classification

Land use/cover classification of the eight-day synthetic NDVI time series was carried out using the Random Forest classifier, as described in Chapter 3 of this thesis. A collection of over 1000 reference points with labels derived from visual inspection of the Google Earth images of 2016 in the test site was used as the training and validation data with a 30:70 split. The land use/cover classes were:

1. Bare land
2. Coffee
3. Forest
4. Grassland
5. Other crop
6. Tea
7. Urban

An overall accuracy of 92.7% and kappa of 0.91 were obtained and Figure A.1.7 shows the land use/cover map including the cropland classes of coffee, tea and other crops. Further validation and refinement of the classification is necessary for two main reasons:

1. Empirical knowledge of cultivation practices was used to distinguish and therefore label the tea, coffee and other crop reference points.



2. Mixed cropping e.g. coffee and maize is common in the test site. More predictors are therefore necessary in order to effectively separate the annual crops such as maize and beans and the perennial crops such as coffee.

These preliminary results thus show that the operational framework presented in this thesis is robust. It can be applied with ease in regions with disparate geoclimatic conditions and agricultural practices to map and monitor croplands that are spatially and temporally heterogeneous and dynamic with regular high frequency.

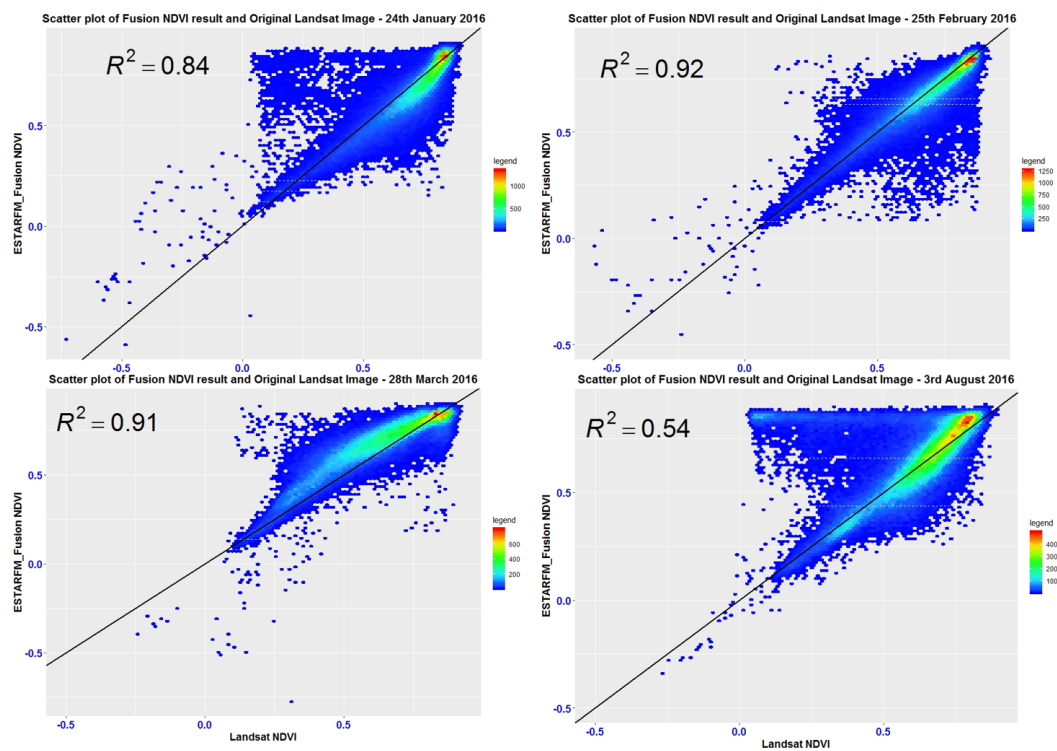


**Figure A.1.6 :** Scatterplots showing results of comparison of synthetic NDVI images with original Landsat NDVI images

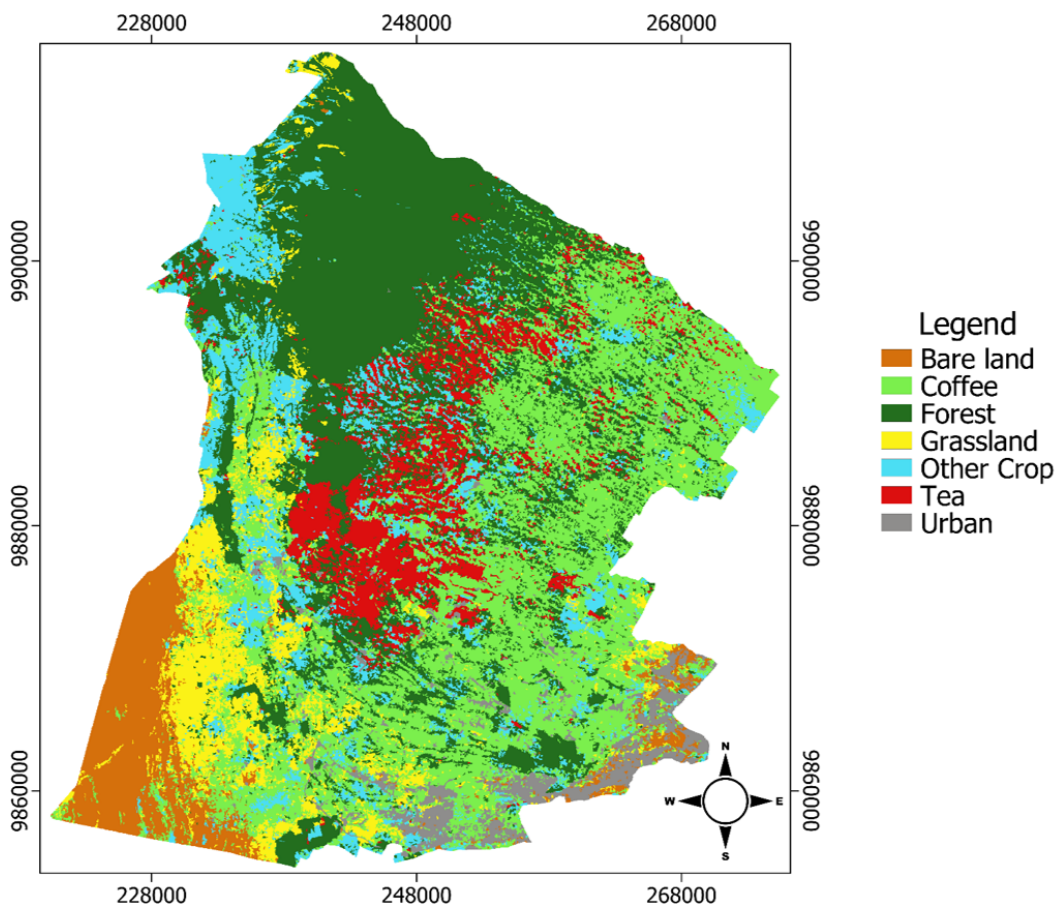


Figure A.1.7 : Land Use/ Cover map of 2016 for the test study area in Kenya

**A.2 Peer Reviewed Journal Paper**

Article

# Cropland Mapping Using Fusion of Multi-Sensor Data in a Complex Urban/Peri-Urban Area

Eunice Nduati <sup>1,\*</sup>, Yuki Sofue <sup>1</sup>, Akbar Matniyaz <sup>1</sup>, Jong Geol Park <sup>2</sup>, Wei Yang <sup>1,3</sup> and Akihiko Kondoh <sup>1,3</sup>

<sup>1</sup> Department of Earth Sciences, Chiba University, 1-33, Yayoi-cho, Inage-ku, Chiba-shi, Chiba 263-8522 Japan; yuki.candy.s126@gmail.com (Y.S.); akbar120311@gmail.com (A.M.); yangwei@chiba-u.jp (W.Y.); kondoh@faculty.chiba-u.jp (A.K.)

<sup>2</sup> Department of Informatics, Tokyo University of Information Sciences, 4-1 Onaridai, Wakaba-ku, Chiba 265-8501 Japan; amon@rsch.tuis.ac.jp

<sup>3</sup> Center for Environmental Remote Sensing, Chiba University, 1-33 Yayoi-cho, Inage-ku, Chiba-shi, 263-8522 Japan

\* Correspondence: nduatie@chiba-u.jp; Tel.: +81-(0)90-9200-1891

Received: 19 November 2018; Accepted: 13 January 2019; Published: 21 January 2019



**Abstract:** Urban and Peri-urban Agriculture (UPA) has recently come into sharp focus as a valuable source of food for urban populations. High population density and competing land use demands lend a spatiotemporally dynamic and heterogeneous nature to urban and peri-urban croplands. For the provision of information to stakeholders in agriculture and urban planning and management, it is necessary to characterize UPA by means of regular mapping. In this study, partially cloudy, intermittent moderate resolution Landsat images were acquired for an area adjacent to the Tokyo Metropolis, and their Normalized Difference Vegetation Index (NDVI) was computed. Daily MODIS 250 m NDVI and intermittent Landsat NDVI images were then fused, to generate a high temporal frequency synthetic NDVI data set. The identification and distinction of upland croplands from other classes (including paddy rice fields), within the year, was evaluated on the temporally dense synthetic NDVI image time-series, using Random Forest classification. An overall classification accuracy of 91.7% was achieved, with user's and producer's accuracies of 86.4% and 79.8%, respectively, for the cropland class. Cropping patterns were also estimated, and classification of peanut cultivation based on post-harvest practices was assessed. Image spatiotemporal fusion provides a means for frequent mapping and continuous monitoring of complex UPA in a dynamic landscape.

**Keywords:** Urban and Peri-urban Agriculture (UPA); heterogeneous; spatio-temporal fusion; synthetic NDVI

## 1. Introduction

Uncertain climatic conditions, high population growth, commodity price fluctuation, urbanization, and allocation of agricultural produce to non-food consumption uses all threaten global and regional food security [1–6]. Eigenbrod and Gruda [3] highlighted the need for analysis of crop area and production that takes into account changing demographics vis-a-vis urbanization. In a global assessment of urban and peri-urban agriculture, Thebo et al. [7] noted that, despite the increasing significance of urban and peri-urban agriculture (UPA), it remains poorly quantified. Common to UPA-related studies is the need for spatially explicit cropland data [7–9]. Numerous studies and projects on cropland and crop-type mapping have been conducted to provide information about crop distribution, crop types, and cropping frequency, at global, regional, and local scales [10–22]. In particular, remote sensing is a critical source of data for agricultural mapping and monitoring, since

it offers synoptic earth observations with repetitive coverage. Teluguntla et al. [13] found that most of the cropland mapping activities were applied to multi-temporal moderate resolution (250 m or more) remotely sensed data or high resolution (Landsat 30 m) limited time-series remotely sensed data, thus limiting mapping of small, fragmented croplands. Due to competing land use demands and the high value attached to land in urban and peri-urban areas, UPA agricultural production units tend to be small, spatially dispersed, and fragmented. This finding is supported by Thebo et al. [7] and Martellozzo et al. [8], who observed that the scale and methods used to generate cropland information are ill-suited to capturing urban croplands and that, given the local nature of UPA, global scale analysis leads to generalizations which can be misleading.

In addition to spatial scale, due consideration for the crop types cultivated and management practices in UPA croplands are necessary. Vegetables and fruits are the most commonly grown crops in UPA [4,9]. Mapping of major staples such as rice, wheat, maize, and soybeans using remote sensing has been successful due to the spatial scale of production and the relatively uniform regional cultivation and management practices [9,16–22]. However, varied crop types, crop varieties, tillage practices, and planting times characterize UPA crop production, resulting in misaligned phenological development and thus necessitating multi-temporal classification approaches which utilize time-series data [22]. Cropland mapping approaches that use time-series data have been shown to perform better than single-date methods [15,23]. One of the main challenges of time-series analysis and classification for cropland mapping is that it requires timely a priori knowledge of the cropland landscape for labeling of clusters (in the case of unsupervised classification), and derivation of the signature files needed to guide supervised classification models [14,15,23–25]. Generally, satellite images are, for most applications, processed and analyzed retrospectively unless the data acquisition and processing are real-time or near real-time, as is the case for meteorological monitoring and prediction applications. The most reliable source of reference data is in situ field observations, collected through farmer surveys and field campaigns [14]. However, the acquisition of this data, especially for large areas and heterogeneous croplands, is an expensive and time-consuming exercise [14]. The collection of ground-truth information for UPA croplands, therefore, remains a daunting task that requires an investigation into the application of novel approaches, such as crop-specific post-harvest practices, for reference data acquisition.

Another challenge of time-series analysis is missing data due to atmospheric artefacts, which results in an irregular sampling frequency of the phenomena of interest [15,24,25]. At any one time, approximately 35% of the global land surface is under cloud cover, thus limiting information retrieval and meaningful interpretation of optical satellite data [25,26]. Various techniques have been developed to deal with cloud cover and other causes of missing data, such as sensor failures [26–28]. Shen et al. [26] broadly classified these methods into spatial, spectral, temporal, and hybrid categories, which vary by the type of images they can be applied to, and the sources of information used to fill the missing data. The synthesis of multisource data with complementary information; data integration in the spatial, spectral, and temporal domains; and development of efficient, accurate, and task-oriented algorithms are areas of potential improvement for missing data reconstruction [26]. The last decade has seen a proliferation in the development of multi-sensor image fusion or blending methods that exploit redundant and complementary information in the spatial and temporal dimensions of remote sensing data, to enhance interpretation and classification accuracy [29,30]. There are several detailed reviews on the types of fusion in remote sensing, state of the art best practices, and advancements [30–32]. Fusion of high spatial–low temporal resolution images (e.g., Landsat 30 m) with low spatial–high temporal resolution satellite images (e.g., MODIS 250 m or 500 m), to generate synthetic high spatial–high temporal resolution data, can enable mapping of small, fragmented, and spatially and temporally heterogeneous UPA croplands at a regular frequency (e.g., seasonally or annually).

This study, therefore, seeks to characterize urban and peri-urban agricultural crop production units in a complex landscape using satellite earth observation data acquired in one year, by identifying horticultural croplands and distinguishing them from other land cover types and uses, including

paddy fields. Using the Normalized Difference Vegetation Index (NDVI) as a phenological indicator, the inter-seasonal variations of various crop production units are investigated at pixel-level, to estimate cropland extent and cropping patterns. An experiment on distinguishing peanuts from other crops within the year of study, using training and validation samples obtained by inference of post-harvest practices, is also evaluated. The objectives of this study are, therefore, to generate a cropland mask, excluding paddy rice fields, determination of cropping patterns intra-annually within the cropland area, and classification of peanuts versus other crops using post-harvest practices information as training data, via classification of a dense regular high resolution (30 m) image time series. The overarching goal of this research is to develop a coherent methodology that promotes acquisition and dissemination of information on agricultural production units in urban and peri-urban areas with regular frequency, and compatibility with global and regional scale datasets for food and nutrition security. The image processing and analysis procedures are implemented mainly using open source software, including R and QGIS [33,34]. For rapidly urbanizing developing countries, this study is relevant for the provision of data to support food security initiatives, and the planning and management of urban spaces.

## 2. Data and Methods

### 2.1. Site Description

The study area, shown in Figure 1, is made up of seven municipalities within the Chiba prefecture, which is in the South-eastern part of Japan and is adjacent to the Tokyo Metropolis to the east. The seven municipalities are Yotsukaido-shi, Inzai-shi, Yachimata-shi, Narita-shi, Sakura-shi, Tomisato-shi, and Shisui-machi, with a total area of 623.15 km<sup>2</sup> and a population of 668,603.

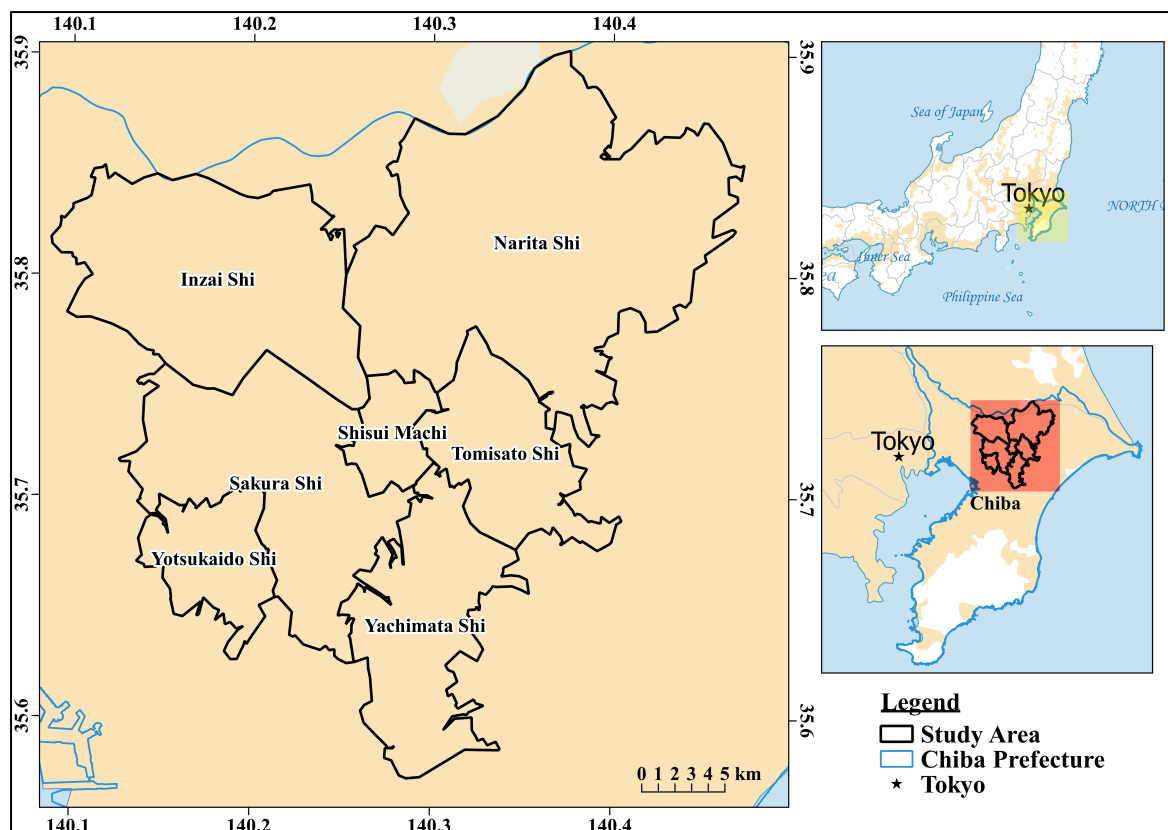


**Figure 1.** The seven municipalities in the Chiba prefecture that constitute the study area.

The Chiba prefecture is a valuable source of agricultural food crops and was ranked sixth in agricultural production in Japan, with vegetable production worth more than half a billion yen in

2015 [35]. It has a varied landscape, comprised of urban or built-up areas, forests (evergreen and deciduous), grasslands (land covered with grass or shrubs), paddy fields, croplands (also described as upland cropland), and water bodies. Grasslands in the area consist of two types: Natural and managed. On the one hand, natural grasslands contain untended grass and shrubs, and include abandoned croplands and paddy fields. On the other hand, there are the managed grasslands, such as golf courses, which are numerous due to proximity to Tokyo.

The Chiba prefecture has an annual average temperature of 16 °C, with annual and monthly average maximum and minimum temperatures of 31 °C and 2 °C, respectively. The annual average precipitation is 1496 mm, and it receives approximately 2113 h of sunlight yearly, making it highly favorable for agricultural production [35,36]. The main crops, in the regions selected, are rice (which is cultivated on irrigated paddy rice fields) and vegetables; including, but not limited to, carrot, daikon radish, taro, cabbage, and spinach.

## 2.2. Data Acquisition and Pre-Processing

The overall flow of processing and analysis activities in this study is as depicted in Figure 2. Two satellite earth observation datasets, Landsat 8 and Moderate Resolution Imaging Spectroradiometer (MODIS) data, were acquired from the United States Geological Survey's (USGS) EarthExplorer site [37]. Landsat 8 has a spatial resolution of 30 m and a temporal resolution of 16 days, while the MODIS data used in this study were daily 250 m images. In an initial application needs assessment, the suitability of the independent use of Landsat with respect to the study's objectives and knowledge of the prevailing conditions on the ground was evaluated. Table 1 shows all of the images for the year 2015 for the Landsat tile, WRS Path/Row 107/035 covering the study area, and their corresponding land cloud cover. Twelve of the images had more than 30% land cloud cover and were excluded from any further evaluation.



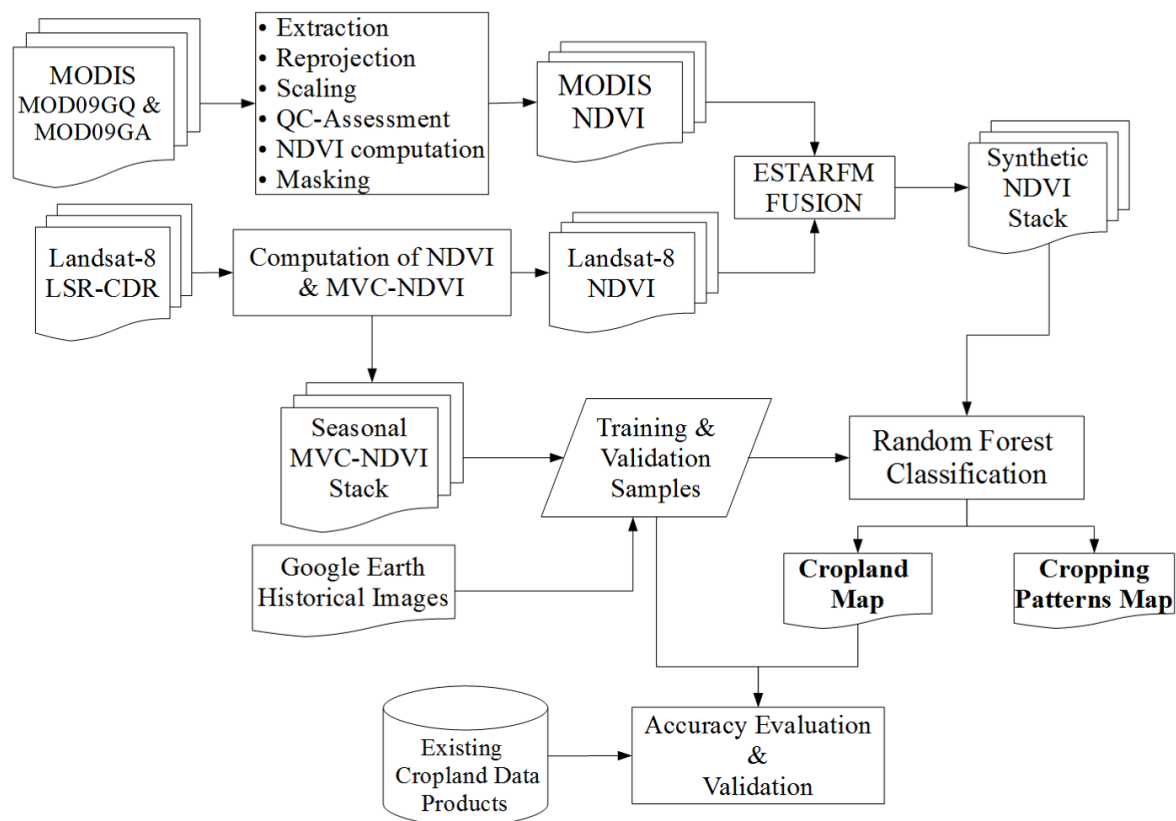


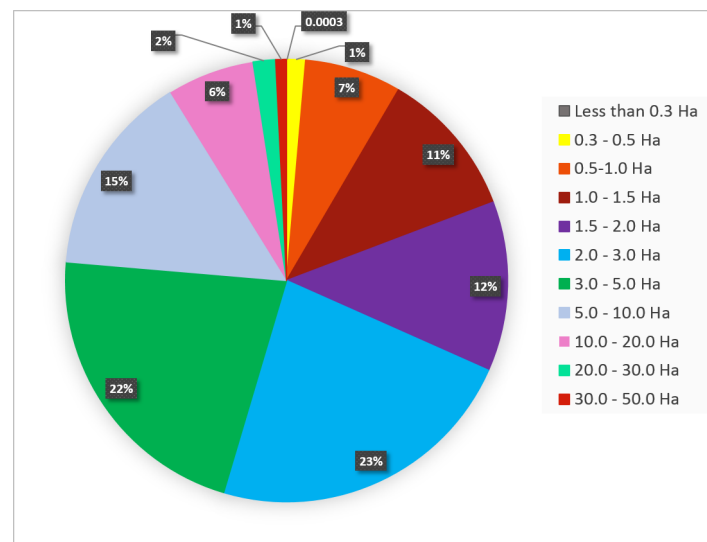
**Figure 2.** Schematic representation of the overall research methodology. The Normalized Difference Vegetation Index (NDVI) was computed for the Moderate Resolution Imaging Spectroradiometer (MODIS) and Landsat Surface Reflectance Climate Data Record (LSR-CDR) datasets. Synthetic NDVI images were generated using the Enhanced Spatio-Temporal Adaptive Reflectance (ESTARFM) Fusion of the NDVI images. The Maximum Value Composite NDVI (MVC-NDVI) was computed using Landsat NDVI and used to generate reference data.

Moreover, the period between April and September (that is, spring to fall) is critical, as crops in the field are in the vegetative phase and are thus useful for remote sensing detection. In June, July, and September, four images had 100% cloud cover—thus ruling out single sensor reconstruction [26,27]. Also, approximately 75% of the cultivated land in the study area is less than 5 Ha, as shown in Figure 3, including paddy rice fields and land under permanent crops. The Landsat 8 30-m resolution is suitable for the mapping of paddy rice fields since they are spatially contiguous, have relatively uniform cultivation and management practices, and the phenology of rice is well understood [38,39].

**Table 1.** Landsat 8 images for the study area's scene Path/Row 107/035 in 2015.

Date (Year 2015)	Day of Year (DOY)	% Land Cloud Cover
10th January	10	16.31
26th January	26	50.37
11th February	42	50.63
27th February	58	31.79
15th March	74	83.76
31st March	90	3.71
16th April	106	9.11
2nd May	122	1.92
18th May	138	59.24
3rd June	154	100
19th June	170	100
5th July	186	100
21st July	202	10.38
6th August	218	3.52
22nd August	234	52.59
7th September	250	100
23rd September	266	19.39
9th October	282	0.92
25th October	298	2.28
10th November	314	68.93
26th November	330	42.17
12th December	346	12.42
28th December	362	15.26

However, the upland croplands tend to be small, fragmented, dispersed, and have diverse cropping patterns and crop varieties, due to varied management practices. Single-date Landsat image classification would therefore not adequately capture these food production units since, at any one time, not all fields have crops and bare or fallow parcels would be classified as bare land or grassland. Thus, time-series classification was more suitable [15,23]. Further evaluation of the Landsat images for cloud cover, focussing on the study area, was carried out, and eight images were finally selected, resulting in an irregular time series.

**Figure 3.** Proportions of cultivated land area in 2015. [35]

Two daily MODIS surface reflectance products (MOD09GA and MOD09GQ) were acquired, for horizontal tile 29 and vertical tile 5 (h29v05), for the period spanning 1 January 2015 to 31 December 2015. The two surface reflectance bands contained in the MOD09GQ scientific dataset (SDS), red (620–670 nm) and near-infrared (NIR) (841–876 nm), and the state 1 km SDS in MOD09GA SDS, were extracted. MODIS data are delivered in the sinusoidal projection, and were therefore reprojected to the Universal Transverse Mercator Projection (UTM) zone 54N. The reflectance bands

and state 1 km SDS were then subset to the Chiba prefecture bounds. A scale factor of 0.0001 was applied to the red and NIR bands, prior to computation of NDVI. The state 1 km SDS was used to retrieve cloud-specific information during quality assessment, because this parameter has not been populated in the reflectance band quality SDS included in the MOD09GQ product since MODIS version 3, as detailed in [40,41]. The Quality Control (QC) masks from the state 1 km SDS were resampled to 250 m using bilinear interpolation, and applied to the NDVI images through masking. The resulting daily NDVI images at 250 m resolution had gaps due to masking, and gap-filling was carried out via linear interpolation in the temporal dimension [42].

### 2.3. Spatio-Temporal Image Fusion

Landsat 8 irregular time-series data and daily MODIS images were fused to generate a regular time series. MODIS data supports Landsat via fusion to inform phenological traits and maintain temporal continuity in the observed phenomena [23,25]. Fusion methods are categorized by the mathematical relationships between the reference and observation data into four groups, including weighted function based, unmixing based, dictionary-pair learning based, and data-assimilation based algorithms [29,43]. The weighted function based methods include the Spatial and Temporal Adaptive Reflectance Fusion Model (STARFM) and the Enhanced STARFM (ESTARFM), which assume that no land cover type changes occur between the reference and prediction dates [43,44]. While this assumption limits the performance of weight function based algorithms in heterogeneous landscapes where rapid, abrupt changes occur, they are popular since they require no auxiliary data as inputs and are robust enough to predict pixels with changes in biophysical attributes [44–46]. In remote sensing, indices enhance spectral information and class separability and are, therefore, an essential basis for the estimation of the biophysical characteristics of land cover, such as vegetation vigor [44,46]. Fusion may be applied to the reflectance bands of images or the indices, via Blend-then-Index (BI) or Index-then-Blend (IB), respectively [43]. Research has found that IB is more computationally efficient and accurate, and its performance is influenced less by choice of algorithm [45,46]. Li et al. [46] found that the use of a MODIS 8-day composite surface reflectance product (MOD09A1 and MYD09A1) with a temporal mismatch between the Landsat and MODIS images resulted in weaker correlations between the observed and synthetic images, due to the day-to-day variation in the MODIS viewing geometry. Table 2 shows the relative distribution of the eight selected Landsat 8 images for this study, and the corresponding available dates in MODIS 8-day composite data, which shows a one-day difference. For this study, we used the daily MODIS surface reflectance products (MOD09GQ and MOD09GA), thus allowing the selection of a start date within the MODIS daily time-series that would fully match the available Landsat image time-series.

**Table 2.** Relative temporal distribution of irregular Landsat 8 time-series to MODIS 8-day composite.

	Day of Year (DOY)							
Available Landsat 8 Images (Cloud Cover < 20%)	10	90	106	122	202	218	282	298
MODIS 8-day Composite	9	89	105	121	201	217	281	297

Spatio-temporal fusion via IB was implemented using the MODIS Daily 250 m NDVI and Landsat 8 intermittent NDVI images, as described in [45]. The MODIS NDVI images were first resampled to 30 m through bilinear interpolation to reduce the effects of geo-referencing error, then cropped to match the extent of the Landsat 8 NDVI images using R (v3.4.4) [33]. Fusion was implemented in ENVI IDL version 4.8 (Exelis Visual Information Solutions, Boulder, Colorado) using the open-source Enhanced Spatio-Temporal Adaptive Reflectance Fusion Model (ESTARFM) [47]. Many spatiotemporal fusion models have been developed, but ESTARFM has been found to be effective in generating synthetic high-resolution images for heterogeneous regions [44–47].

ESTARFM requires at least two pairs of temporally coincident fine-resolution (moderate to high spatial resolution–low temporal resolution) and coarse resolution (low spatial resolution–high temporal

resolution) images as inputs. Using a specified moving window size within the image, and thereby having a central pixel, similarity of pixels with reference to the central pixel is evaluated and weights computed. Working on the assumption that, for a heterogeneous landscape, the changes in reflectance within a mixed pixel are representative of the weighted sum of changes for each land cover type, and that these changes do not change significantly over a short period of time, the relationship then can be inferred from the pixel value of the fine resolution pixels [45]. Additionally, given that predictions for fine-resolution pixels are likely to be more accurate from a pure coarse-resolution pixel, larger weights are assigned to these pixels, and so conversion coefficients are thus computed and used to predict the fine-resolution reflectance or index value per pixel. As the objective of this study was to classify land cover annually and, specifically, to discriminate cropland from non-cropland, the prediction of land cover changes was not necessary and the ESTARFM algorithm has been found to predict phenology changes satisfactorily [43–47]. The fine-resolution reference images, used in the fusion process, were the most cloud-free Landsat 8 NDVI images for 2015, acquired in late winter (10th January), early spring (16th April), and mid-fall (9th and 25th October). For computational efficiency, an 8-day interval was chosen.

#### 2.4. Training and Validation Data Collection

Two main land cover and cropland datasets were evaluated as potential sources of training and validation data. The Japan Aerospace Exploration Agency's (JAXA's) High Resolution Land Use and Land Cover map of Japan (HRLULC Ver.18.03) is a 30 m land cover map of Japan, generated using multi-temporal, multi-source data. The data includes Landsat 8 OLI collection 1 images, 10 m geographical and topographic data from the Geographical Survey Institute (GSI) of Japan, Advanced Land Observing Satellite (ALOS-2)/ Phased Array type L-band Synthetic Aperture Radar (PALSAR) 25 m 2015 mosaic dataset, and ALOS Panchromatic Remote-sensing Instrument for Stereo Mapping (PRISM) Digital Surface Model (DSM). A Bayesian estimation classifier, followed by post-classification editing, was used for the latest version. The JAXA High Resolution land use/land cover maps have a regular update frequency, and were identified in Waldner et al. [48] as a freely available regional cropland-related dataset for Japan. It has ten land use/land cover classes, including water, urban, rice paddy, crop, grass, deciduous hardwood forest, deciduous softwood forest, evergreen broad-leaved forest, evergreen conifers forest, and bare land. The reported producer's and user's accuracy for the cropland class are 83.8% and 74.1%, respectively. However, since the data used in its production is not temporally specific and ranges from 2014 to 2016, it was decided to use this dataset for validation of the results of this study. Further details on its production are available in [49].

In addition, the recently released Global Food Security-Support Analysis Data at 30 m (GFSAD30), benchmarked for 2015, was evaluated [50]. The Southeast and Northeast Asia dataset (GFSAD30SEACE) were acquired and assessed for suitability as a source of training and validation data in this study. The cropland extent in this dataset represents all cultivated land including paddy, irrigated, and rainfed areas. As the discrimination between paddy rice fields and other croplands was an objective of this study, the GFSAD30SEACE dataset was used for validation of our result, in terms of total cropland extent.

In the absence of a reference dataset that was temporally specific to the year 2015 and representative of the intended cropland class, reference data samples were generated using the Maximum Value Composite NDVI (MVC-NDVI), computed between consecutive NDVI images of the sparse Landsat image time series. In addition to minimizing the effects of cloud cover, the seasonal MVC-NDVI Red-Green-Blue (RGB) composite stacks, as shown in Figure 4, revealed inter-seasonal pixel-level NDVI changes which made it possible to determine seasonal behavior of the major land cover types and set rules for distinguishing the major land cover classes and cropping patterns. Through raster math of the MVC-NDVI layers, masks were generated for each land cover class. The raster masks were then vectorized and cleaned-up, by comparison with the Google Earth (GE) image available for 9th October 2015. A dense point cloud was then generated for each land cover class by

joining the vector land cover masks with a 30 m point vector grid of the study area. The training and validation points were then selected via stratified random sampling of the dense point cloud.

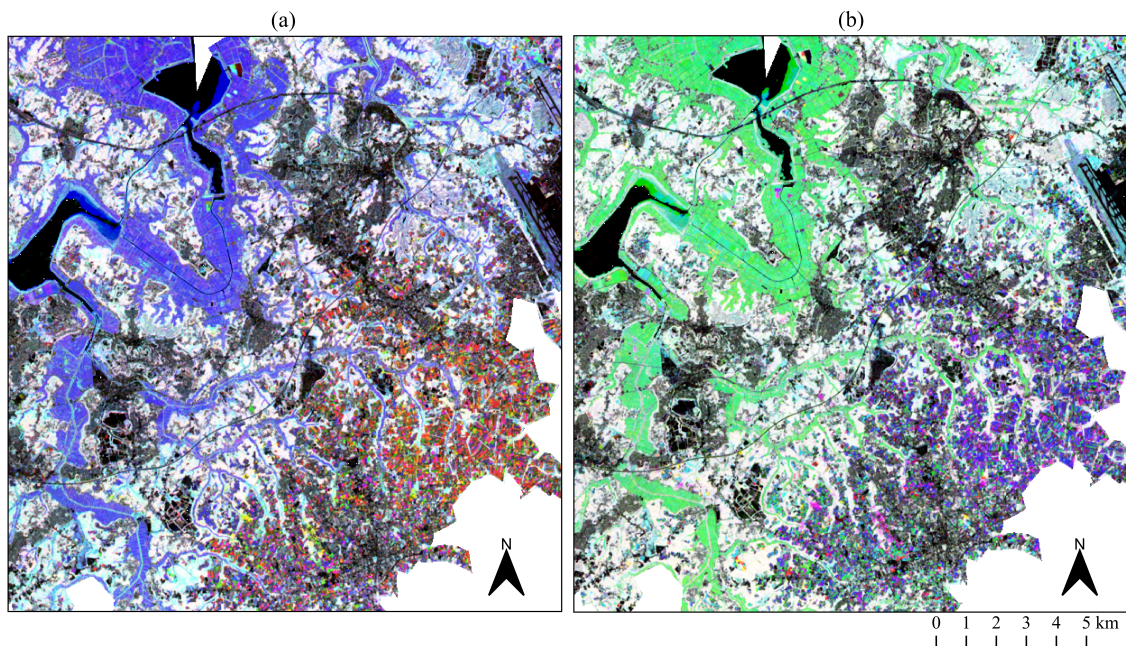


**Figure 4.** Red-Green-Blue (RGB) composites of the seasonal Maximum Value Composite-Normalized Difference Vegetation Index (MVC-NDVI). (a) The winter-spring-summer composite, and (b) the spring-summer-fall composite for 2015. Off-white regions in both (a) and (b) depict dense vegetation, such as forests, which have high NDVI with minimal variation intra-annually. The black and grey regions are urban and water features, which have low NDVI with minimal variation within the year. Red, blue, green, cyan, yellow, and magenta regions represent vegetation whose maximum NDVI corresponds with the seasonal order in the RGB composite.

In this study, distinguishing peanuts from other crops growing in the study area was tested. Peanuts, grown for their commercial value, are a popular crop in this region. Approximately 75% of Japan's domestic supply of peanuts comes from the Chiba prefecture [51–53]. From moderate resolution satellite images, it is impossible to distinguish, with certainty, one crop (e.g., peanuts) from another (e.g., carrots) during the growing season. As such, to know which crop was growing at a certain location at a given time, field photos or farm surveys are necessary during the growing season in every year, since farmers regularly change crops cultivated, especially in the case of horticultural food crops. Constant and regular acquisition of crop type information is time-consuming and costly. Thus, creative means of inferring and deciphering such information from existing data are necessary. In this study, the post-harvest practice of *jiboshi* by peanut farmers in Japan makes it possible to know where peanuts had been growing, within at least a month from harvesting.

After harvest, peanut pods have approximately 50% moisture which renders them prone to contamination with mycotoxins, which are a major food safety concern and may lead to considerable economic losses [54,55]. Peanut farmers in the Chiba prefecture will, after harvest, leave the peanut plants and pods in inverted windrows, which allows air to circulate around the pod and for the moisture content to diminish significantly, for about a week [55]. Thereafter, the peanut plants and pods are piled into solitary heaps, as shown in Figure 5a, in a process referred to as *jiboshi* (drying on the ground) for about a month. These piles or heaps are referred to as *bocchi*, and are visible from GE images (as shown in Figure 5b), thus allowing one to infer that peanuts had been growing on that field within at least a month of acquisition of the image. Training and validation samples were collected within the study area, for locations which were visible in the GE image of 9th and 29th October 2015.



**Figure 5.** The post-harvest practice of on-field drying of peanuts, known as jiboshi; (a) shows the heaps (bocchi), as seen on Google Maps Street View on 29th October, 2015, and (b) shows the aerial view of the same field, as seen on Google Earth (35°37'N, 140°14'E) on 9th October, 2015.

### 2.5. Time Series Classification

The Random Forest (RF) classification algorithm was used in this study. RF is a robust ensemble machine learning classifier, which has been used in numerous agricultural mapping application studies [56–61]. RF has been found to be stable and efficient, with better performance in classification of croplands with high intra-class variability than other classifiers, such as conventional decision trees and time-weighted dynamic time warping (TWDTW) [15,61]. In this study, RF was implemented using the RStoolbox (ver.0.2.3) package in R, by use of the 'superClass' function [62]. The function takes, as input, the raster image and reference data—either as spatial points or a spatial polygon data frame, containing position and class attribute information. A separate validation dataset can also be provided but, if not, the training dataset is split based on a partition proportion ranging from zero to one, provided by the user. The model tuning parameters are the number of samples per land cover class, the number of levels for each tuning parameter, and the number of cross-validation resamples, for robust prediction performance [56]. To ensure non-overlap between training and validation data, a minimum distance, in terms of pixels, can be provided [62]. Several combinations of the tuning parameters, informed by the RStoolbox package literature, were tested with a 70% training data and 30% validation data split. The configuration with the best sensitivity in the cropland class was chosen.

### 2.6. Accuracy Assessment

The classification results were evaluated using error matrix accuracy assessment metrics, which include producer's, user's, and overall accuracy, as well as the kappa coefficient, as defined in Equation (1). The mathematical notation of the kappa coefficient, with respect to the error matrix, is shown in Equation 2 [63,64].

$$\hat{K} = \frac{\text{Observed accuracy} - \text{Expected accuracy}}{1 - \text{Expected accuracy}} \quad (1)$$

$$\hat{K} = \frac{N \sum_{i=1}^r x_{ii} - \sum_{i=1}^r (x_{i+} * x_{+i})}{N^2 - \sum_{i=1}^r (x_{i+} * x_{+i})}, \quad (2)$$

where  $\hat{K}$  is the kappa coefficient,  $N$  is the total number of observations,  $r$  is the number of rows in the error matrix,  $x_{ii}$  is the number of observations in row  $i$  and column  $i$ , and  $x_{i+}$  and  $x_{+i}$  are the marginal totals of row  $i$  and column  $i$ , respectively [64]. The kappa coefficient provides a measure of how much better the classification performed, compared to the probability of randomly assigning pixels to the correct class.

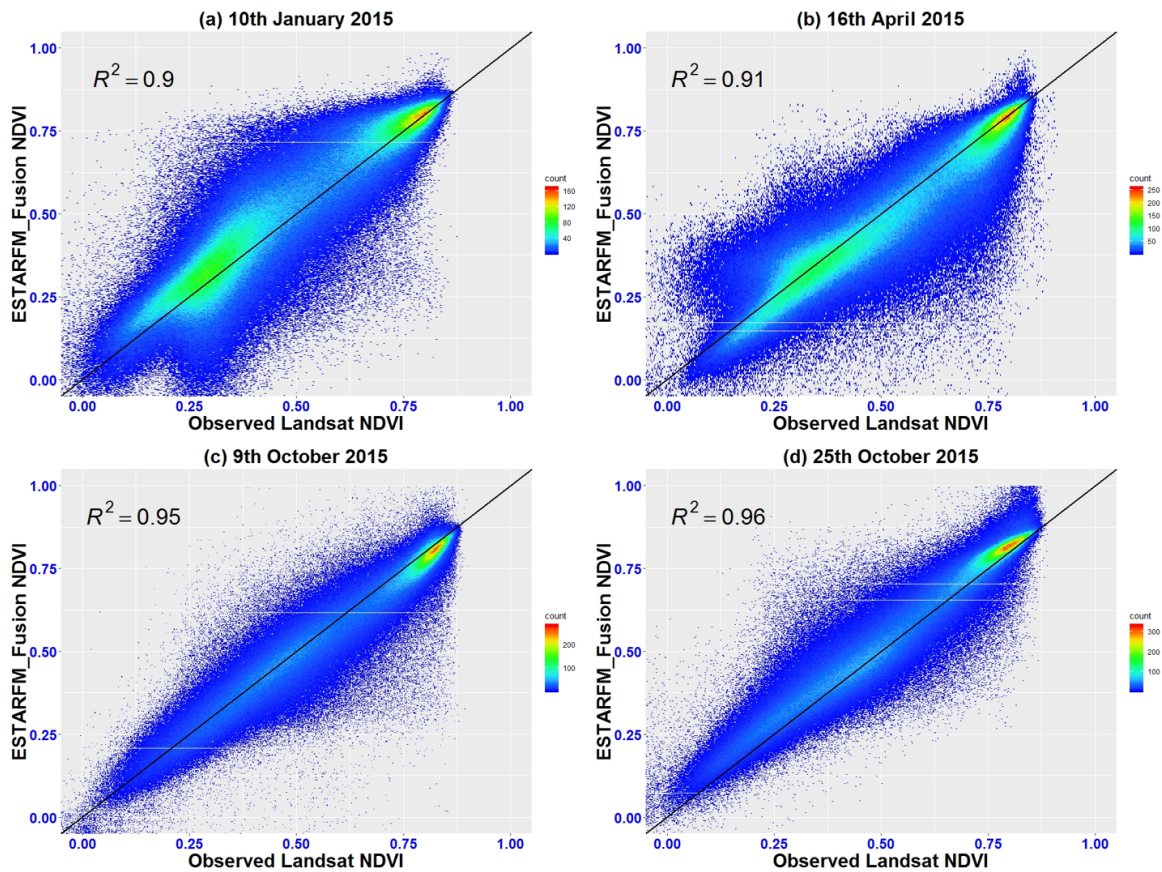
### 3. Results

#### 3.1. Fusion Results

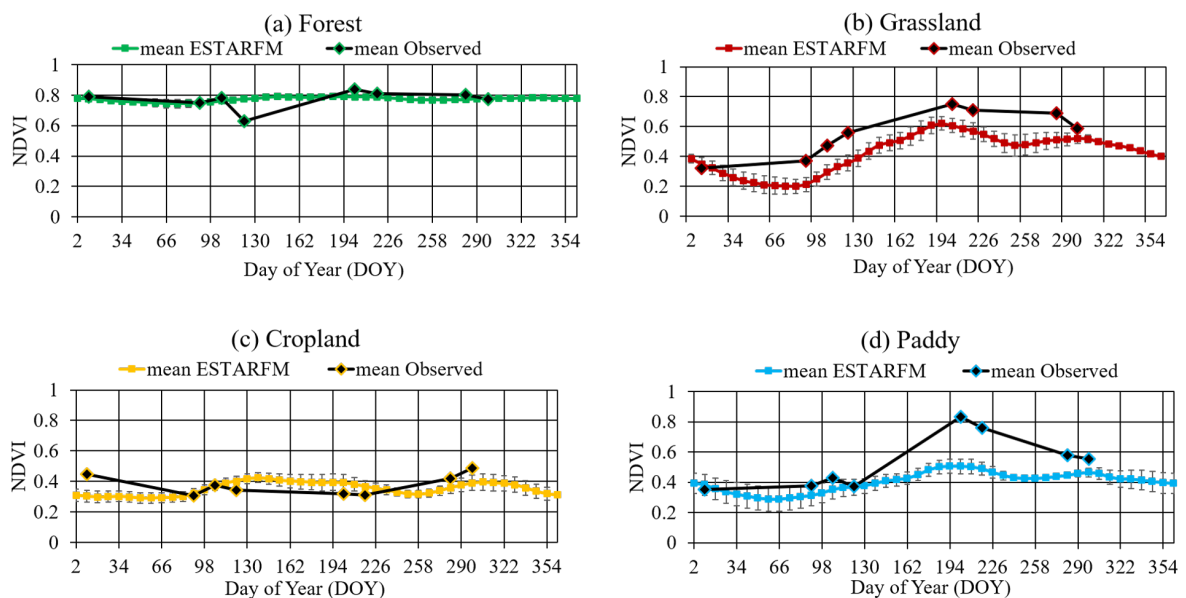
Performance of the fusion process in generating synthetic NDVI images was evaluated quantitatively by comparing the synthetic NDVI images to the reference observed Landsat NDVI images. Overall, there was a strong agreement between the synthetic images and the observed Landsat images, with  $R^2 > 0.9$  for all dates, as depicted in Figure 6. A higher association was found in the mid-fall images (9th and 25th October) (Figure 6c,d), than in the late winter (10th January) (Figure 6a) and early spring (16th April) (Figure 6b) images. Phenological changes in the landscape can also be inferred from the point density in the scatterplots, shown by color—with blue being low density and red showing high density. In the late winter and early spring images (when vegetation vigor is low), there are two data clusters. The first, albeit lower density, lies in the mid NDVI ranges (0.125 to 0.5), and the second within the higher NDVI ranges (0.6 to 0.8). However, in the mid-fall images (when vegetation vigor is high), the scatterplot tapers with high density in the higher NDVI ranges. This may be attributed to the intra-annual changes in vegetation density, and is demonstrative of more pure vegetation pixels in the fall than in late winter and early spring. These observations may not hold for other years of study for the same region, or other regions with different land cover and climate, and require further investigation.

Figure 7 shows the qualitative assessment of the fusion results, in terms of the temporal evolution of NDVI in the smoothed fusion series and the original Landsat 8 series for the main vegetation cover types in the study area. The shape or configuration of the temporal profiles of the synthetic NDVI time series are analogous to those of the observed NDVI, for all of the main vegetation cover classes. The standard error in the synthetic NDVI time-series are also reflective of intra-class behavior. For forest or dense vegetation, there is minimal variation throughout the year also detected in the observed MVC-NDVI, as shown in Figure 4.

Internal variability is exhibited in the other vegetation types, and varies with season. In the case of the grassland temporal evolution of NDVI, sample points were taken from both the artificial and natural grasslands, and therefore exhibit high intra-class variability. However, towards the end of the year (as winter commences), vegetation vigor decreases and the intra-class variability diminishes, as seen from the error bars in that profile. The observed images do not cover this later part of the temporal behavior of the grassland land cover, as the series ends in early fall, and demonstrates the predictive capabilities of the ESTARFM fusion model. Based on the temporal information inferred from the available coarse resolution images, the changes in the biophysical characteristics of land cover features can be elicited, even in the absence of complete annual coverage of the fine resolution images.



**Figure 6.** Scatterplots of the comparisons of synthetic Landsat images (generated by fusion) with the original Landsat images: (a) 10th January 2015; (b) 16th April 2015; (c) 9th October 2015; (d) 25th October 2015.



**Figure 7.** NDVI temporal evolution of the major vegetation land cover types in the study area, in the fusion and original Landsat NDVI time-series. Dates along the time series are expressed as Day of Year (DOY).

The temporal profiles of the cropland and paddy classes also reveal characteristics inherent to these land cover classes. Intra-class variability in the cropland class exhibits a double cropping pattern,



where fluctuations are detected during the growing seasons and abate (albeit minimally when the curve is in decline and recovery). Contrastingly, for the paddy class, fluctuations are detected most when it is expected that paddy rice is not on-field. That is, January to April and October to December, or late winter to spring and late fall into the winter. This behavior is akin to that observed within the grassland class, and is indicative of post-harvest vegetation whose vigor is not subject to management practices by the farmer. However, as in the case of grassland land cover, the concluding part of the year and the information elicited arises from the synthetic dataset, and would not have been available within the available Landsat imagery. Overall, both the quantitative and qualitative assessments of the fusion result, in comparison to the observed Landsat dataset, vis-à-vis conventional land cover temporal changes, establish the value of fusion in providing information about land cover prior to classification. Figure 8 depicts the temporal evolution of NDVI in the synthetic time-series stack for representative sample points in the major land cover types of the study area. From this graph, the significance of the synthetic time-series dataset is substantiated further, since we see that for grassland, paddy, and cropland, the spring-summer seasons provide the best distinction points with continuity. The observed Landsat image time-series was sparse, due to inundation with cloud cover during this crucial period, hence making information unavailable; especially in the cropland class.

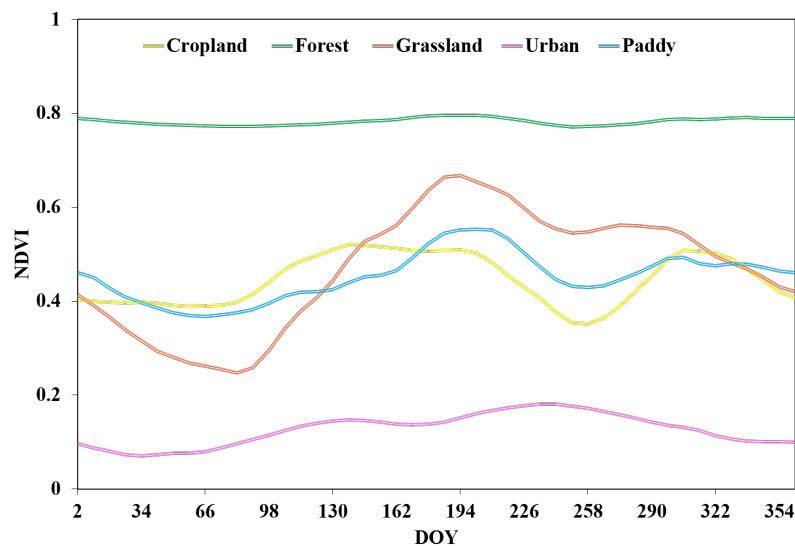


**Figure 8.** NDVI temporal evolution of the major land cover types of the study area in the fusion NDVI time-series.

### 3.2. Classification Results

#### 3.2.1. Cropland Extent

The cropland extent in the context of this study is all land used for crop cultivation, excluding paddy fields. An initial land use/land cover classification was carried out for the main land use/cover types in the region, as shown in Figure 9. An overall accuracy of 91.7% was achieved, with a stratified random sample of over 1000 points per class. The dominant land use/cover classes of forest, grassland, paddy, and urban and water had the highest producer's (PA) and user's accuracies (UA), both more than 90%. The cropland area estimation had the lowest PA and UA, of 79.8% and 86.4%, respectively, but was deemed to be acceptable, given the heterogeneity of the landscape. The estimated area of croplands, excluding paddy fields, for the study area in 2015 was 85.5 Km<sup>2</sup>, as is depicted in Figure 10. Table 3 shows the classification's error matrix. Vegetation along urban features and banks of water bodies were also misclassified as cropland and paddy. Within the paddy field class, the timing

of post-harvest vegetation in the fall within some paddy fields manifested as two peaks, similar to croplands with double cropping, leading to misclassification as croplands.

**Table 3.** Confusion matrix of cropland extent classification.

	Cropland	Forest	Grassland	Paddy	Urban & Water	Total	User's Accuracy (UA) (%)
Cropland	542	2	38	15	30	627	86.4
Forest	7	691	4	0	0	702	98.4
Grassland	38	0	638	27	0	703	90.8
Paddy	36	0	11	597	7	651	91.7
Urban & Water	56	0	0	12	640	708	90.4
Total	679	693	691	651	677	3391	
Producer's Accuracy (PA) (%)	79.8	99.7	92.3	91.7	94.5		
Overall Accuracy (OA) (%)	91.7						
Kappa	0.9						

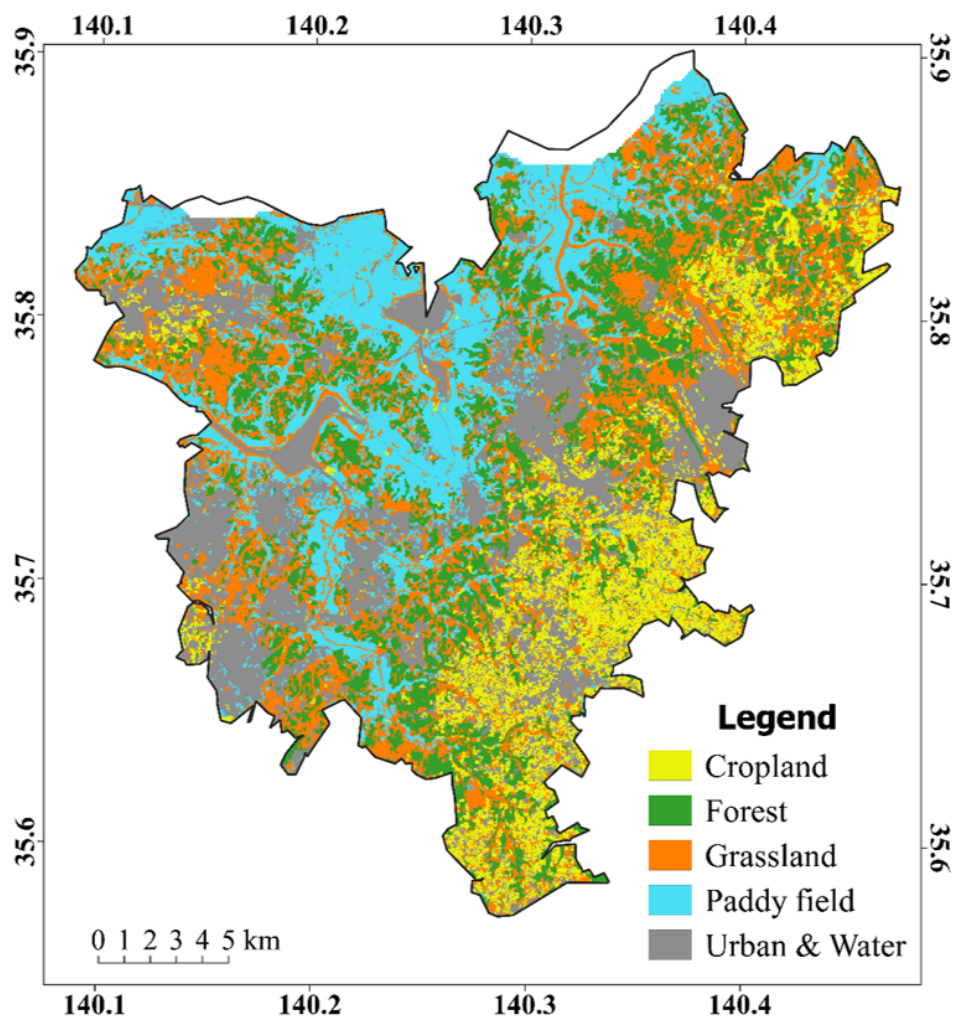


**Figure 9.** Cropland extent map and other land cover types in 2015.

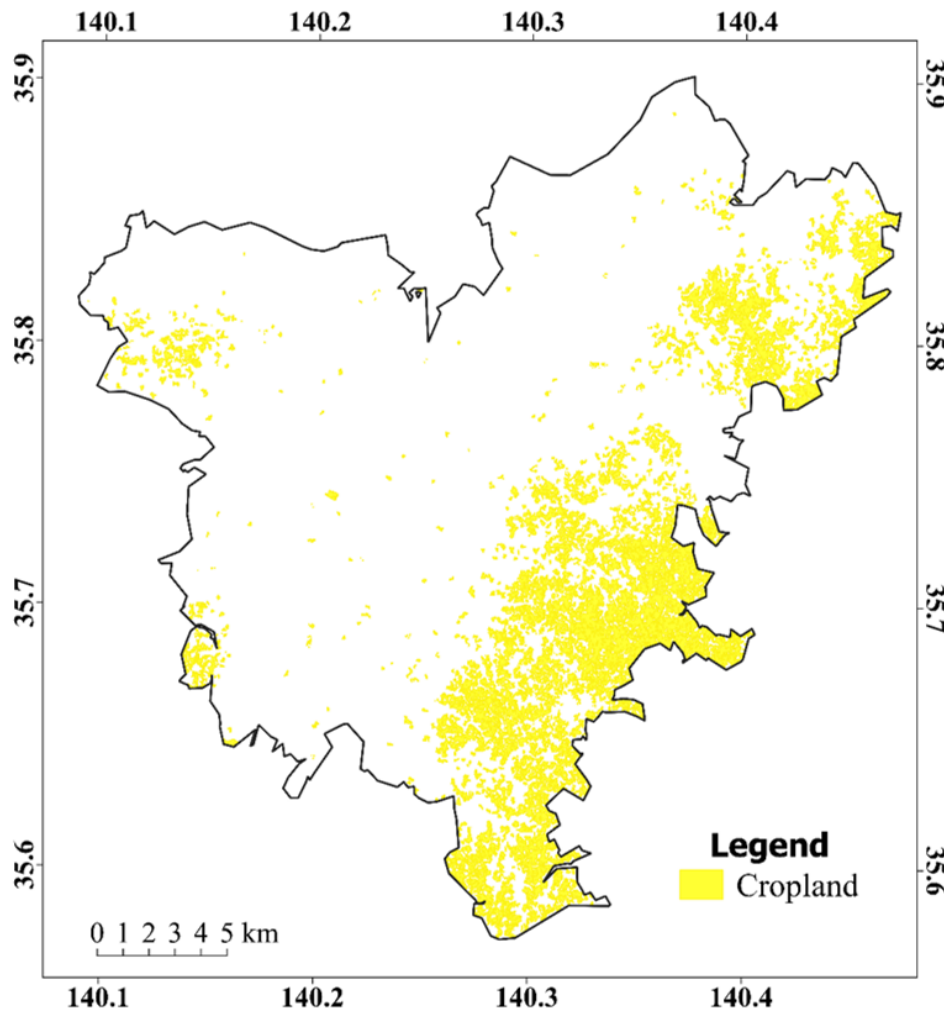


Figure 10. Cropland extent in 2015, derived from this study.

### 3.2.2. Cropping Regimes

Two main cropping patterns or regimes were estimated, as shown in Figure 11: Single cropping, where a pixel had a singular peak within the year, in a season or within two consecutive seasons; and double cropping, for pixels with two peaks in non-consecutive seasons—that is, winter-summer, winter-fall, and spring-fall. The cropping regimes estimation confusion matrix is as shown in Table 4. Most of the croplands were found to be under double cropping intensity, while paddy rice was under single cropping. This is expected, since the upland cropland is used mainly for the production of horticultural food crops that have short durations of growth. Table 5 shows the best periods of market availability for some of the Chiba prefecture's representative crops. This table can be taken to represent an inverse crop calendar, where periods of non-availability represent the growing periods. Therefore, apart from taro and peanuts, which have high market availability for only one period within a year, the rest of the crops can be said to be planted twice by one farmer or continuously by various farmers, within the year. Taro has a long growth period between transplanting and maturation, approximately six to eight months. The table also does not take into account market availability as a result of imports from other regions or countries. Consequently, it is expected that most upland croplands will exhibit double cropping, as our result indicates. Most paddy rice fields had a single cropping pattern, with the exception of a few. This can be attributed to the fact that paddy rice fields are highly sensitive to changes in soil composition, and therefore farmers prefer to leave the land fallow post-harvest in order to maintain the soil nutrient balance necessary for paddy rice. In addition, paddy rice cultivation is a highly specialized skill in Japan and is resource- and labor-intensive. Therefore, apart from the

cultivation of other crops for subsistence consumption, which is normally carried out on other parcels of land, paddy rice farmers tend to focus only on paddy rice.

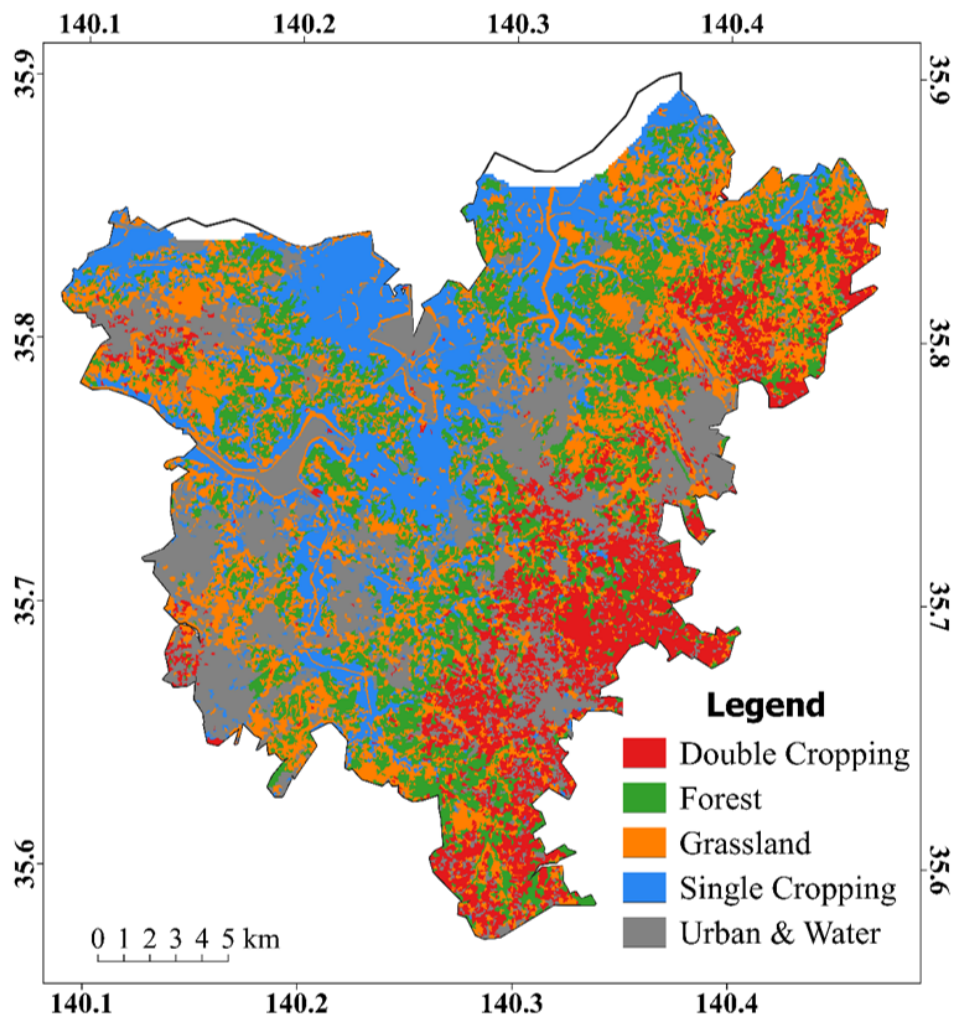


Figure 11. Cropping patterns estimated for 2015 in this study.

Table 4. Confusion matrix of cropping regimes estimation

	Double Cropping	Forest	Grassland	Paddy	Single Cropping	Urban & Water	Total	User's Accuracy (UA) (%)
Double Cropping	1546	4	65	17	716	48	2396	64.5
Forest	11	3217	1	0	104	0	3333	96.5
Grassland	124	1	3015	109	312	0	3561	84.7
Paddy	49	0	44	2467	82	41	2683	91.9
Single Cropping	735	27	173	80	1295	84	2394	54.1
Urban & Water	125	0	0	60	328	3068	3581	85.7
Total	2590	3249	3298	2733	2837	3241	17,948	
Producer's Accuracy (PA) (%)	59.7	99.0	91.4	90.3	45.6	94.7		
Overall Accuracy (OA) (%)	81.4							
Kappa	0.776							

**Table 5.** Market availability of various crops.

Crop Type	Market Availability
* Cabbage	March~May; September and October
* Carrot	April and May; September~December
* Spinach	April and May; September~December
* Taro	September~December
* Turnip	May; October~January
** Peanuts	September~December

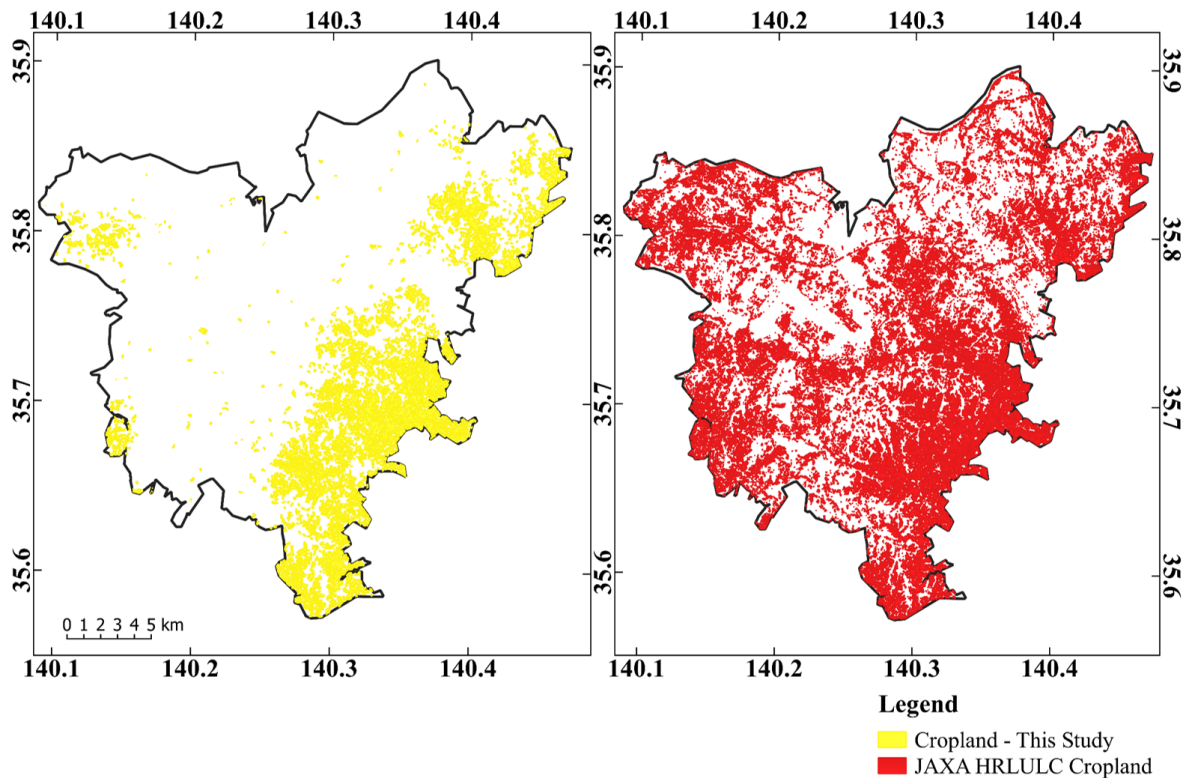
\* [51]. \*\* Inferred from this study; Does not consider imports.

### 3.2.3. Peanuts and Other Crops

A total of 378 sample points representing peanuts were collected, as described in Section 2.4. Non-cropland land cover classes including forest, grassland, paddy, and urban and water were masked out from the fusion time-series, using the cropland mask produced in this study. A stratified random sampling of the peanut samples and other croplands not designated as peanuts was carried out to yield 200 points per class, and a binary classification was implemented. The overall accuracy was 67.1%, and the PA and UA for the peanut class were 63.2% and 71.2%, respectively. Given the limited amount of reference data and the fact that peanuts are cultivated at the same time as other crops, as seen in Table 5, we found this classification accuracy to be sufficient. The phenological similarity between peanuts and other crops, as well as high intra-class variability within the cropland class, requires that a large number of training datasets is used to train the RF classifier [57]. Further research on the determination of the distinct spectral-temporal characteristics of peanuts and other crops cultivated in the region, with more training data and predictors, could improve the classification accuracy.

## 4. Discussion

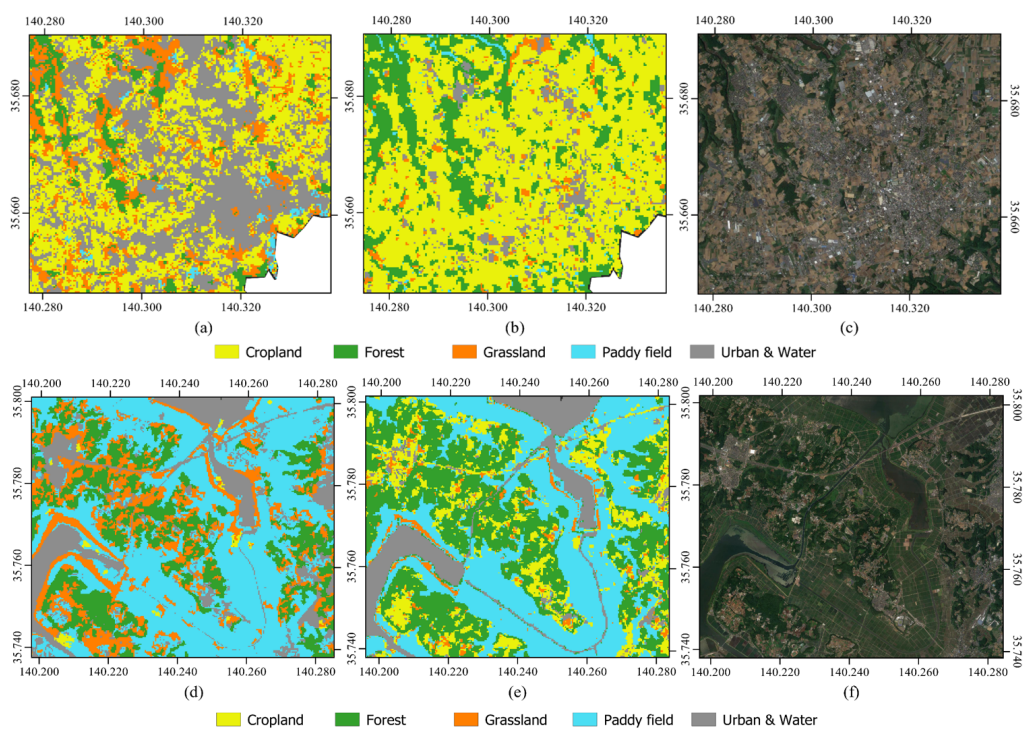
In this study, the application of a high temporal density image time-series to intra-annual cropland extent and cropping regime estimation was evaluated. Validation of the cropland extent or distribution was carried out by comparing this study's result with two existing cropland maps; that is, the regional JAXA HRLULC and the global GFSAD30SEACE datasets. The upland cropland extent, according to the JAXA HRLULC (version 18.03) map, was approximately 367.9 Km<sup>2</sup>, while, in the GFSAD30SEACE data set (which includes paddy fields), it was 129.4 Km<sup>2</sup>. The cropland extent in this study was 85.5 Km<sup>2</sup>. Sharma et al. [65] produced a land use/land cover map of Japan for 2013 to 2015, the JpLC-30m map, and compared their result to the JAXA HRLULC map (version 14.02). Disparities between the JpLC-30m map and the JAXA HRLULC map (version 14.02) were detected, including: Croplands in forests, water-bodies in forests, water in croplands, and herbaceous land cover in croplands. Based on this comparison, the classification of croplands in the JAXA HRLULC map (version 14.02) was severely affected. The improvement over the earlier version (16.03) in cropland classification accuracy is significant. In version 16.03, the reported producer's and user's accuracy for the cropland class were 63.9% and 45.2%, respectively, while, in version 18.03, the producer's and user's accuracy for the cropland class were 83.8% and 74.1%, respectively. Figure 12 depicts the cropland extent, as per this study, excluding paddy fields, and the JAXA HRLULC (version 18.03) cropland. The cropland extent within the JAXA HRLULC (version 18.03) map far exceeds the extent in this study. Further inspection of the land use/land cover map shows misclassification of urban land cover as cropland in the JAXA map, as shown in Figure 13. This phenomenon, which has also been observed in other regional land use/land cover maps, such as the GlobeLand30 map, may be attributed to spatial heterogeneity, but further investigations are necessary [46].



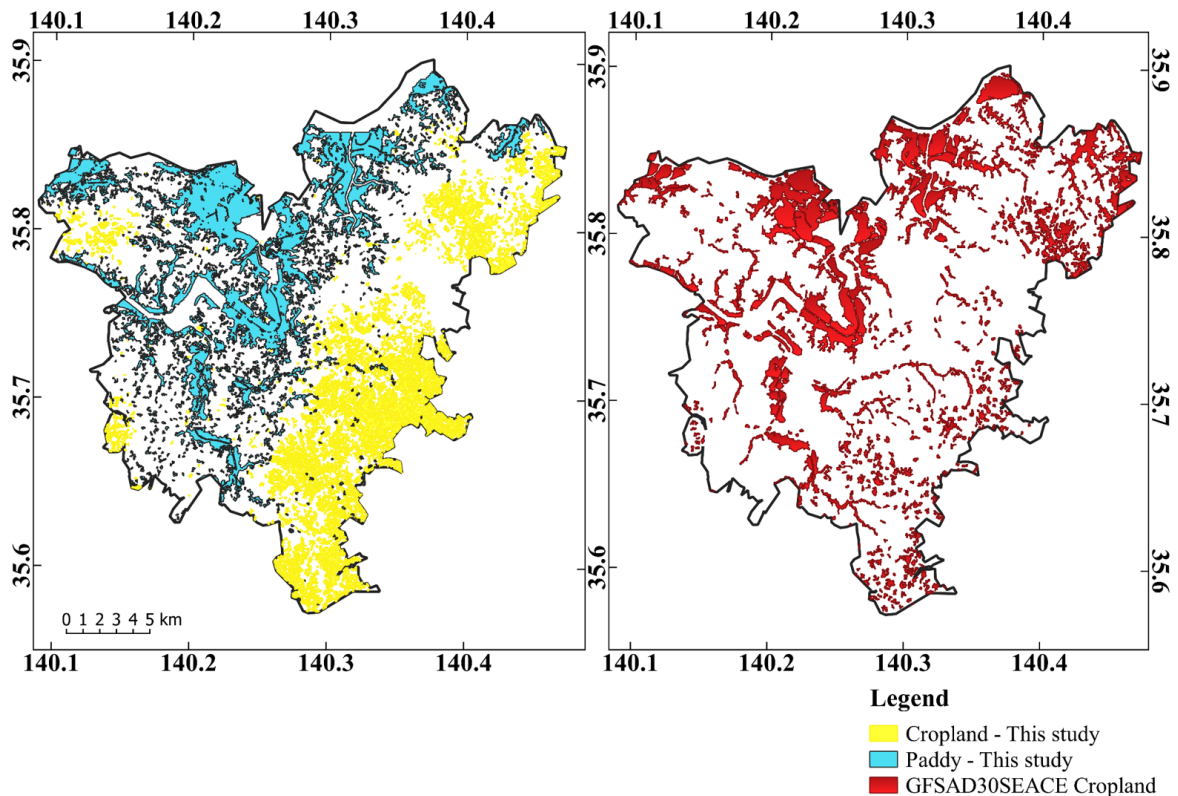
**Figure 12.** Cropland extent for 2015 in this study and in the JAXA HRLULC map.

Figure 14 shows our cropland and paddy extent, and the GFSAD30SEACE cropland extent. The GFSAD30 product does not make a distinction between types of croplands—that is, upland cropland and paddy rice—and, while it adequately captures the paddy fields and compares favorably with our result, it underestimates the upland cropland. This may be attributed to the heterogeneous nature of the upland croplands, which leads to misclassification of upland cropland as non-cropland in the GFSAD30 framework. Our result overestimated paddy fields, with commission errors of 2.3% and 4.15% as cropland and grassland, respectively. However, this was almost balanced out by misclassification of some paddy fields as croplands, and can be attributed to the fact that only NDVI was used as a classification metric. Using other metrics for the same one-year data-set, such as the NDWI index or shape and texture features, may solve this [66].

Statistical survey data at local and national scales can be useful in assessing the results of remote sensing classification and estimates. While it can be time consuming and expensive, it allows for various government agencies and stakeholders to engage directly with farmers. However, there is no standard approach to collection and dissemination of such data and, for regional and global upscaling, statistical data can prove to be problematic due to (among other issues) language barriers. Understanding what variables are measured and how they are measured is key to consideration of statistical data for reference.



**Figure 13.** Comparison of the land use/land cover map of this study with the JAXA HRLULC map. Figures (a,d) show the land use/land cover map produced in this study, while (b,e) show the JAXA HRLULC map. Figures (c,f) show the Google Earth images of the areas shown in (a,b,d,e).



**Figure 14.** Cropland extent for 2015 in this study and in the GFSAD30SEACE map.

Japan carries out an agricultural census every five years via questionnaires, and the last census was released on 1 February 2015. It is, therefore, not representative of the agricultural production situation in the year 2015 but, rather, represents the preceding five years. Farmers respond to questionnaires by regions referred to as ‘agricultural villages’, and respond to (among other questions) how much land is under cultivation, whether the production is for commercial or subsistence purposes, and what they grow. However, the boundaries of the agricultural villages do not match the current national administrative boundaries. This, therefore, makes merging and comparison of this data with data obtained based on administrative boundaries difficult. The total reported area of cropland in the statistical data was 129.5 Km<sup>2</sup>. This figure is close to our estimated area of paddy rice fields (123.21 Km<sup>2</sup>), and also matches the GFSAD30 cropland area. Spatial distribution of crops and cropping regimes could not be inferred, due to the incongruence between the boundaries used in this study with those of the statistical data. The results of this study, therefore, provide a base-map compatible with national administrative boundaries, for future analysis and monitoring of agriculture in the region.

The fusion results confirmed that implementing Index-then-Blend with MODIS dates matching the Landsat dates generates synthetic images with a strong agreement with the observed images. However, the fusion process takes a long time and, for this reason, we applied fusion to a subset of the Landsat scene covering the Chiba prefecture, rather than the entire scene. This led to the loss of data in the northern part of our study area, which also coincides with the boundary of Chiba prefecture. It would, therefore, be better to apply fusion to entire Landsat scenes or a mosaic of scenes, then subset to the intended study area.

This study demonstrates that using the simple, yet robust, NDVI with high temporal frequency, dynamic heterogeneous landscapes can be adequately mapped and monitored using data available within a year. From a policy development perspective, this aspect of our methodology is desirable, as it allows for changes taking place within the landscape to be catalogued using the most recent data and disseminated with reasonable frequency and accuracy.



## 5. Conclusions

Intra-annual cropland area estimation and distinction from other land cover types in heterogeneous landscapes can be challenging, due to inadequate information. In this study, we demonstrated how, using the intermittent moderate resolution Landsat and daily MODIS surface reflectance imagery, information that can be used to distinguish croplands from other land cover types can be retrieved. Fusion of the MODIS NDVI and Landsat NDVI images yielded synthetic Landsat imagery with  $R^2 > 0.9$ , indicating strong agreement with the observed NDVI. The regular moderate resolution image time-series, with an 8-day interval, proved to be adequate for the task of estimating cropland area and cropping patterns in a complex heterogeneous urban landscape. In addition, using knowledge of post-harvest practices of peanut farmers in the region, we were able to distinguish peanuts from other crops with reasonable accuracy. The Random Forest classifier requires a large amount of training data, which was acquired based on the seasonal MVC-NDVI. However, this was made possible by the availability of images in each season which met the cloud-cover threshold, and may not be the case when carrying out analysis in other years or regions that are heavily inundated with cloud cover. In this regard, efforts to establish spectral-temporal libraries for various land cover types in disparate geographical locations would go a long way in enhancing local- and national-scale annual cropland mapping. This study also demonstrates the importance of local-scale cropland mapping towards validating regional- and global-scale cropland datasets. Future research work will involve evaluation of the applicability of the methodology to larger regions, and in different geographical locations which have different land cover and climate characteristics.

**Author Contributions:** E.N. formulated the research design and methodology, processed and analyzed the data and wrote the final manuscript. A.M. assisted in refining the methodology and revising the manuscript. Y.S. assisted in revising the manuscript. A.K., Y.W., and J.G.P. revised the manuscript and supervised. All authors contributed and approved the final manuscript before submission.

**Funding:** This research was funded by the Japan International Cooperation Agency (JICA), grant number D1511645.

**Acknowledgments:** The authors would like to thank the reviewers and the editors for the invaluable and constructive comments and suggestions. Eunice Nduati is grateful to the Japan International Cooperation Agency (JICA) for the financial support that made this work possible.

**Conflicts of Interest:** The authors declare no conflict of interest. The funders had no role in the design of the study; in the collection, analyses, or interpretation of data; in the writing of the manuscript, and in the decision to publish the results.

## References

1. Brown, M.E.; Funk, C.C. Food security under climate change. *Nat. Clim. Chang.* **2008**, *6*, 10–13.
2. Porter, J.R.; Dyball, R.; Dumaresq, D.; Deutsch, L.; Matsuda, H. Feeding capitals: Urban food security and self-provisioning in Canberra, Copenhagen and Tokyo. *Glob. Food Secur.* **2014**, *3*, 1–7.
3. Eigenbrod, C.; Gruda, N. Urban vegetable for food security in cities. A review. *Agron. Sustain. Dev.* **2015**, *35*, 483–498.
4. Opitz, I.; Berges, R.; Piorr, A.; Krikser, T. Contributing to food security in urban areas: Differences between urban agriculture and peri-urban agriculture in the Global North. *Agric. Hum. Values* **2016**, *33*, 341–358.
5. Besthorn, F.H. Vertical farming: Social work and sustainable urban agriculture in an age of global food crises. *Aust. Soc. Work* **2013**, *66*, 187–203.
6. Lang, T.; Barling, D. Food security and food sustainability: Reformulating the debate. *Geogr. J.* **2012**, *178*, 313–326.
7. Thebo, A.L.; Drechsel, P.; Lambin, E.F. Global assessment of urban and peri-urban agriculture: Irrigated and rainfed croplands. *Environ. Res. Lett.* **2014**, *9*, 114002.
8. Martellozzo, F.; Landry, J.S.; Plouffe, D.; Seufert, V.; Rowhani, P.; Ramankutty, N. Urban agriculture: A global analysis of the space constraint to meet urban vegetable demand. *Environ. Res. Lett.* **2014**, *9*, 064025.

9. d'Amour, C.B.; Reitsma, F.; Baiocchi, G.; Barthel, S.; Güneralp, B.; Erb, K.A.; Haberl, H.; Creutzig, F.; Seto, K.C. Future urban land expansion and implications for global croplands. *Proc. Natl. Acad. Sci. USA* **2017**, *114*, 8939–8944.
10. Waldner, F.; Canto, G.S.; Defourny, P. Automated annual cropland mapping using knowledge-based temporal features. *ISPRS J. Photogramm. Remote Sens.* **2015**, *110*, 1–13.
11. Thenkabail, P.S. Global Food Security Support Analysis Data at Nominal 1 km (GFSAD1km) Derived from Remote Sensing in Support of Food Security in the Twenty-First Century: Current Achievements and Future Possibilities. In *Remote Sensing Handbook-Three Volume Set*, CRC Press. **2019**, 865–894.
12. Teluguntla, P.; Thenkabail, P.S.; Xiong, J.; Gumma, M.K.; Congalton, R.G.; Oliphant, A.; Poehnelt, J.; Yadav, K.; Rao, M.; Massey, R. Spectral matching techniques (SMTs) and automated cropland classification algorithms (ACCAs) for mapping croplands of Australia using MODIS 250-m time-series (2000–2015) data. *Int. J. Digit. Earth* **2017**, *9*, 944–977.
13. Teluguntla, P.; Thenkabail, P.; Oliphant, A.; Xiong, J.; Gumma, M.K.; Congalton, R.G.; Yadav, K.; Huete, A. A 30-m Landsat-derived cropland extent product of Australia and China using random forest machine learning algorithm on Google Earth Engine cloud computing platform. *ISPRS J. Photogramm. Remote Sens.* **2018**, *144*, 325–340.
14. Matton, N.; Canto, G.S.; Waldner, F.; Valero, S.; Morin, D.; Inglada, J.; Arias, M.; Bontemps, S.; Koetz, B.; Defourny, P. An automated method for annual cropland mapping along the season for various globally-distributed agrosystems using high spatial and temporal resolution time series. *Remote Sens.* **2015**, *7*, 13208–13232.
15. Belgiu, M.; Csillik, O. Sentinel-2 cropland mapping using pixel-based and object-based time-weighted dynamic time warping analysis. *Remote Sens. Environ.* **2018**, *204*, 509–523.
16. Jakubauskas, M.E.; Legates, D.R.; Kastens, J.H. Crop identification using harmonic analysis of time-series AVHRR NDVI data. *Comput. Electron. Agric.* **2002**, *37*, 127–139.
17. Mingwei, Z.; Zhou, Q.; Chen, Z.; Liu, J.; Zhou, Y.; Cai, C. Crop discrimination in Northern China with double cropping systems using Fourier analysis of time-series MODIS data. *Int. J. Appl. Earth Obs. Geoinf.* **2008**, *10*, 476–485.
18. McNairn, H.; Champagne, C.; Shang, J.; Holmstrom, D.; Reichert, G. Integration of optical and Synthetic Aperture Radar (SAR) imagery for delivering operational annual crop inventories. *ISPRS J. Photogramm. Remote Sens.* **2009**, *64*, 434–449.
19. Siachalou, S.; Mallinis, G.; Tsakiri-Strati, M. A hidden Markov models approach for crop classification: Linking crop phenology to time series of multi-sensor remote sensing data. *Remote Sens.* **2015**, *7*, 3633–3650.
20. Inglada, J.; Arias, M.; Tardy, B.; Hagolle, O.; Valero, S.; Morin, D.; Dedieu, G.; Sepulcre, G.; Bontemps, S.; Defourny, P.; et al. Assessment of an operational system for crop type map production using high temporal and spatial resolution satellite optical imagery. *Remote Sens.* **2015**, *7*, 12356–12379.
21. Immitzer, M.; Vuolo, F.; Atzberger, C. First experience with Sentinel-2 data for crop and tree species classifications in central Europe. *Remote Sens.* **2016**, *8*, 166.
22. Vladimir, C.; Lugonja, P.; Brkljač, B.N.; Brunet, B. Classification of small agricultural fields using combined Landsat-8 and RapidEye imagery: Case study of northern Serbia. *J. Appl. Remote Sens.* **2014**, *8*, 083512.
23. Gómez, C.; White, J.C.; Wulder, M.A. Optical remotely sensed time series data for land cover classification: A review. *ISPRS J. Photogramm. Remote Sens.* **2016**, *116*, 55–72.
24. Petitjean, F.; Jordi, I.; Pierre, G. Satellite image time series analysis under time warping. *IEEE Trans. Geosci. Remote Sens.* **2012**, *50*, 3081–3095.
25. Petitjean, F.; Kurtz, C.; Passat, N.; Gançarski, P. Spatio-temporal reasoning for the classification of satellite image time series. *Pattern Recognit. Lett.* **2012**, *33*, 1805–1815.
26. Shen, H.; Li, X.; Cheng, Q.; Zeng, C.; Yang, G.; Li, H.; Zhang, L. Missing information reconstruction of remote sensing data: A technical review. *IEEE Geosci. Remote Sens. Mag.* **2015**, *3*, 61–85.
27. Cheng, Q.; Shen, H.; Zhang, L.; Peng, Z. Missing Information Reconstruction for Single Remote Sensing Images Using Structure-Preserving Global Optimization. *IEEE Signal Process. Lett.* **2017**, *24*, 1163–1167.
28. Julien, Y.; Sobrino, J.A. Comparison of cloud-reconstruction methods for time series of composite NDVI data. *Remote Sens. Environ.* **2010**, *114*, 618–625.
29. Zhao, Y.; Huang, B.; Song, H. A robust adaptive spatial and temporal image fusion model for complex land surface changes. *Remote Sens. Environ.* **2018**, *208*, 42–62.

30. Pohl, C.; Van Genderen, J.L. Review article multisensor image fusion in remote sensing: Concepts, methods and applications. *Int. J. Remote Sens.* **1998**, *19*, 823–854.
31. Solberg, A.H.S. Data fusion for remote sensing applications. *Signal Image Process. Remote Sens.* **2006**, 249–271.
32. Schmitt, M.; Zhu, X.X. Data fusion and remote sensing: An ever-growing relationship. *IEEE Geosci. Remote Sens. Mag.* **2016**, *4*, 6–23.
33. R Core Team. *R: A Language and Environment for Statistical Computing*; R Foundation for Statistical Computing: Vienna, Austria, 2013. Available online: <http://www.R-project.org/> (Accessed April 19, 2018).
34. QGIS Development Team. QGIS Geographic Information System. Open Source Geospatial Foundation. 2009. Available online: <http://qgis.osgeo.org> (Accessed March 10, 2018).
35. Ministry of Agriculture, Forestry and Fisheries(MAFF), Japan. FY 2016 Summary of the Annual Report on Food, Agriculture and Rural Areas in Japan. 2016. Available online: [http://www.maff.go.jp/j/wpaper/w\\_maff/h28/attach/pdf/index-28.pdf](http://www.maff.go.jp/j/wpaper/w_maff/h28/attach/pdf/index-28.pdf) (Accessed October 16, 2018).
36. Tivy, J. *Agricultural Ecology*; Routledge 2014.
37. EarthExplorer. Available online: <https://earthexplorer.usgs.gov/> (Accessed January, 2018).
38. Mosleh, M.; Hassan, Q.; Chowdhury, E. Application of remote sensors in mapping rice area and forecasting its production: A review. *Sensors* **2015**, *15*, 769–791.
39. Motohka, T.; Nasahara, K.N.; Miyata, A.; Mano, M.; Tsuchida, S. Evaluation of optical satellite remote sensing for rice paddy phenology in monsoon Asia using a continuous in situ dataset. *Int. J. Remote Sens.* **2009**, *30*, 4343–4357.
40. NASA LP DAAC. MODIS Land Products Quality Assurance Tutorial: Part-1. **2013**. Available online: [https://lpdaac.usgs.gov/sites/default/files/public/modis/docs/MODIS\\_LP\\_QA\\_Tutorial-2.pdf](https://lpdaac.usgs.gov/sites/default/files/public/modis/docs/MODIS_LP_QA_Tutorial-2.pdf). (Accessed February 23, 2018).
41. Vermote, MOD09A1 MODIS/Terra Surface Reflectance 8-Day L3 Global 500m SIN Grid V006. *NASA EOSDIS Land Processes DAAC*, **2015**, Volume 10.
42. Lobell, David B. and Asner, Gregory P. Cropland distributions from temporal unmixing of MODIS data. *Remote Sensing of Environment* **2004**, *93*(3), 412–422.
43. Liao, C.; Wang, J.; Pritchard, I.; Liu, J.; Shang, J. A spatio-temporal data fusion model for generating NDVI time series in heterogeneous regions. *Remote Sens.* **2017**, *9*, 1125.
44. Zhu, X.; Chen, J.; Gao, F.; Chen, X.; Masek, J.G. An enhanced spatial and temporal adaptive reflectance fusion model for complex heterogeneous regions. *Remote Sens. Environ.* **2010**, *114*, 2610–2623.
45. Jarihani, A.A.; McVicar, T.R.; van Niel, T.G.; Emelyanova, I.V.; Callow, J.N.; Johansen, K. Blending Landsat and MODIS data to generate multispectral indices: A comparison of “Index-then-Blend” and “Blend-then-Index” approaches. *Remote Sens.* **2014**, *6*, 9213–9238.
46. Li, L.; Zhao, Y.; Fu, Y.; Pan, Y.; Yu, L.; Xin, Q. High resolution mapping of cropping cycles by fusion of landsat and MODIS data. *Remote Sens.* **2017**, *9*, 1232.
47. Remote Sensing and Spatial Analysis Lab, ESTARFM. 27 July 2018. Available online: <https://xiaolinzhu.weebly.com/open-source-code.html> (Accessed March 10, 2018).
48. Waldner, F.; Fritz, S.; di Gregorio, A.; Defourny, P. Mapping priorities to focus cropland mapping activities: Fitness assessment of existing global, regional and national cropland maps. *Remote Sens.* **2015**, *7*, 7959–7986.
49. Japan High Resolution Land Use Land Cover (2014–2016) (Version 18.03). Available online: [https://www.eorc.jaxa.jp/ALOS/lulc/lulc\\_jindex\\_v1803.htm](https://www.eorc.jaxa.jp/ALOS/lulc/lulc_jindex_v1803.htm) (Accessed February 9, 2018).
50. Oliphant, AJ, Thenkabail, PS, Teluguntla, P, Xiong, J, Congalton, RG, Yadav, K, Massey, R, Gumma, MK and Smith, C. NASA Making Earth System Data Records for Use in Research Environments (MEaSUREs) Global Food Security-support Analysis Data (GFSAD) Cropland Extent 2015 Southeast Asia 30 m V001; *NASA EOSDIS Land Processes DAAC, USGS Earth Resources Observation and Science (EROS)*, **2017**.
51. Japan CROPS. Available online: <https://japancrops.com/en/prefectures/chiba/> (Accessed October 16, 2018).
52. Japan External Trade Organization (JETRO). Jitsukawa Foods: Chiba: A Peanut Paradise. Available online: <https://www.jetro.go.jp/en/mjcompany/jitsukawafoods.html> (Accessed October 16, 2018).
53. Ito, K.; Aoki, S.T.; Shimuzu, A. Japan’s Peanut Market Report. Global Agricultural Information Network; USDA Foreign Agricultural Service, GAIN Report Number: JA9532, 22 December 2009. Available online: <https://www.fas.usda.gov/>. (Accessed October 16, 2018)

54. Dickens, J.W. Peanut curing and post-harvest physiology. In *Peanuts Culture and Uses*; American Peanut Research and Education Society: APRES Inc. **1973**.
55. Allen, W.S.; and Sorenson, J.W.; Person, N.K., Jr. Guide for Harvesting, Handling and Drying Peanuts. Texas Agricultural Extension Service. *Leaflet/Texas Agricultural Extension Service*; no. 1029; **1971**.
56. Sonobe, R.; Tani, H.; Wang, X.; Kobayashi, N.; Shimamura, H. Random forest classification of crop type using multi-temporal TerraSAR-X dual-polarimetric data. *Remote Sens. Lett.* **2014**, *5*, 157–164.
57. Tatsumi, K.; Yamashiki, Y.; Torres, M.A.C.; Taïpe, C.L.R. Crop classification of upland fields using Random forest of time-series Landsat 7 ETM+ data. *Comput. Electron. Agric.* **2015**, *115*, 171–179.
58. Hao, P.; Zhan, Y.; Wang, L.; Niu, Z.; Shakir, M. Feature selection of time series MODIS data for early crop classification using random forest: A case study in Kansas, USA. *Remote Sens.* **2015**, *7*, 5347–5369.
59. Wang, L.A.; Zhou, X.; Zhu, X.; Dong, Z.; Guo, W. Estimation of biomass in wheat using random forest regression algorithm and remote sensing data. *Crop J.* **2016**, *4*, 212–219.
60. Vogels, M.F.A.; De Jong, S.M.; Sterk, G.; Addink, E.A. Agricultural cropland mapping using black-and-white aerial photography, object-based image analysis and random forests. *Int. J. Appl. Earth Obs. Geoinf.* **2017**, *54*, 114–123.
61. Lebourgeois, V.; Dupuy, S.; Vintrou, É.; Ameline, M.; Butler, S.; Bégué, A. A combined random forest and OBIA classification scheme for mapping smallholder agriculture at different nomenclature levels using multisource data (simulated Sentinel-2 time series, VHRS and DEM). *Remote Sens.* **2017**, *9*, 259.
62. Leutner, B.; Horning, N. *RStoolbox: Tools for Remote Sensing Data Analysis*, CRAN–Package RStoolbox, bf 2017. Available online: <https://cran.r-project.org/web/packages/RStoolbox/index.html> (Accessed 5 February 2018)
63. Cohen, J. Weighted kappa: Nominal scale agreement provision for scaled disagreement or partial credit. *Psychol. Bull.* **1968**, *70*, 213.
64. Congalton, R.G. 4A review of assessing the accuracy of classifications of remotely sensed data. *Remote Sens. Environ.* **1991**, *37*, 35–46.
65. Sharma, R.C.; Tateishi, R.; Hara, K.; Iizuka, K. Production of the Japan 30-m land cover map of 2013–2015 using a Random Forests-based feature optimization approach. *Remote Sens.* **2016**, *8*, 429.
66. Dong, J.; Xiao, X. Evolution of regional to global paddy rice mapping methods: A review. *ISPRS J. Photogramm. Remote Sens.* **2016**, *119*, 214–227.



© 2019 by the authors. Licensee MDPI, Basel, Switzerland. This article is an open access article distributed under the terms and conditions of the Creative Commons Attribution (CC BY) license (<http://creativecommons.org/licenses/by/4.0/>).